AD-A194 658 CONSTRUCTION OF GALLIUM ARSENIDE SOLAR CONCENTRATOR FOR SPACE USE(U) NAVAL POSTGRADUATE SCHOOL MONTEREY CA C L HUDEC MAR 88 1/2

UNCLASSIFIED F/G 9/1 NL

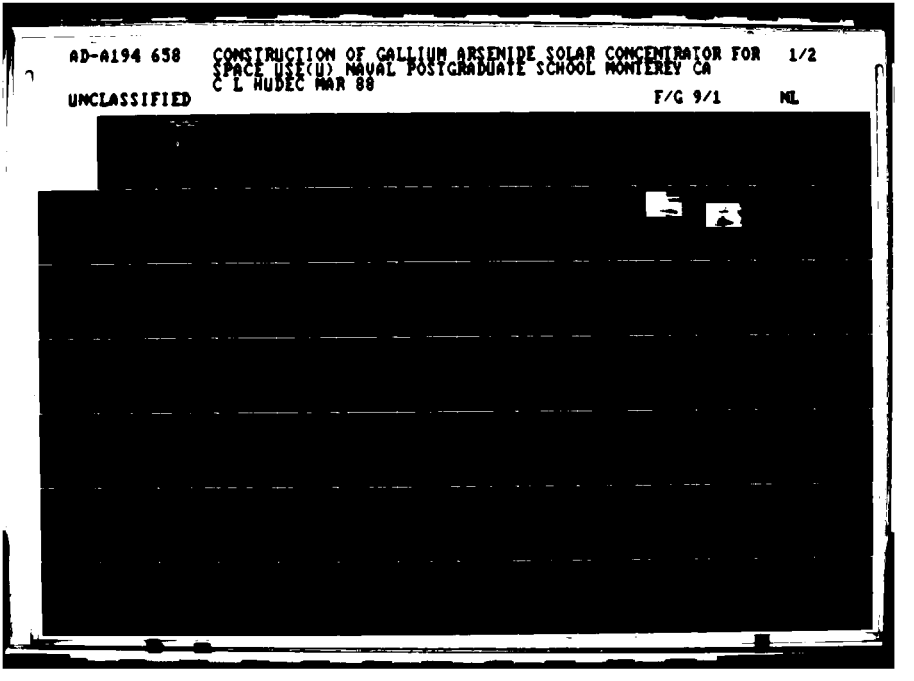

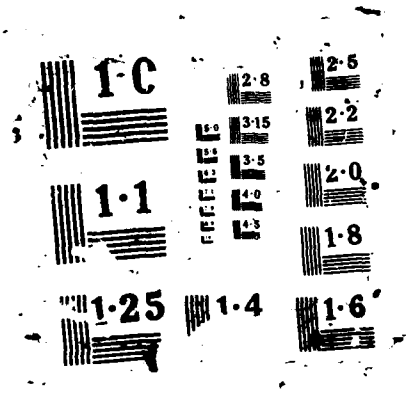
1·C
1·1
1·25
2·8
3·15
3·5
4·0
4·5
1·4
2·5
2·2
2·0
1·8
1·6

(2)

NAVAL POSTGRADUATE SCHOOL
Monterey, California

THESIS

CONSTRUCTION OF GALLIUM ARSENIDE SOLAR CONCENTRATOR FOR SPACE USE

by

Chris L. Hudec

March 1988

Thesis Advisor Dr. Sherif Michael

Unclassified

security classification of this page

A194658

REPORT DOCUMENTATION PAGE

1a Report Security Classification: Unclassified	1b Restrictive Markings
2a Security Classification Authority	3 Distribution Availability of Report: Approved for public release; distribution is unlimited.
2b Declassification Downgrading Schedule	
4 Performing Organization Report Number(s)	5 Monitoring Organization Report Number(s)
6a Name of Performing Organization: Naval Postgraduate School; 6b Office Symbol (if applicable): 39	7a Name of Monitoring Organization: Naval Postgraduate School
6c Address (city, state, and ZIP code): Monterey, CA 93943-5000	7b Address (city, state, and ZIP code): Monterey, CA 93943-5000
8a Name of Funding Sponsoring Organization; 8b Office Symbol (if applicable)	9 Procurement Instrument Identification Number
8c Address (city, state, and ZIP code)	10 Source of Funding Numbers: Program Element No; Project No; Task No; Work Unit Accession No

11 Title (Include security classification): CONSTRUCTION OF GALLIUM ARSENIDE SOLAR CONCENTRATOR FOR SPACE USE

12 Personal Author(s): Chris L. Hudec

13a Type of Report	13b Time Covered	14 Date of Report (year, month, day)	15 Page Count
Master's Thesis	From To	March 1988	120

16 Supplementary Notation: The views expressed in this thesis are those of the author and do not reflect the official policy or position of the Department of Defense or the U.S. Government.

17 Cosati Codes			18 Subject Terms (continue on reverse if necessary and identify by block number)
Field	Group	Subgroup	GaAs Solar Concentrator Array; Fresnel Lens

19 Abstract (continue on reverse if necessary and identify by block number)

A Gallium Arsenide (GaAs) Solar Concentrator Array (SCA) was constructed using the recently developed fresnel lens technology. The parts used were a mixture of space qualified components and readily available off-the-shelf items. The objective of the test was to verify that the SCA would substantially increase the array's power output and reject the high thermal radiation it would encounter in space. It was found that the 3 by 3 GaAs SCA power output increased from 29.88 mW to 433.71 mW. The thermal analysis and the steady state cell operating temperature calculation showed that the SCA's thermal design would keep the GaAs solar cells at a steady state temperture of 50.7° C. However, because of the low intensity level of the light source available for use the cell operating temperature was only 27° C. This was considered to be inconclusive in determining the adequacy of the thermal design.

20 Distribution Availability of Abstract	21 Abstract Security Classification	
☒ unclassified unlimited ☐ same as report ☐ DTIC users	Unclassified	
22a Name of Responsible Individual: Dr. Sherif Michael	22b Telephone (include Area code): (408) 646-2252	22c Office Symbol: 62Mi

DD FORM 1473,84 MAR

83 APR edition may be used until exhausted
All other editions are obsolete

security classification of this page

Unclassified

Approved for public release; distribution is unlimited.

Construction of Gallium Arsenide Solar Concentrator For Space Use

by

Chris L. Hudec
Major, United States Army
B.S., The Ohio State University, 1975

Submitted in partial fulfillment of the
requirements for the degree of

MASTER OF SCIENCE IN ELECTRICAL ENGINEERING

from the

NAVAL POSTGRADUATE SCHOOL
March 1988

Author: 

Chris L. Hudec

Approved by: 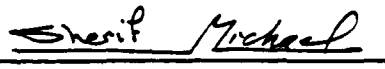

Dr. Sherif Michael, Thesis Advisor

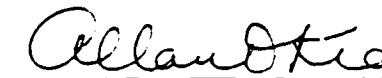

Allan D. Kraus, Second Reader

John P. Powers, Chairman,
Department of Electrical and Computer Engineering

Gordon E. Schacher,
Dean of Science and Engineering

ABSTRACT

A Gallium Arsenide (GaAs) Solar Concentrator Array (SCA) was constructed using the recently developed fresnel lens technology. The parts used were a mixture of space qualified components and readily available off-the-shelf items. The objective of the test was to verify that the SCA would substantially increase the array's power output and reject the high thermal radiation it would encounter in space. It was found that the 3 by 3 GaAs SCA power output increased from 29.88 mW to 433.71 mW. The thermal analysis and the steady state cell operating temperature calculation showed that the SCA's thermal design would keep the GaAs solar cells at a steady state temperture of 50.7° C. However, because of the low intensity level of the light source available for use the cell operating temperature was only 27° C. This was considered to be inconclusive in determining the adequacy of the thermal design.

TABLE OF CONTENTS

LIST OF TABLES

LIST OF FIGURES

ACKNOWLEDGEMENTS

The author would like to thank Professor S. Michael for his guidance in the preperation of this thesis and his knowledge on solar cells. The author also thanks Professor A. Kraus for his guidance in the thermal design and analysis of the solar concentrator array. Finally the author would like to thank his wife, Jeanne, for her continual support, positive atitude, and typing skills which made a seemingly impossible task possible.

I. INTRODUCTION

Satellite systems are constantly changing. They have gone from relatively simple payloads by today's standards to massive complex payloads able to do a multitude of complex tasks. With this increase in complexity comes an increase in the overall weight of the satellite and an increase in the power required to operate it. The solar arrays currently used to provide this power would also have to be enlarged, further adding to the size and weight of the satellite.

A viable power alternative is to use a solar concentrator array (SCA). The SCA not only provides a substantial increase in power, but also uses fewer solar cells. The weight reduction in the array will help offset the increase in weight from the payload.

The Cassegrainian Solar Concentrator Arrays are the primary SCAs used in space today. These concentrators use reflecting technology to reflect light onto the solar cell. Unfortunately, mirror technology has reached its limits in efficiency, dimension, weight, and tolerance to tracking and alignment errors. Fortunately, there has been a recent development in optics that has already overcome these limits. This new development is the fresnel lens.

The fresnel lens has many distinct advantages over the Cassegrainian mirror. First, the fresnel lens uses refracting technology that reduces the overall volume of the solar concentrator array. Second, the lens has a lighter weight that helps reduce the overall satellite weight. Third, it has a higher efficiency. This will allow more light to reach the solar cell which will in turn increase the cell's efficiency and power output. Finally, it has a higher tolerance to tracking and alignment errors. Higher errors mean less fuel needed for attituded control of the satellite. Therefore, the satellite's lifetime can be increased because of this reduction in fuel consumption.

With the development of the fresnel lens comes the need to put this technology together with the solar array to build a new type of solar concentrator. Hence, the subject of this thesis is to build a Gallium Arsenide (GaAs) Solar Concentrator Array using fresnel lenses, show that it is capable for space use, and verify that the total output power of the array increases.

A critical factor in determining the SCA's effectiveness in space will be its ability to keep the solar cells within their operating temperature limits [Ref. 1: p. 109]. The operating temperature is strongly related to the thermal design of the SCA. The cell oper-

ating temperature will be used as the criteria for determining if the SCA can operate in space.

Chapter II discusses the environment in which the SCA will be throughout its lifetime.

Chapter III discusses the components that make up a SCA. It also includes a discussion on the reasons a particular component will be used in building the SCA.

The thermal design considerations for the SCA is addressed in Chapter IV. The calculation of the steady-state cell operating temperature is performed. This temperature will be verified by performing a nodal analysis.

Chapter V discusses the equipment, software, and procedures used in conducting the test of the SCA. The results of the test are given and explained.

The conclusions and recommendations based on the findings in Chapter V are presented in Chapter VI.

II. THE ENVIRONMENT

The operating enviroment of the SCA will have a major impact on its design. There are four different environments that the SCA will encounter during its lifetime, namely, terrestrial, launch, space, and radiation. Each of these will be briefly discussed. A detailed discussion of this subject can be found in Rauschenbach [Ref. 2].

A. TERRESTRIAL ENVIRONMENTAL EFFECTS ON THE SCA

The SCA will be affected by the terrestrial environment up to and including part of the launch. These environmental effects must not be taken lightly by the SCA designer, or substantial damage and mission delay could occur. This damage may not show until the SCA has been launched into space causing the mission to end prematurely and loss of millions of dollars. The four major concerns of which the SCA designer must be aware of are, exposure to extreme temperature cycles, high humidity, surface contamination, and mishandling of the SCA.

When the SCA has to be stored for a significant length of time, steps must be taken to keep the array parts at the same temperature. If there are temperature differences among the SCA parts, additional stresses will be introduced. Over a long period of time, these stresses can weaken or cause permanent fractures in the parts. [Ref. 2: p. 419]

If the temperature cycling is in the presence of high humidity, corrosion on the solar cell contacts will occur, leading to a power loss in the solar cell. Partial solutions to this problem are soldering of the contacts or by using adhesive to completely cover them. Both of these solutions are not 100 percent effective. Solder becomes porous during temperature cycling, and the adhesive absorbs water during the curing process. The best solution is to store the SCA in a temperature and humidity controlled environment. This not only prevents the temperature cycling and high humidity, but reduces the surface contamination. [Ref. 3: p. 2.1-3]

Surface contamination of the SCA comes mainly from sand and dust. The sand can cause errosion to the thermal control paint, anti-reflective coatings, coverglasses, and the fresnel lenses. In addition, it can cause short circuiting of the components on the SCA. Large amounts of dust particles will reduce the amount of light received by the solar cells. [Ref. 3: p. 2.1-5]

The last terrestrial environmental effect - mishandling the array - has the greatest potential for damage the SCA. Dropping tools, bumping into the SCA, and handling thermal control paint with oily hands are examples of improper handling.

B. LAUNCH ENVIRONMENTAL EFFECTS

The SCA is considered to be in the launch environment from lift-off until the spacecraft reaches its mission orbit. The rocket engines cause the majority of damage to the SCA. The forces that are a by-product of the engines are vibration, acoustics, shock, and high acceleration loads.

1. Vibration

The rocket engine will transmit vibrational forces to the SCA via the structural members. The magnitude and the frequency of this vibration is either attenuated or amplified by the transmitting media. If the vibrational force is near the SCA's resonant or natural frequency, the force will be amplified until it causes permanent damage. The majority of the damage comes from the deformation and separation of the different SCA parts. To prevent this, the designer must avoid or dampen the SCA's resonant frequency.

Minimizing the effects of vibration can be accomplished by using several different techniques. Some of the pertenent ones are [Ref. 2: p. 432]:

1. Isolating the SCA's substrate from the rest of the spacecraft.
2. Changing the SCA's resonant frequency by modifying the shape, mass, or stiffness.
3. Dissipate the energy and reduce the amplitude by using dampers and additional tie-downs.
4. Spot bond wires and joints to the substrate at irregular intervals.
5. Rivet members to provide interface friction.

2. Acoustics

Any acoustic vibration that is generated by the launch will be transmitted to the SCA. The majority of acoustic vibration is generated by the rocket engine and by aerodynamic excitation of the shrouds as the rocket passes through the sound barrier. The acoustical vibration force on the SCA is usually larger than the structural vibration force. Reduction of these forces is accomplished by using the same methods used to reduce the vibrational forces. [Ref. 2: p. 433]

3. Shock

Shock loads only have to be considered when the SCA is located close to the booster interface. In this case, shock isolation must be accomplished, otherwise there

is a risk of potiential damage to the SCA. An example of this damage is the cracking of the coverglass or the solar cell itself. During the launch, shock forces are present on the SCA when the rocket engines are ignited. [Ref. 2: p. 430]

4. High Acceleration

During the launch, parts of the SCA not rigidly mounted will be deflected. Depending on the material, the deflection may or may not be temporary. For example, adhesive mounted solar cells will temporarily move, while blocking diodes will be permanently bent. This problem is reduced or eliminated by orienting the SCA to minimize the effects of acceleration. There are several ways to minimize acceleration effects. One way is to use stress reliefs and fasteners on the wires and secure them at short, regular intervals to the substrate. [Ref. 2: p. 429]

C. SPACE ENVIRONMENT

The space environment is characterized by a high vacuum, meteoroids, electromagnetic fields, temperature cycling, and radiation. All of them will have an effect on the SCA operation.

1. High Vacuum

The problem with high vacuum is that certain metals vaporize in space when heated. These metals are magnesium, cadium, and zinc [Ref.2: p. 435]. These should not be used in the SCA because as they vaporize, they could condense on the fresnel lenses and on the coverglasses causing a reduction in the light received by the cell. In addition, these condensing metals could cause short circuiting of two closely spaced parallel strings of solar cells.

If the above metals must be used on the SCA, certain preventive measures must be taken to insure that they do not vaporize. These measures are, keeping them at a low temperature, or overcoating them with a metal that does not vaporize at high temperatures. [Ref. 2: p. 435]

Even though some materials are adversely affected by the high vacuum of space, some materials such as glass, are actually strengthened. Glass is three times stronger in space than on earth. If a glass surface cracks on earth, the cracks absorb gases from the atmosphere. The absorbed gases act as wedges causing cracks to widen until they eventually break the glass. It is important that the materials used for the SCA be chosen carefully so that they perform well in space and do not contribute to a failure of the SCA. [Ref. 2: p. 436]

The high vacuum of space not only has an effect on certain metals, but will cause polymers to vaporize. This causes the polymer to become brittle in space. Fortunately, many of the polymers of engineering importance, such as the polymers used in the fresnel lens, do not evaporate in space. [Ref. 4]

2. Meteoroids

Meteoroid environment is unlike the high vacuum environment in that meteoroids cannot be controlled by the SCA designer. Meteoroids come in various sizes with the greater majority having a mass between 10^{-6} grams to 10^{-3} grams. These sized meteoroids cause the majority of damage to the SCA. A large part of the damage comes from the erosion of SCA parts, especially of the fresnel lens, solar cell coverglass, and the thermal control paint.

While meteoroid collision possesses the potential for catastrophic damage to an SCA, to date no satellite solar array has recorded any significant damage as the result of this phenomenon. Because of this, the SCA degradation output due to meteoroid impact is assumed to be zero. [Ref. 2: p. 438]

3. Magnetic Fields

The next effect on the SCA comes from the earth's magnetic field. When the solar cells produce a current, the current produces a magnetic field. This magnetic field interacts with the earth's field producing a torque on the SCA. This torque must be corrected by the spacecraft attitude controls. Constant use of the attitude controls causes the fuel supply to be used at a faster rate. This will reduce the lifetime of the spacecraft.

Fortunately, this is very easy to correct. Field negation is accomplished by placing the solar cell strings in such a way as to cancel the magnetic field produced by the SCA. Figure 1 on page 7 shows two possible solar cell string configurations. Both of these configurations are effective.

4. Solar Eclipse

The solar eclipse has the quickest and the most pronounced effect on the output of the SCA in the space environment. The majority of spacecraft in low earth orbit (LEO) will experience a solar eclipse. When the spacecraft goes into the earth's shadow, no light will fall on the SCA. The SCA will cease to produce power and will act as a current sink. If no design measures are taken to prevent this, the on-board batteries will be drained. One measure is to place blocking diodes at strategic locations on the SCA. These diodes will prevent the SCA from acting as a current sink. Diodes are discussed in greater detail in Chapter III.

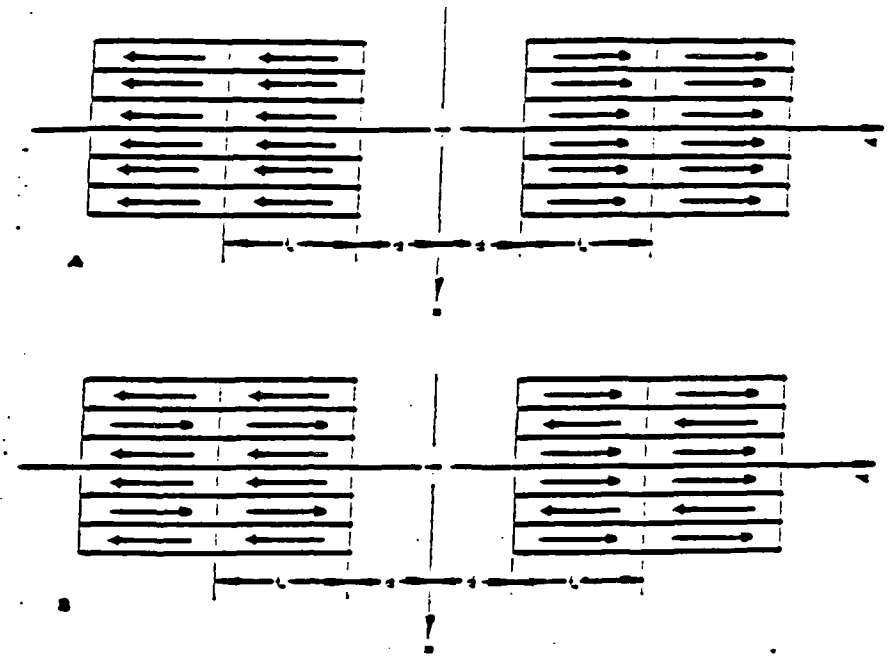

Figure 1. Solar Cell String Configuration for Magentic Field Cancellation [Ref. 2: p. 149]

Solar eclipses also have an effect on the operating temperature of the solar cell. The lowest operating temperature of the cell is reached when the SCA is in the solar eclipse. It is important that the cell's operating temperature in its eclipse and the operating temperture in the sun are not too extreme. Chapters III and IV go into greater detail on this subject.

5. Effects of Rocket Engine Exhaust and Monoatomic Oxygen

Another area of concern are the deposits resulting from outgassing of the engine exhaust plume onto the SCA. This outgassing condensation could land on the fresnel lenses and on the solar cell coversglasses. This would decrease the amount of light being transmitted to the solar cells. [Ref. 2: p. 438]

Another problem with this condensation is that it increases the solar cell operating temperature. It deteriorates the thermal-optical characteristics of the solar cell coverglass and the thermal control surfaces on the backside of the SCA. For SCAs used on a three-axis stabilized spacecraft, no significant problem has been detected. However, for a body mounted SCA, this could cause some reduction of power. [Ref. 2: p. 438]

A significant problem for all SCA's that use fresnel lens in LEO is the problem of monoatomic oxygen. Monoatomic oxygen causes a substantial discoloration to the fresnel lenses in a very short period of time. According to Mark J. O'Neill of ENTECH, Inc., the only material presently found to protect the fresnel lens from monoatomic oxygen is glass. Adding glass to the fresnel lens would take away its light weight advantage over other types of solar concentrators. There is currently much research being conducted in this area to find a suitable material that will not degrade in a monoatomic oxygen environment. [Ref. 4]

The deposits of the engine exhaust plume could reduce the output power to the SCA by as much as two percent [Ref. 2: p. 438]. This problem is considered minor compared with the damage to the SCA caused by radiation.

D. RADIATION ENVIRONMENT

Radiation may be classified as either electromagnetic radiation or particulate radiation. Electromagnetic radiation has a zero rest mass, while particulate radiation has a finite rest mass. Ultraviolet (UV) light, gamma rays and x-rays are examples of electromagnetic radiation. Particulate radiation, which is also known as corpuscular radiation, includes protons, neutrons, electrons and alpha particles. Of these two types of radiation, the majority of damage to the SCA comes from particulate radiation. [Ref. 2: p. 447]

1. Particulate Radiation

Within the particulate radiation, the vast majority of the damage comes from the electrons and protons. This follows from the fact that electrons and protrons are the most common particles in space. Damage from the neutrons and alpha particles are considered to be negligible. [Ref. 2: p. 446]

The electrons and protons not only possess different energy levels among themselves, but they also propagate at different velocities. The different velocity levels will cause varying degrees of damage, but the main damage comes from the different energy levels. The energy levels for these particles ranges from 0.2 MeV to 1.0 MeV for electrons and 4 MeV to 40 MeV for protons. [Ref. 2: pp. 446-447]

The particulate radiation energy spectrum is modified by certain components on the SCA. This signifies that the amount of radiation damage the solar cells receive is design related. The main components that modify this radiation are the fresnel lens, the coverglass, and the substrate. The SCA designer can choose the type, size, and thickness of these components.

Even though the solar cells are better protected due to the fresnel lenses and the coverglasses, output power of the solar cells may still decrease. Both the fresnel lens and the solar cell coverglass are damaged by this radiation. Radiation damages the coverglass by causing a discolorization or darkening. This will cause more light to be absorbed which not only reduces the amount of light transmitted, but increases the operating temperature of the solar cell. [Ref. 2: p. 447]

The fresnel lens is also subjected to particulate radiation damage. The polymer material discolors under extended radiation exposure. Particulate radiation causes the fresnel lens to becomes brittle over an extended period. This is due to the bonded electrons in the polymeric material which are removed by the radiation.

Other components of the SCA are affected in addition to those mentioned above. These components are the electrical insulation on the wires, terminals, connectors, adhesives and the blocking, shunt and zener diodes [Ref. 2: p. 448]. If the SCA is to be put in an orbit where significant amounts of particulate radiation are present, steps must be taken by the designer to protect its components.

One measure is to harden the components. This will protect them against radiation damage. The price paid for this protection will be an increase in the weight of the SCA and hence, to the overall weight of the spacecraft.

2. Effects of Corpuscular and Ultraviolet Radiation Together

Corpuscular and UV radiation exist simultaneously in most orbits. There is currently two divergent views on the effects that they have on the SCA, more specifically on the fresenl lens and solar cell coverglass. [Ref. 2: p. 448]

One view, which is supported by ground testing, is that the UV radiation will reverse the effects of the darkening of the material. The other view, which is supported by comparing ground-test data with orbital data, states that the combined effects from both radiations cause an increase in darkening rather than a decrease. From these conflicting views, it can be concluded the darkenening mechanism done to the different parts of the SCA is not completely understood [Ref. 2: p 448]. Further research must be conducted in order to get an understanding on what combined effects, if any, that particulate and UV radiation have on the SCA components.

III. THE GALLIUM ARSENIDE SOLAR CONCENTRATOR ARRAY

A. GENERAL

Figure 2 shows a diagram of a fresnel lens module conceptual design of the GaAs solar concentrator array (SCA). As can be seen from this figure, each module will consist of a fresnel lens, upper and lower interconnector, GaAs solar concentrator cell, silicon adhesive, dielectric, and aluminum substrate.

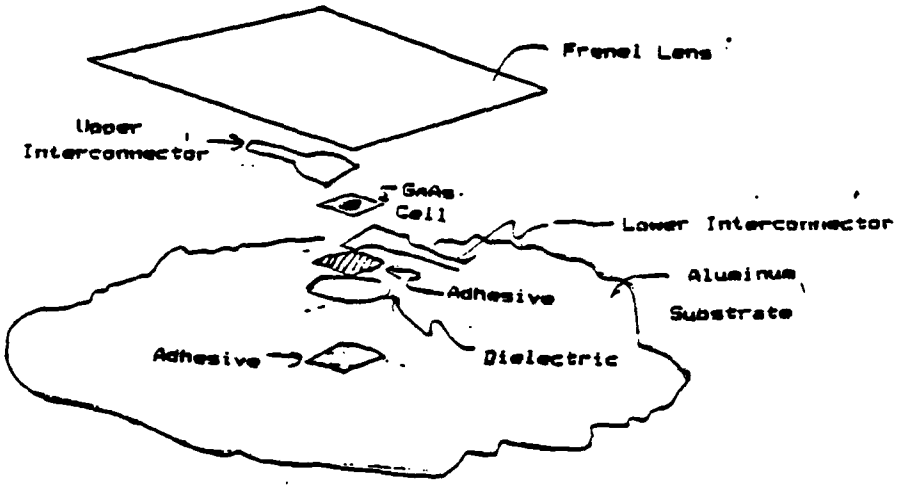

Figure 2. Fresnel Lens Module Conceptual Design

Figure 3 on page 11 shows the complete GaAs SCA. The SCA consists of nine 183X fresnel lenses supported on a 0.232m (9.125") high copper frame. The substrate is a 0.7m by 0.7m aluminum sheet.

The components used in the SCA were selected based on four primary criteria. These criteria are proven reliability in space, availability, cost, and concentration ratio. The concentration ratio of economic interest is between 50X and 200X [Ref. 5: p. 2]. Building the SCA within this concentration ratio range would minimize the total system cost.

The rest of this section contains a detailed discussion on the components used to build the SCA. The first component to be discussed is the fresnel lens.

Figure 3. 183X Fresnel Lens GaAs Solar Concentrator Array.

B. FRESNEL LENS

1. General Discussion

The refractive fresnel lens is the optics of choice over the reflective technology due to many advantages. Some of these advantges are light weight, tolerance to tracking and alignment errors, high efficiency, and ability to be stowed. All of these make it attractive for space use.

The fresnel lens does have some disadvantages. Because the lens is made of a polymeric material, it reacts with monoatomic oxygen particles in low earth orbit. This causes the lens to darken which prevents light from hitting the solar cell. At present, the only solution to this problem is to either making the fresnel lens out of glass or putting a coverglass on the lens [Ref. 4]. Both of these solutions will reduce its light weight advantage. Another disadvantage of the fresnel lens is its vulnerability to reflection loss on its front surface. This, however, can be easily corrected by using an antireflection coating similar to the ones used on solar cells.

2. Fresnel Lens Description

The fresnel lens selected for use is manufactured by the 3M Company at a cost of $200.00 per sheet. The sheet is configured into a parquet of two by seven lenses. Each lens is 8.16" squared, 0.060" in depth, with a lens-to-cell spacing of 9.125". A lens produces a 0.68" diameter area. The reason for the circular area is the prism pattern on the lens is circular. The lens has an optical efficiency of 82% and a concentration ratio of 183X. See Figure 4 for a picture of the fresnel lens.

Figure 4. Fresnel Lens

The fresnel lens consists of an optical grade acrylic material. This polymeric material, however, does not posses the necessary stiffness to prevent the sheet from sagging. This sagging must be corrected, otherwise the concentration ratio will be reduced. The sagging can be corrected by either lamination or by the use of a frame that is designed to support each lens. Lamination is a costly process that will provide the stiffness necessary to prevent sagging. The lamination process consists of adding a thicker, transparent superstrate material to the fresnel lens. Of the two, the frame is the less expensive method, but it will add more weight to the SCA.

The reason for the sagging of the sheet is due to gravity. When the SCA is placed into orbit, the affects of gravity on the sheet will be eliminated. However, since

this SCA is being tested on earth, the frame design method was used. For this particular fresnel lens, the sheet will sag approximately 0.040" [Ref. 6: p. 2].

3. Geometric and Actual Concentration Ratio Calculation

An important parameter of any concentrator is its geometric and actual concentration ratio. The geometric ratio is a ratio of the lens area to spot size area. This assumes 100% transmissivity of sunlight. However, there will be some loss of sunlight due to the imperfections in the lens. The actual concentration ratio accounts for this loss. This is found from the formula

$$C_a = \eta_0 \times C_g \tag{3.1}$$

where C_a is the actual concentration ratio, η_0 is the efficiency of the lens and C_g is the geometric concentration ratio. The geometric concentration ratio is

$$C_g = \frac{A_a}{A_t} \tag{3.2}$$

where A_a is the area of the fresnel lens and A_t is the area of the spot size. The respective areas are

$$A_a = 66.59 \text{ in}^2 \tag{3.3}$$

$$A_t = 0.363 \text{ in}^2 \tag{3.4}$$

Substituting these results into equation (3.2) yields a geomeric ratio of $C_g = 183X$ From the manufactor specification sheet, $\eta_0 = 82\%$ substituting these values into equation (3.1) yields an actual concentration ratio of 150X.

C. THE SOLAR CELLS

1. General Discussion

The next component used in the SCA is also the most important. It is the solar cell. There are many types of solar cells in use today. Each type has been classified according to certain criteria. The criteria for a solar cell used in a solar concentrator array are the cell must be optimized for the high intensity sunlight, be able to withstand high temperatures, and have a low internal resistance. The type of solar cell that meets this criteria is the high intensity or concentrator cell.

Solar concentrator cells are made up of two different semiconductor materials--silicon and GaAs. Of the two, GaAs is by far the superior material. However, before

going into the advantages of GaAs over silicon, it is necessary to have an understanding of how the solar cell operates and what electrical characteristics or parameters are used to judge its performance.

2. Solar Cell Operation

a. General

This section will present a brief discussion of solar cell operations. A detailed discussion of the construction and operating characteristics is contained in the Solar Cell Radiation Handbook [Ref. 7].

b. Electric Current

When sunlight hits the solar cell, three things can happen. The sunlight passes through the cell, it is reflected or it is absorbed by the cell. The solar cell can only produce an electrical current from absorbed sunlight. This can only happen if the sunlight hits an electron in the valence band with enough energy to cause an electron to be moved to the conduction band. When this happens, an electron-hole pair is generated.

In the conduction band, the electron is free to roam from one atom to the next. If there is no external mechanism present, the electrons will eventually lose their energy by collision and return to their valence position. The mechanism used to prevent this is the potential barrier formed at the p-n (or n-p) junction of the semiconductor material.

The potential barrier prevents the electron-hole recombination by sweeping electrons to the front surface and holes to rear surface or vice versa depending on the type of material used. At the front surface, the electrons will reach the cell contacts and is then delivered to an external electrical load.

The process of creating an electrical current in a solar concentrator cell is basically the same as in the conventional cell. Due to the high intensity light and high temperature the cell will receive in an SCA there are some differences to its design. The differences are pointed out throught this section.

c. Effects of Increasing the Concentration Ratio.

The whole purpose of a solar concentrator is to increase the sunlight intensity falling on the solar cell. By increasing the intensity, the cell's maximum power output and efficiency of will be increased. An increase in efficiency means a decrease in the number of solar cells used to power a spacecraft. On the other hand, using the same amount of solar cells, the power output of the solar array would increase. This means better, more complex missions can be performed by the spacecraft without increasing its size. Either way, this represents a substantial cost savings in accomplishing the mission.

The increased sunlight intensity causes more electron-hole pair generation which in turn increases the short-circuit current and increases, though not as much, the open-circuit voltage. These increases produce an increase in the maximum power output and solar cell efficiency.

Figure 5 shows an I-V curve[1] of a solar cell under three different illumination levels. Notice that the increase in the maximum power output in mainly from the increase in the short-circuit current.

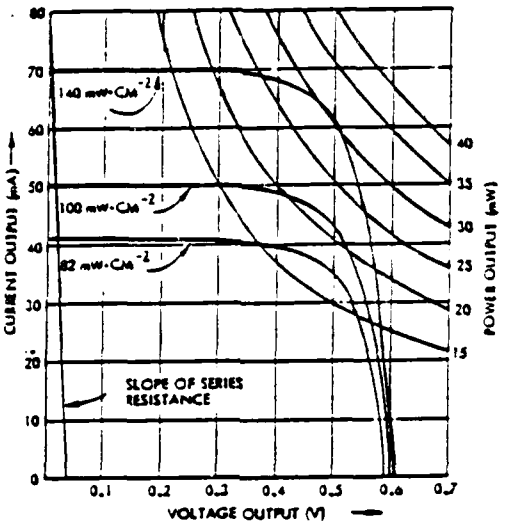

Figure 5. I-V Curve of Solar Cell at Three Different Illumination Levels [Ref. 2: p. 173]

Sunlight intensity on the SCA depends on other parameters besides the concentration ratio. These are the angle of incident of the sunlight to the SCA, the distance from the sun to the SCA, the transmission loss of light through the fresnel lens, the solar cell coverglass, cover adhesives, and solar eclipse. Each one of these must be taken into account by the SCA designer. Some of these parameters, such as solar eclipses and angle of incidence, will depend on the particular mission of the spacecraft. [Ref. 2 p. 172]

d. Effects of Temperature on the Solar Cell

In the above discussion, the solar cell operating temperature was assumed to be held at a constant temperature. In actuality, if the intensity is increased, the cell's efficiency and power output will decrease. Figure 6 on page 16 shows an I-V curve of

---

1 I-V curves are discussed in Electrical Characteristics Section in this Chapter.

the same solar cell at different operating temperatures. Notice that in both sets of curves, the efficiency of the solar cell decreases as the cell temperature increases. This decrease in cell efficiency comes predominently from the decrease in the open-circuit voltage of the solar cell.

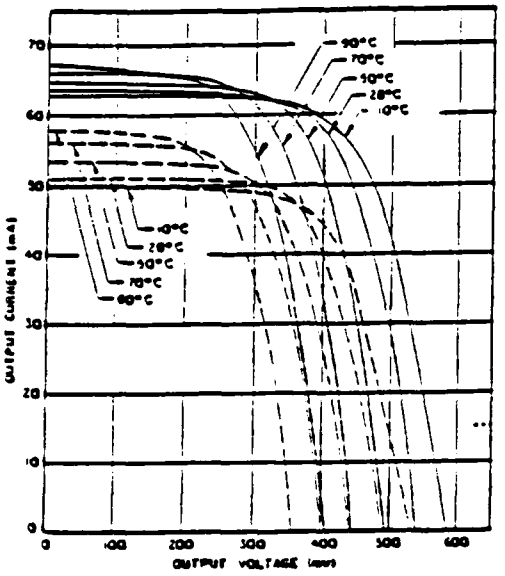

Figure 6. Variation of I-V Curves At Different Operating Temperature [Ref. 2: p. 173]

The change in the voltage is due to the change in the diode construction characteristics of the solar cell. As the temperature increases, the entire I-V curve translates at approximately 2.2 to 2.3 mV/°C towards the lower voltage. [Ref. 2: p. 173]

For the solar concentrator array, the solar cell operating temperature will be increased significantly due to the substantial increase in sunlight intensity. Steps must be taken to maintain the solar concentrator cell within its optimum temperature limits. These steps are discussed in Chapter IV.

3. Electrical Characteristics

a. I-V Curve

The current-voltage characteristic or I-V curve is used to describe the solar cell's electrical characteristics. From the I-V curve, one can obtain all the information needed to satisfactorily judge the solar cell's performance. Useful information obtained from the curve is the short-circuit current, I_{sc}, open-circuit voltage, V_{oc}, the maximum power, P_{max}. With this information, the solar cell's efficiency, fill factor (FF), optimum

load resistance, R_{Lopt}, maximum current, I_{max}, and maximum voltage, V_{max} can either be read directly from the curve or calculated.

Figure 7 shows a typical I-V curve for a solar cell. I_{sc} , I_{max}, V_{oc}, V_{max} , and P_{max} are read directly from the curve. The maximum power point corresponds to the maximum conversion efficiency, η_{max}, of the solar cell. This is represented by the shaded area in the figure. This signifies the largest rectangle that can be placed within the curve. By drawing a straight line from the origin through P_{max}, the optimum load resistance, R_{Lopt}, is obtained.

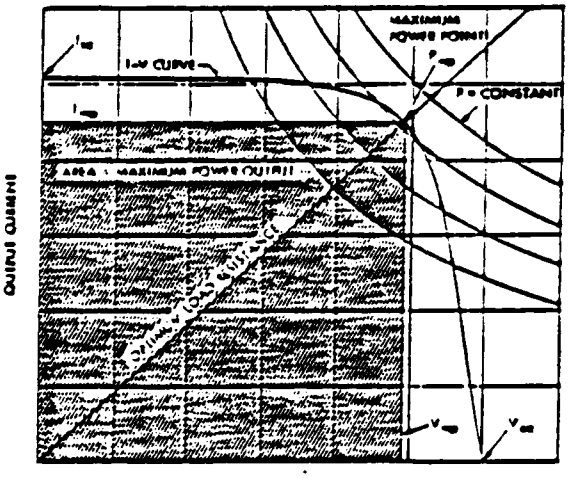

Figure 7. I-V Curve [Ref. 2: p. 167]

b. Fill Factor.

The fill factor, FF, is a term that describes the "squareness" of the I-V curve. The squarer the curve, the higher the maximum power output and the higher the conversion efficiency of the solar cell. The FF is defined by this equation

$$FF = \frac{V_{max} \times I_{max}}{V_{oc} \times I_{sc}} = \frac{P_{max}}{V_{oc} \times I_{sc}} \tag{3.5}$$

Note that since V_{max} and I_{max} are always less than or equal to V_{oc} and I_{sc} ,the fill factor is always less than or equal to one.

The fill factor is used to compare different solar cells under the same operating conditions. However, it can be misleading when it is used to determine changes in the cell's I-V curve shape due to environmental degradation. It can be shown that when

the solar cell operating temperature or illumination intensity is varied over a range in which the I-V curve shape does not change, the calculated value of the fill factor will change. [Ref. 2: p. 171]

c. Solar Cell Efficiency

As mentioned earlier, the solar cell efficiency can be obtained from the I-V curve. It is also found from the equation

$$\eta = \frac{P_{out}}{P_{in}} = \frac{P_{out}}{p_{in} \times A_c} \tag{3.6}$$

where P_{out} is the electrical power output of the solar cell, P_{in}, is the energy input to the solar cell, p_{in} is the solar illumination level per unit area and A_c is the active area of the solar cell. In the case of the solar concentrator, P_{in} is the solar constant, S_0, multiplied by the actual concentration ratio, C_a, or

$$P_{in} = C_a \times S_0 \tag{3.7}$$

where S_0 is equal to 1353 W/m^2. A solar cell operates at its maximum efficiency, η_{max}, when the its maximum power output capability is utilized by an optimized load at a particular illumination intensity and cell operating temperature. [Ref. 2: p. 171]

The maximum solar cell conversion efficiency depends on several different aspects of the solar cell. These are the solar cell internal construction, active area, specific material properties, photovoltaic junction characteristics, anti-reflective coating, surface texture, contact and grid configuration, illumination levels, cell operating temperature, particulate irradiation damage, and temperature cycling.

Figure 8 on page 19 shows the theoretical efficiency of different types of semiconductor materials used in solar cells. Notice that a GaAs solar cell has a higher efficiency than silicon.

d. Series Resistance

The series resistance is a measure of the cell's discipative internal electrical losses and is observed from the cell's terminal behavior. This resistance is a lumped parameter consisting of the resistance from the semiconductor material of the cell, its ohmic contacts, the semiconductor/contact interface, and the diffused layer. [Ref. 2: p. 169]

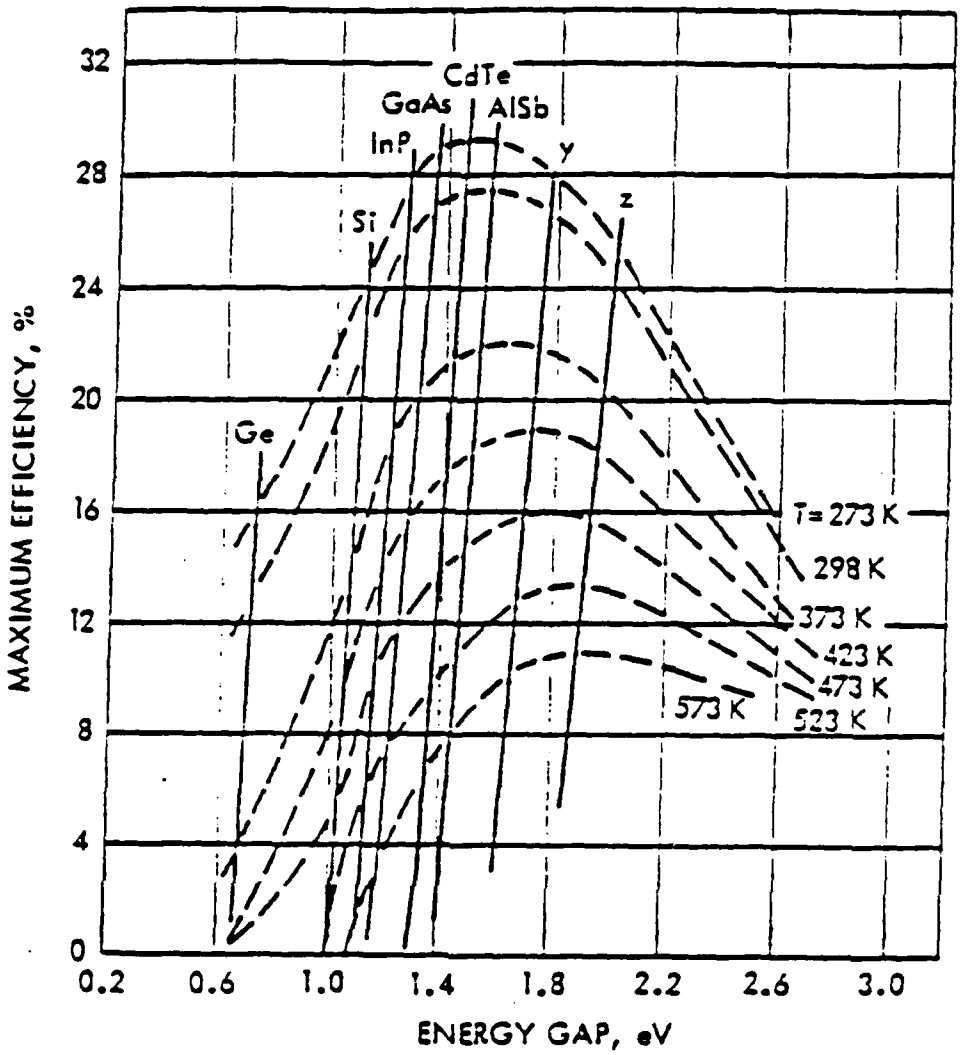

Figure 8. **Theoretical Solar Cell Efficiencies** [Ref. 7: p. 1-32]

Variation in the series resistance will cause changes in the solar cell's power output. Environmental conditions such as changing temperature, illumination levels, and radiation damage will cause this resistance to vary significantly

As can be seen from Figure 9 on page 20, an increase in the series resistance will cause a decrease in the output power of the solar cell. It is important that this resistance be reduced in the solar cell. One way is by decreasing the solar cell's temperature. Another way is by reducing the amount of radiation the solar cell receives. This was clearly shown in Figure 6 on page 16 where the set of dashed I-V curves is for the same solar cell after it was irradiated.

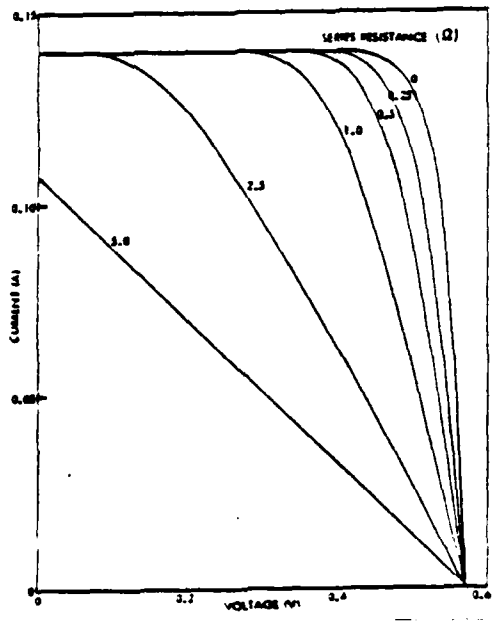

Figure 9. Series Resistance [Ref. 2: p. 170]

In a solar concentrator cell, the largest contribution to the series resistance comes from the diffusion layer and contact resistances. This is particularly true at high intensities. To reduce this resistance, the solar concentrator cell uses a denser gridline pattern that is optimized to reduce the series resistance at a specific operating temperature and concentration ratio. [Ref. 2: p. 178]

Figure 10 on page 21 shows an I-V curve of two different solar cells at the same high intensity and temperature. One solar cell has thirteen gridlines (solid line) the other has five (dashed line). Notice that the solar cell with the higher gridline density has the squarer I-V curve, even at the higher temperature, than the less dense gridline cell.

e. Shunt Resistance

Another resistance that is important to the solar cell's maximum output power is the shunt resistance, R_{SH}. A portion of the electrical energy is lost due to internal leakage. There are three shunt resistance paths that exist in a solar cell. They are the recombination current at the p-n junction, along the outer cell edge (surface leakage), and through n-contact metalization shunting junction at micorscopic flaws. An example of a flaw is surface scratches. [Ref. 2 : p. 170]

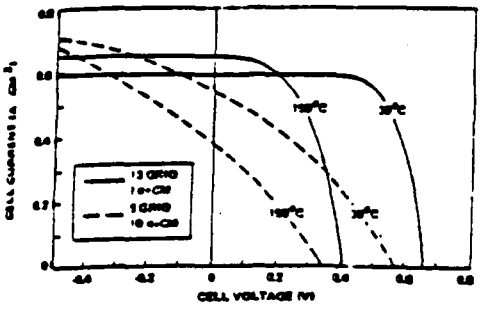

Figure 10. I-V Curves of Two Different Grideline Density Solar Cells at High Intensity [Ref. 2: p. 179]

As can be seen in Figure 11 on page 22, by increasing the shunt resistance, the output power is increased. Lowering it, however, would significantly reduce the cell's output power.

4. Gallium Arsenide vs Silicon Solar Cells

The GaAs solar cell is the superior cell compared with silicon. GaAs cells have now equalled or surpassed the best silicon cells in terms of efficiency, radiation resistance, annealibility, and operating temperature.

Referring back to Figure 8 on page 19, GaAs has a 28% theoretical efficiency at 0°C, compared to a 25% theoretical efficiency of silicon. Moreover, as the operating temperature of the solar cell increases, the silicon cell's efficiency drops more rapidly than GaAs. This drop in efficiency is even more evident when comparing the two cells' power output. Silicon has a power loss of approximately 0.45% per degree Celsius while GaAs has a power loss of 0.22% per degree Celsius [Ref. 1: p. 110]. In addition, GaAs has the ability to self-anneal at temperatures greater than 100°C [Ref. 1: p. 110]. From the above reasons, GaAs solar cells are more suitable for use in solar concentrators.

Another reason for GaAs superiority over silicon is GaAs has a wider bandgap (1.4eV) between the valence band and conduction band than silicon (1.1eV) [Ref. 1: p. 110]. This energy bandgap nearly coincides with the peak efficiency of the solar spectrum. This means more electron-hole pair generation.

GaAs has not only demonstrated higher radiation resistance than silicon to electrons and protons, but also to X-rays and gamma rays. This makes GaAs extremely attractive for use in space. [Ref. 1: p. 111]

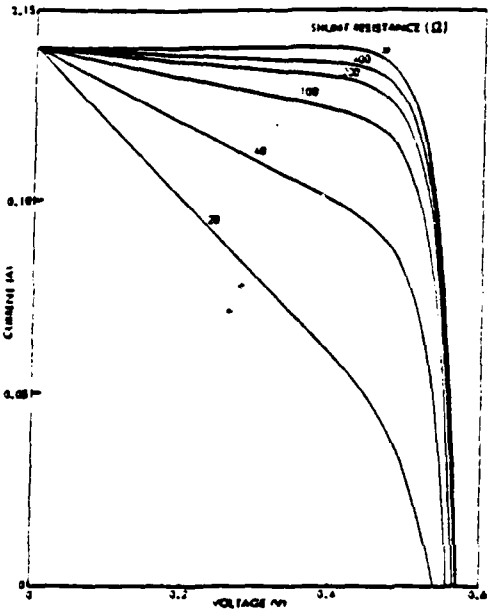

Figure 11. Effect of Shunt Resistance on I-V Curve [Ref. 2: p. 170]

GaAs does have some disadvantages. The main disadvantages are its high production cost, limited production, and higher mass ratio. The problem with production cost and quantity is being reduced as new and better production techniques are being used. The higher mass ratio is offset by the fact that less solar cells are needed for the same amount of power.

5. Solar Cells Chosen for the SCA

Because of the above reasons, GaAs cells were the logical choice for this SCA. Twelve GaAs solar cells used were purchased from Applied Solar Energy Corporation (ASEC). Nine of these cells will be used in the SCA. The three extra cells were purchased for backup reasons in case three of the nine solar cells fail. The GaAs solar cells have a 4mm diameter active area. At AM0 cell efficiency is 16% or greater. It is designed such that its optimum temperature is around 80°C and has an approximate 1.0 volt output. The nine solar cells will be placed in a three-by-three array. There will be three solar cell strings in parallel, with three solar cells per string.

D. INTERCONNECTORS

1. General

The purpose of the interconnector is to conduct electrical power from the individual solar cell to the load. This must be accomplished throughout the lifetime of the

spacecraft. To accomplish this task, the interconnectors must meet certain physical, environmental and electrical requirements. [Ref. 3: p. 5.2-1]

For the physical requirements, the interconnectors must be light weight and posses the ability to be rolled, folded or bent. This is important especially when the SCA must produce a high voltage. Many SCAs have several of solar cells in a string. The strings are usually longer than the length of the module and must be doubled back. Because of these size constraints, the cells will be packed side-by-side.

Other physical properties of importance for the interconnector are that they must be nonmagnetic, manufacturable, flexible, and repairable. The interconnector must be able to withstand the terristrial, launch, space, and radiation environment mentioned in Chapter II.

The main concerns for the interconnectors' electrical requirements are that they remain electrically continuous and posses adequate conductivity. Any break in the interconnectors would prevent the currents and voltages generated by the strings from getting to the load. The lower the conductivity means higher resistance and a larger power loss. This power loss is due mostly to the dissipation of heat.

2. Interconnector Failure

One of the major failures with the interconnectors comes from the stresses in the joints and loops. These are caused by temperature variations and external forces. Temperature variations cause the different materials to expand. The problem is they expand at different lengths. To reduce the stress problem, the materials must be choosen to have closely matched linear expansion coefficients. If imbedded interconnectors are used instead of solder joints, they may fail if the strength of the surrounding material becomes greater than the strength of the interconnector.

Figure 12 on page 24 shows the number of temperature cycles for various spacecraft missions. Notice that for near earth orbits the number of temperatures cycles is anywhere from 5,000 to 50,000 cycles with a temperature range from $-70°C$ to $110°C$.

To reduce the thermal stresses, alternate interconnector configuration and materials have been developed. These configuration use new interconnector techniques such as parallel resistance welding, ultrasonic bonding and thermal compression bonding. New interconnector materials such as silver-plated molybdenum and silver-plated Invar have been used. The advantage of using this material is that these interconnectors do not require an intermediate layer like solder. [Ref. 8 : p. 341]

Mission	Life (years)	Number of Cycles	Temperature Limits (°C)	
			Low	High
Near-earth orbits: scientific, manned or unmanned	1 to 3	5000 to 50,000	0 to -70	70 to 110
Synchronous earth orbits: communications	1 to 10	100 to 700	-80 to -180	0 to 80
Interplanetary probes				
Inbound	1 to 3	<5	-100	175
Outbound	1 to 3	<5	-190	90
Lunar surface, stationary	1 to 2	<25	-180	130

Figure 12. Temperature Cycling for Various Spacecraft Missions [Ref. 3: p. 5.2-1]

3. Interconnector Type and Selection

a. Types

There are two basic types of solar cell interconntectors. One type is the mesh, the other is a formed strips. The formed strip is further broken down into coplanar or in-plane loops and out-of-plane loops. The easiest to handle is the out-of-plane loop. It deforms by bending. It is this deformation that helps alleviate stress. Figure 13 shows a typical out-of-plane loop.

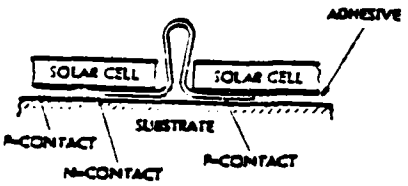

Figure 13. Out-of-Plane Loop Interconnector [Ref. 3: p. 5.3-9]

b. Selection

The selection of the material and interconnector configuration used should be done so that they will reduce the stress in the solar cell interconnector joints and the interconnector expansion loops to a permissible value. Because this SCA is only a small module that will not go through 5,000 temperature cycles, this was not a major concern. All that was necessary to consider was the material that had the best conductivity and was readily available. This was solved by simply using 30 AWG wire. It has a high conductivity and can be soldered or welded to the solar cell. Out-of-plane loops were added to reduce any possible stress due to material expansion.

E. ADHESIVE AND SOLDER

1. Adhesive

There are two basic types of adhesives. The first type is the silicon rubber adhesive or better known as RTV (room temperature vulcanization). It is used to bond the solar cell to the the dielectric, the dielectric to the substrate, and the coverglass to the solar cell. There are two generic types of RTV adhesives. They are meythl-phenyl silicon and dimethyl silicon. Of the two, the dimethyl silicon is superior RTV. Figure 14 on page 26 gives a list of commonly used adhesives. The clear or transparent adhesives, such as CW-93-500, is used to bond the coverglass to the solar cell. The nontransparent adhesive, such as RTV-566, are used to bond the solar cell to the dielectric and the dielectric to the substrate.

The second type of adhesive is the conducting adhesive. It is used to electrically attach the solar cell to the interconnector and circuitry during array repairs. In addition this adhesive can be used to insure a reliable electrical connection has been made between ground straps and metallic surfaces. It is important to note that this adhesive serves only as a conductive medium, not as a bonding element. Additional structural elements must be used to provide the bonding for those connections.

There are a number of properties an adhesive must have if it is to be used to bond solar cells to the dielectric or substrate. First and most important, it must have a high thermal conductivity to pass the majority of heat from the solar cell to the substrate. Secondly, the adhesive must have low outgassing because of the environmental problems discussed in Chapter II. Thirdly, the thermophysical and mechanical properties of the adhesive must be compatable with the solar cells and the substrate used. Otherwise over a period of time the adhesive will crack and eventually fail due to the high number of temperature cycling it will go through. Fourth, the adhesive must be repairable during the fabrication process. Finally, the adhesive must have adequate strength. It must be able to resist vibrational forces and thermally induced stresses that it will go through during the spacecraft's lifetime. [Ref. 2: p. 464]

2. Adhesive Selected For Use

The adhesives listed in Figure 14 on page 26 are very expensive. Since this SCA will not be subject to the harsh space and radiation environments, the properties needed by an adhesive can be relaxed. The only necessary property for the adhesive used on this SCA is that it has a high thermal conductivity. This property is found in any inexpensive heat sink compound purchase at any local store.

Material	Manufacturer	Color	Density ($g \cdot cm^{-3}$)
6-1104	Dow Corning	White, translucent	1.12
93-500	Dow Corning	Clear	1.08
RTV-40	General Electric	White	1.35
RTV-41	General Electric	White	1.31
RTV-118	General Electric	Clear	1.04
RTV-511	General Electric	White	1.20
RTV-560	General Electric	Red	1.42
RTV-566	General Electric	Red	1.51
RTV-567	General Electric	Clear	1.00
RTV-577	General Electric	White	1.35
RTV-580	General Electric	Red	1.49
RTV-602	General Electric	Clear	0.995
Silastic 182	Dow Corning	Clear	1.05
Silastic 184	Dow Corning	Clear	1.08
R6-3488	Dow Corning	Clear	1.05
R6-3489	Dow Corning	Clear	1.02

Figure 14. **Commonly Used Adhesives.** [Ref 2: p. 468]

The heat sink adhesive selected is a silicon type Z9 manufactured by GC Electronics. It has a high thermal conductivity and it is used as a heat sink bond in electronic equipment. It is important to note that the adhesive, if it had been used, must be applied as thinly as possible. The thinner adhesive will help keep the temperature gradient small so that a larger amount of heat can be transfered from the solar cell to the dielectric or the substrate.

The heat sink will be used on this SCA to bond the solar cell to the dielectric and the dielectric to the substrate. Bonding the solar cell to the interconnector is the subject of the next subsection.

3. Solder

There is another method that can be used to bond a solar cell to the dielectic and a dilectric to the substrate besides adhesive. This method is to solder these components together. Solder, however, is mainly used to bond the interconnectors to the solar cells. In fact, most solar cells have been bonded to their interconnectors by this method. There are, however, some limitations to the use of solder. Solder, first of all, has a lower strength at higher temperatures. Solder will have zero strength at 170°C. It has a problem with its fatigue life in that it will fracture and crack much sooner than adhesive. This problem is even more compounded if the spacecraft is in low earth orbit. As mentioned earlier, the spacecraft will go through a large number of temperature cycles. It also has a problem with creep in that it will cause an open-circuit failure at temperatures in excess of 100°C. [Ref. 2: p. 271]

An option to soldering is welding. However, there are many things that have not been resolved as to which is the better method, especially whether soldered or welded joints will exhibit the longer temperature cycling fatigue life [Ref. 2: p. 273].

F. DIELECTRIC

Dielectrics are used to insulate wires and the rear contact of the solar cells from the metal substrate. All dielectrics are not perfect insulators in that they have some leakage current associated with them. This is due to the imperfection of the material, such as pin holes, and due to moisture absorbed by material. [Ref. 2: p. 493]

The important parameters of the dielectic are its voltage breakdown characteristics, its leakage through the material and its leakage resistance of the material. It turns out that the higher the voltage breakdown and leakage resistance, the lower the leakage current will be. The lower the leakage current, the better the dielectric material.

The voltage breakdown is directly related to the dielectric strength. In general, the dielectric strength, hence the voltage breakdown, will increase with decreasing material thickness, but it will also decrease with increasing time during which the electrical stress is applied. Increasing the thickness will increase the leakage resistance but will also increase the weight to the SCA unnecessarily and the voltage breakdown will not be increased by much as will will be seen later.

A solution to this problem can be seen from the equation of resistivity. Namely,

$$R_L = \rho \frac{t}{A} \tag{3.8}$$

where ρ the volume resistivity of the dielectric, t is the sheet thickness, and A is the area of the dielectric covered with solar cells and other non-insulated conductors. By increasing the volume resistivity and decreasing the area, the leakage resistance will be increased. This will increase the voltage breakdown too.

With this information, it became easy to select a good dielectric for this SCA. Figure 15 and Figure 16 shows the volume resistivity and dielectric strength vs temperature of Kapton, respectively. From Figure 16 going to a thinner material, 1 mil instead of 5 mil, the dielectric strength is increased significantly. Notice in Figure 15 that the lower the operating temperature the higher the volume resistivity. Kapton has a proven and reliable track record for space use and was readily available for use. It does not melt at high temperatures. Kapton has a high cut-through resistance and creep strength at higher temperatures. [Ref. 2: p. 465]

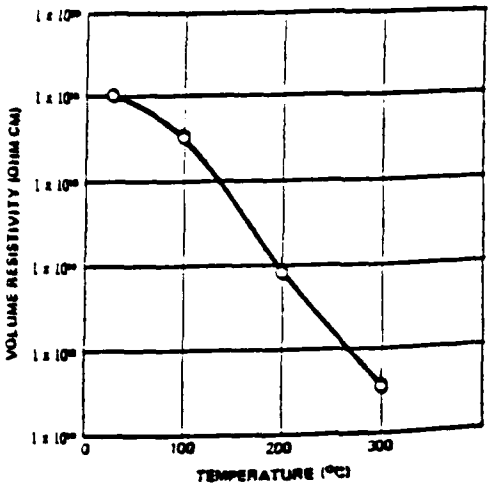

Figure 15. Volume Resistivity of Kapton [Ref. 2: p. 496]

G. SUBSTRATE

The next item in the SCA is the substrate. By definition, the substrate is the structural element that mechanically supports and holds in place the solar cells, interconnectors and associating wiring [Ref 2: p. 314]. In an SCA, it must also function as a radiator to dissipate the excessive heat from the solar cells.

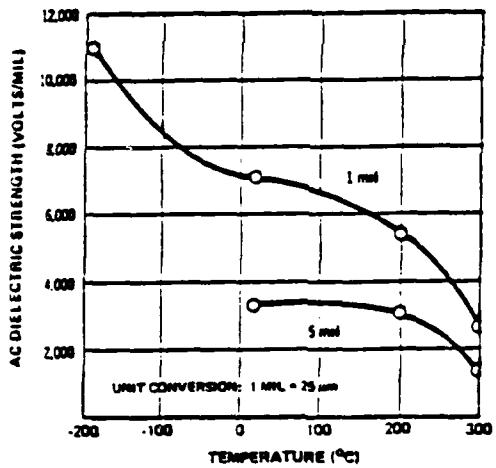

Figure 16. Dielectric Strength of Kapton [Ref. 2: p. 496]

The substrate design and material will be a factor affected by the size of the array. The larger the substrate area, the more solar cells can be placed in the array. Likewise,

the larger the substrate area, the larger the emitting area. This will help reduce the solar cell operating temperatures.

In addition to the area of the substrate, the thickness of the substrate will have an impact on the operating temperature. It turns out that the cell temperature will decrease as the substrate thickness is increased [Ref. 5: p. 3]. Figure 17 shows a graph of a fin substrate vs cell temperature. As the thickness of the fin is increased the temperature is decreased. Even though this is a graph of a circular substrate vs temperature, the same conclusions can be drawn from a square substrate.

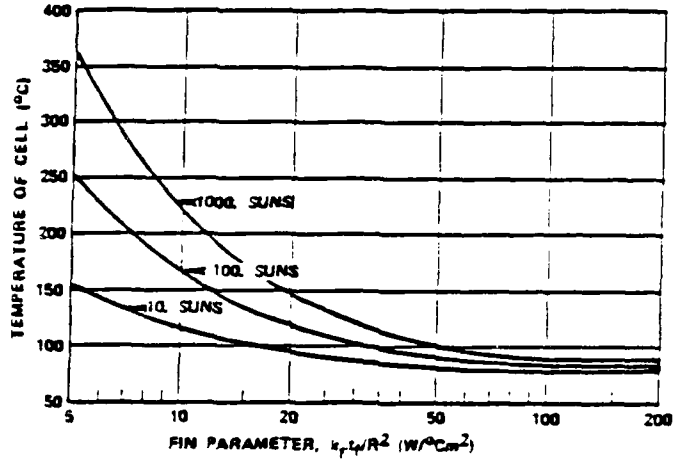

Figure 17. Cell Temperature as a Function of Fin Parameter and Solar Intensity [Ref. 5: p. 3]

The substrate material most used is solar arrays, both concentrator and nonconcentrator, is aluminum [Ref. 2: pp. 332-341]. Aluminum has a high thermal coefficient and a low mass compared with most metals. For a flexible solar array, Kapton or FEP Teflon are used. These materials have excellent creasing and folding characteristics.

The substrate used in this SCA is aluminum (type 1100) because of the information pointed out in the previous paragraphs. The dimension of the substrate is 0.7m by 0.7m with a sheet thickness of 1.59 mm. The thickness was chosen based on the availability of the aluminum sheet. The thickness is larger than actually needed. However, as a general rule, the thinner the substrate the greater the temperature extremes and the less the radiation output [Ref. 3: p. 6.1-2]. Chapter IV goes into a greater detail on design of the substrate.

H. DIODES

The last item in the SCA is the diode. There are three major uses for them in an SCA. These are for blocking, shunting and voltage regulation.

1. Blocking Diode

Blocking diodes are used to isolate solar cell strings such that they will permit the flow of current from the string to the power bus, but will prevent or block the current going from the bus bar to the string whenever the string voltage is lower than the power bus. These diodes prevent the solar cell string from becoming a current sink that takes away power, from the load. Blocking diodes can also be used for fault isolation.

Solar cell strings can have a lower voltage than the power bus for many reasons. One of which is when the solar cell or a string of cells become nonilluminated due to shadowing, or a solar eclipse. Another reason is a solar cell in a string could become defective or have a reduced power output due to absorbing more radiation than the surrounding cells.

A problem with using blocking diodes is that they cause a voltage drop of around 0.7V. This means that the power output from the string will drop. A decision must be made on the number of blocking diodes needed versus the amount of power loss one is willing to accept from the SCA. Figure 18 on page 31 shows four possible locations for blocking diodes. The circled areas show potential electrical failure.

2. Shunt Diode

Shunt diode is also known as a bypass diode. Its purposes are to minimize output losses and to protect the solar cells. It will permit the flow of electrical current in a solar cell string when one or more cells in that string become shadowed, fractured or failed in an open-circuit mode. The shunt diode is placed in parallel with the solar cell string such that when the cells are illuminated the shunt diode is in reverse bias. The shunt diode will become forward bias when one of the aforementioned problems happen. Figure 19 on page 31 shows conventional rectifier type diodes used as shunt diodes. [Ref 2: p. 300]

3. Zener Diode

The Zener diode is used to limit the maximum voltage that can develop across a string of solar cells. The Zener diode will only conduct when the string voltage exceeds the breakdown voltage of the diode. The use of Zener diodes will insure that a string of solar cells will not cause other strings in parallel to be reversed bias.

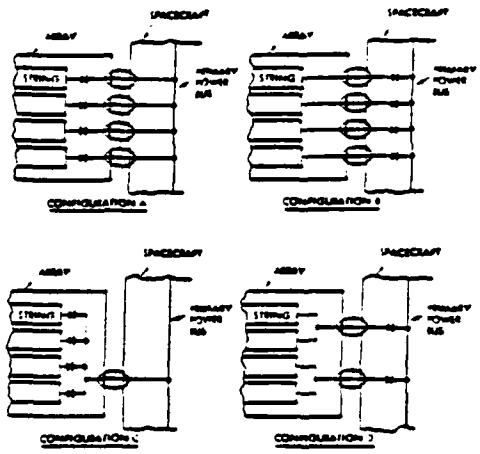

Figure 18. Possible Blocking Diode Locations [Ref 2: p. 298]

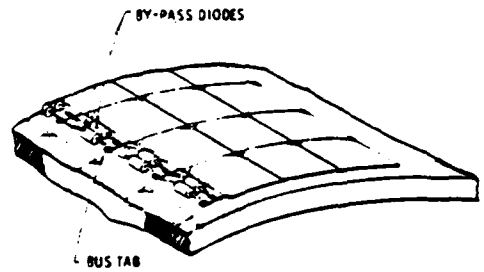

Figure 19. Shunt Diode [Ref. 2: p. 300]

4. Diode Usage On This SCA

All three diodes mentioned above would be used on any SCA. Quantities to be used and their location would be based on trade offs between how much energy loss one is willing to accept.

GaAs solar cells have a problem that they are easier to be damaged under reverse bias conditions than silicon. However, this requires at least five or more volts to do so. Since this SCA is actually only a small part of a larger array, all three types of diodes are not needed and therefore will not be used. If this SCA was a little larger, some, possible all three, would have to be used.

IV. THERMAL DESIGN AND ANALYSIS OF THE SCA

A. GENERAL

As mentioned in Chapter III, the cell's efficiency and power output is strongly dependent on its temperature. Solar cell have operating temperature limits between −160°C and 80°C [Ref. 8: p. 266]. The maximum and the minimum operating temperature of the cell is determined by the design and manufacturing process. As long as the cell temperature does not go above its temperature limits, the solar cell will not lose its efficiency. For example, the GaAs solar concentrator cell used for this SCA has a design maximum operating temperature of 80°C [Ref. 9]

The solar cell's operating temperature is largely affected by the intensity of sunlight incident on it. As the intensity is increased, such as the case for the SCA, the cell operating temperature will rise. This is because the solar cell converts ten to twenty percent of the incident sunlight. This means the remaining 80 to 90 percent of the unreflected light is converted into heat. If this heat is not dissipated, the cell's temperature will continue to increase. Eventually, it will reach a point where the power output will start to decrease, reducing the cell's efficiency. This was shown in Figure 6 on page 16. For a SCA, the cell temperature will rise well beyond this point causing permanent damage to the solar cell. For example, the operating temperature of the GaAs solar cell in this SCA would be 859.9°C if no thermal design was used.[2] At this temperature, not only the solder used in bonding the solar cells to the interconnectors would be affected, but the cell's contacts and gridlines would have also melted. Thermal design is a critical part of the overall SCA's design process.

B. THERMAL DESIGN

1. General

The objective of thermal design is to provide the proper heat transfer between all of the array components so that the solar cells will remain within their design operating temperature limits during all mission environmental conditions. To meet this objective, the thermal design of the SCA must be concerned with the following [Ref. 3: p. 8.5-1]:

---

2 This temperature was calculated by using equation 4.1 with cell's front and back area, A_F and A_B respectively, equal to each other and the emissivity of the cell's back area ε_B, equal to 0.88. All othervalues used were as stated in Section C of this chapter.

- Solar cell operating temperature control.
- Thermal control surface design.
- Thermal gradients in structure elements.
- Local high temperature (hot spots).
- High temperature operation.

Solar cell operating temperature control is strongly influenced by the thermal control surface design and the thermal gradient in the structure elements. This is because heat transfer in a SCA in space is achieved by conduction and radiation modes. The heat in the solar cells will be transferred via conductive heat-transfer paths to the array's external surface. There the heat is radiated into space.

The analysis of local high temperature (hot spots) and high temperature operation on the SCA is normally carried out by thermodynamic and heat specialists [Ref. :ref refid=rbach2.: p. 8.5-1]. This analysis is accomplished by using thermal analysis computer programs that calculate the temperature throughout all parts of the array. The last section in this chapter briefly discusses the results of a thermal analysis (thermal analyzers) of this array.

2. Thermal Control Techniques

Temperature control of the solar cells is accomplished by using two types of thermal control techniques. These types are active thermal control and passive thermal control.

Active thermal control is used on a SCA when there is a great variation to surface thermo-optical properties due to space degradation, large solar flux variation during the mission, and when the extra mass required by passive thermal control becomes too inefficient. Examples of active thermal control elements that can be used on an SCA are heat pipes, louvers, and electrical heaters. [Ref. 8: p. 298]

Passive thermal control maintains the solar cell temperature to within the desired temperature range by the control of the conductive and radiative heat paths through different geometric configuration and different thermo-optical properties of SCA's exterior surface. In-orbit, cell operating temperatures of approximately 80°C and lower are achievable by purely passive thermal control techniques [Ref. 5: p. 1]. Passive thermal control techniques for a SCA include thermal coating, heat sinks, and phase-change materials.

For a SCA in an earth orbit, passive thermal control is more cost efficient than active thermal control. Passive thermal control has the advantage of not requiring any

moving parts, moving fluids, or electrical power input where the active thermal control elements do. For these reasons, passive thermal control techniques were used to provide the solar cell temperature control on this SCA.

3. Temperature Control

As was pointed out in Chapter II, most SCAs in a low earth orbit (LEO) will be eclipsed by the earth during each orbital period. This causes a large temperature range on the solar cells which will increase the chances of a cell failure. It is important that the temperature of the cells coming out of a solar eclipse be close to the cells' operating temperature when illuminated. The best approach in achieving this comes from the thermal control surface design. More specifically, the SCA's average solar absorptance must first be lowered, then, if necessary, its heat emissions must be increased.

The average effective solar absorptance, $\bar{\alpha}_s$, of the SCA can be lowered by any one or a combination of the following [Ref. 2 : p. 134]:

- Put spectrally selective reflecting filters on the solar cell coverglass and or fresnel lens.
- Minimize darkening of the fresnel lens, solar cell coverglass, and cover adhesive at the end-of-mission life.
- Cover all or partial array areas not covered by solar cells with a highly reflective material.
- Maximize the end-of-mission solar cell energy conversion operating efficiency, η_{op}.
- Reduce the absorption area.

Improving the heat emission is achieved by increasing the average emittance, $\bar{\varepsilon}$, of the SCA. The average emittance is increased by any one or combination of the following [Ref. 3: p. 8.5-2]:

- Increase the solar cell cover emittance.
- Cover all array areas not covered by solar cells with a highly emitting, but also reflecting material.
- Cover the SCA's back side with highly emitting material such as white or black paint.
- Increase the emitting area.

The degree to which the improvements given in the foregoing two lists are accomplished depends on the desired cell operating temperature. For example, a SCA that uses solar with a higher operating temperature would not have to reduce the absorption area as much as a SCA using cells with a lower operating temperature.

4. The Thermal Design Used for This SCA

A decrease in the average solar absorptance, $\bar{\alpha}_s$, was accomplished by reducing the SCA's absorption area. According to Dr. Dennis Flood of the NASA Lewis Research Center in Cleveland, Ohio, the front area is where the concentrated light physically touches the array [Ref. 10]. This means that the SCA's absorption area has some initial reduction due to its inherent design. It turns out, in this case, further reduction is still required.

Each fresnel lens has a spot diameter of 0.68" (17.2 mm) which produces a 2.34×10^{-4} m² area. The parts of the SCA that fall within this area besides the solar cell are the solder, interconnector, dielectric (Kapton) and part of the aluminum substrate. The solder and interconnector areas are negligible and can be discarded. On the other hand, the part of the aluminum substrate and the Kapton will influence the average solar absorptance. The aluminum substrate was eliminated by reducing the spot area by 25 percent to 1.757×10^{-4}m². This was accomplished by placing a highly reflective tape on the aluminum substrate that fell within the concentrated light. Kapton's solar absorptance is approximately equal to the gallium arsenide solar cell used. Gallium arsenide solar absorptance is equal to 0.81 [Ref. 11] and hence the average solar absorptance is 0.81.

Because aluminum has a very low emittance ($\varepsilon = 0.039$) the emittance for the SCA had to be increase. This was accomplished by painting the SCA's back surface with white paint. White paint has an emittance value of approximately 0.85.

C. CALCULATION OF THE CELL OPERATING TEMPERATURE

1. Definition and Explanation of Values

The solar cell steady state operating temperature is given by

$$T_{op} = \left[(\bar{\alpha}_s - F_p \eta_{op}) \frac{A_F}{(\bar{\varepsilon}_F A_F + \varepsilon_B A_B)} \frac{S \cos \Gamma}{\sigma} \right]^{\frac{1}{4}} \tag{4.1}$$

where the symbols are defined as:

$\bar{\alpha}_s$ is the average solar absorptance and is equal to 0.81.

F_p is the solar cell packing factor. This is the ratio of the total active area of the solar cells to the total area of the substrate.

η_{op} is the solar cell operating efficiency and is equal to 16%. This value was obtained from the cell manufacturer.

A_F is the array front side area ($A_F = 9 \times 1.757 \times 10^{-4} = 1.58 \times 10^{-3}$m²).

A_B is the array back side area ($A_B = (0.7m)^2 = 0.49m^2$).

$\bar{\varepsilon}_F$ is the average emittance of the array front side.

ε_B is the emittance of array back side. This is equal to 0.85.

S is the value of the solar constant multiplied by the actual concentration ratio and is equal to 2.0295×10^5 W/m^2.

σ is the Stephan Boltzmann's constant (5.699×10^{-8} W/m^{2}K^4).

Γ is the angle of incident of sunlight on the SCA. For this case, Γ is equal to zero.

The solar cell packing factor, F_p, is given by

$$F_p = \frac{NA_c}{A_s} \tag{4.2}$$

N is the number of solar cells and is equal to nine. A_c is the solar cell active area and is equal to 1.257×10^{-5} m^2 (active area diameter is equal to 4 mm). A_s is the total area of the substrate and is equal to 0.49 m^2. Substituting these values into equation (4.2) yields a packing factor of 2.308×10^{-4}.

The average emittance of the SCA's front side, $\bar{\varepsilon}_F$, is found by this equation

$$\bar{\varepsilon}_F = \frac{\sum_{i=1}^{m} \varepsilon_i A_i}{\sum_{i=1}^{m} A_i} \tag{4.3}$$

where m is the number of different surface materials, ε_i is the emittance of the ith material, and A_i is the area of the ith material.

As was the case for the average solar absorptance, only the Kapton and solar cell will have any influence on this value. The solar emittances for Kapton and the Gallium Arsinide solar cell are 0.75 and 0.88, respectively. The Kapton has a total surface area equal to 1.46×10^{-3} m^2 . The solar cell's total surface area is equal to 1.13×10^{-3} m^2. Substituting these values into equation (4.3) yields a value of $\bar{\varepsilon}_F$ is equal to 0.7.

Substituting the values into equation (4.1) yields a solar cell operating temperature, T_{op}, of 50.7°C. This operating temperature is within the gallium arsenide solar cell operating temperature limits.

D. THERMAL ANALYSIS

1. General

The thermal analysis of the SCA was accomplished by using a steady-state thermal analyzer computer program written by Dr. Allan D. Kraus. This computer program performed a nodal analysis of the SCA. The output produced a list of steady-state temperature for each node from which hot spots could be identified. In addition, the gallium arsenide cell temperatures could be cross-checked with the operating temprature calculation performed earlier.

The thermal analyzer software consisted of several computer programs of which only two were used. The first program, THANSS, was the model builder program. It writes an input file which is used by the thermal analyzer program to calculate the steady-state temperature. The thermal analyzer program is called TASS200 and is used when the model has less than 200 nodes. For a more detail description of the operation and use of the two programs refer to Kraus [Ref. 12].

2. The Model

The SCA was modeled by ten parallel planes, one large plane on the the bottom with nine small planes on top of it. The nine small planes were arrange in a 3 by 3 matrix. The middle plane was centered on the centered on the center of the bottom plane. The lower plane represented the aluminum substrate. The upper plane represented the nine gallium arsenide solar cells. Figure 20 on page 38 shows a sketch of the model's bottom plane.

The model was divided into 178 sub-volumes of various dimensions. Each sub-volume was represented by a node in the computer. As shown in the Figure 20, the bottom plane consisted of nodes 1 through 169. The upper plane contained nodes 170 through 178. These were located above nodes 29, 33, 37, 81, 85, 87, 133, 135, and 137 in the bottom plane.

From this model, 668 branches were identified and input into the program THANSS. The branches represented all of the different heat flow paths from each node to its surrounding nodes.

3. The Results

The lines of code were input into the computer by typing THANSS.EXE and following the user friendly instructions. Upon completion, TASS200.EXE was called and the user friendly instructions were followed.

The result of the thermal analyzer program are listed in Figure 21 on page 38. Notice that the temperature of all nine gallium arsenide solar cells are approximately

52°C . This agrees with the operating temperature calculation performed earlier. In addition, the temperatures show that there are no hot spots.

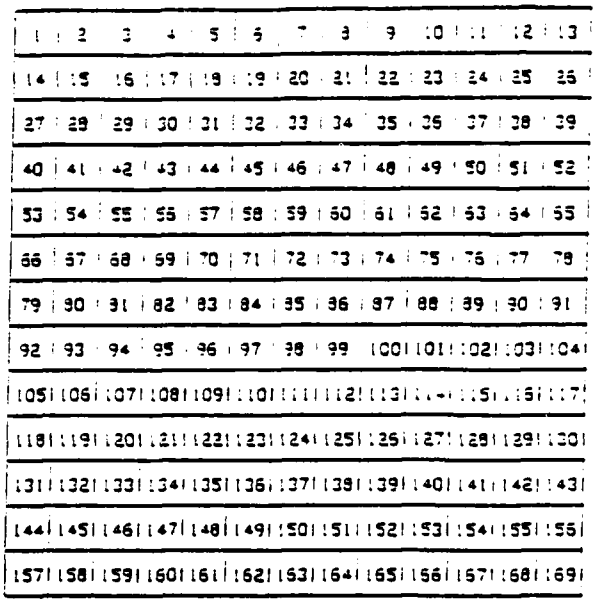

1	2	3	4	5	6	7	8	9	10	11	12	13
14	15	16	17	18	19	20	21	22	23	24	25	26
27	28	29	30	31	32	33	34	35	36	37	38	39
40	41	42	43	44	45	46	47	48	49	50	51	52
53	54	55	56	57	58	59	60	61	62	63	64	65
66	67	68	69	70	71	72	73	74	75	76	77	78
79	80	81	82	83	84	85	86	87	88	89	90	91
92	93	94	95	96	97	98	99	100	101	102	103	104
105	106	107	108	109	110	111	112	113	114	115	116	117
118	119	120	121	122	123	124	125	126	127	128	129	130
131	132	133	134	135	136	137	138	139	140	141	142	143
144	145	146	147	148	149	150	151	152	153	154	155	156
157	158	159	160	161	162	163	164	165	166	167	168	169

Figure 20. SCA Thermal Analysis Sketch

Page No. 1

GaAs SOLAR CONCENTRATOR ARRAY
Temperatures, degC

1	32.05	2	32.45	3	32.56	4	32.64	5	32.59	6	32.82
7	32.84	8	32.82	9	32.59	10	32.64	11	32.56	12	32.45
13	32.05	14	32.45	15	33.45	16	34.24	17	33.66	18	33.14
19	33.86	20	34.56	21	33.86	22	33.14	23	33.66	24	34.24
25	33.45	26	32.45	27	32.56	28	34.24	29	50.87	30	34.42
31	33.29	32	34.63	33	51.29	34	34.63	35	33.29	36	34.42
37	50.87	38	34.24	39	32.56	40	32.64	41	33.66	42	34.42
43	33.88	44	33.37	45	34.09	46	34.75	47	34.09	48	33.37
49	33.88	50	34.42	51	33.66	52	32.64	53	32.59	54	33.14
55	33.29	56	33.37	57	33.24	58	33.58	59	33.61	60	33.58
61	33.24	62	33.37	63	33.29	64	33.14	65	32.59	66	32.82
67	33.86	68	34.63	69	34.09	70	33.58	71	34.30	72	34.97
73	34.30	74	33.58	75	34.09	76	34.63	77	33.86	78	32.82
79	32.84	80	34.56	81	51.29	82	34.75	83	33.61	84	34.97
85	51.74	86	34.97	87	33.61	88	34.75	89	51.29	90	34.56
91	32.84	92	32.82	93	33.86	94	34.63	95	34.09	96	33.58
97	34.30	98	34.97	99	34.30	100	33.58	101	34.09	102	34.63
103	33.86	104	32.82	105	32.59	106	33.14	107	33.29	108	33.37
109	33.24	110	33.58	111	33.61	112	33.58	113	33.24	114	33.37
115	33.29	116	33.14	117	32.59	118	32.64	119	33.66	120	34.42
121	33.88	122	33.37	123	34.09	124	34.75	125	34.09	126	33.37
127	33.88	128	34.42	129	33.66	130	32.64	131	32.56	132	34.24
133	50.87	134	34.42	135	33.29	136	34.63	137	51.29	138	34.63
139	33.29	140	34.42	141	50.87	142	34.24	143	32.56	144	32.45
145	33.45	146	34.24	147	33.66	148	33.14	149	33.86	150	34.56
151	33.86	152	33.14	153	33.66	154	34.24	155	33.45	156	32.45
157	32.05	158	32.45	159	32.56	160	32.64	161	32.59	162	32.82
163	32.84	164	32.82	165	32.59	166	32.64	167	32.56	168	32.45
169	32.05	170	32.37	171	32.88	172	32.37	173	32.88	174	33.24
175	32.88	176	32.37	177	32.88	178	32.37				

Figure 21. Results of Thermal Analyzer Program TASS200

V. TEST AND ANALYSIS

A. GENERAL

The SCA was tested in the Applied Solar Laboratory in the basement of Halligan Hall. The original objective was to test the SCA as a complete entity under AM0 conditions. This, however, could not be accomplished due to the light source intensity problem. The test was changed to testing one GaAs solar cell under AM0 comditions with unconcentrated and concentrated light. From this data, an output analysis of the SCA's electrical parameters could be obtained [Ref. 2: p. 84]. The light source intensity problem is discussed further in this chapter.

In addition to testing one solar cell, the three strings on the SCA were tested. The purpose of doing this test was to verify that the fresnel lenses were providing 150X concentration ratio and to check the SCA's operating temperature.

B. TEST EQUIPMENT

The solar simulator system consisted of five major componnents. These are the IBM PC XT computer, Data Acquisition and Control elements, Hewlett Packard (HP) 59501B Power Supply Programmer HP 6825A Bipolar Power Supply combinatic Karatos SS 2500 Solar Simulator, and temperature control water ciculator and cell test block. An excellent detailed description of the equipment settings, calibration, and operation is found in Gold [Ref. 13]. Gold's procedures were followed for the single GaAs cell test. The software used was different. This is discussed in Section C of this chapter. A simplified block diagram of the system is shown in Figure 22 on page 40.

A slight modification of the system had to be accomplished before testing the SCA's three strings. The modification consisted of rotating the Kratos SS 2500 Solar Simulator's output mirror and changing the cell input lines to the switching module. The mirror was rotated approximately 75 degrees in order to shine the light on the SCA. The SCA negative and positive wire replaced the cells test block input wire to the switching module. The negative wire was placed in input A and a shorting wire was used to connect A to D. Similarily, the positive wire was plugged into input marked B. A shorting wire connected B to C. The purpose of shorting the wire was to change the input points from four to two. By changing the box marked test block to SCA and replacing the four on the line from the test block to switching module to a two, Figure 22 would be the test equipment set up for the SCA string test.

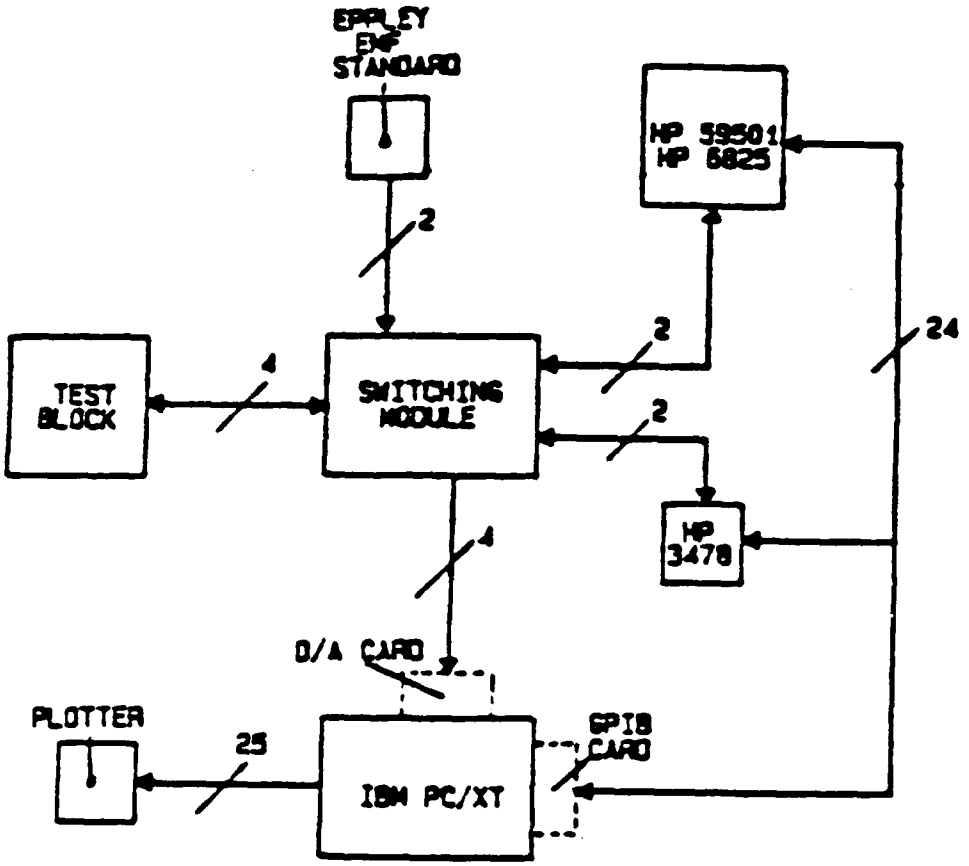

Figure 22. Test Equipment Configuration for Testing One Solar Cell. [Ref. 13: p. 17]

C. SOFTWARE

The I-V characteristic curves and electrical parameters of the solar cells were obtained through five computer programs. All five programs were obtained through modification of previously written programs. Two programs, SCA1 and SCACON, were used to test one 4 mm diameter GaAs solar cell under AM0 conditions. SCA1 was used for unconcentrated light while SCACON was used for concentrated light. The programs called SCAV3 and SCAVC3 were used to test the string of cells. The first one was for unconcentrated light while SCAVC3 was for the concentrated light. In addition, both SCAV3 and SCAVC3 had to be programmed to place the power supply into the high output range. The fifth program, SCALOG, converted the linear scale I-V curve to

logarithmic scales. It was used to compare the unconcentrated test with the concentrated test.

1. SCA1 and SCACON

Both SCA1 and SCACON initially measured I_{sc} by setting the power supply voltage to zero. Next the power supply was incremented by +1.5mV and the current measurement was taken. This procedure continued until the current was less than zero. The computer then measured the V_{oc} by interpolation. The maximum power is calculated by the computer from which the maximum current and voltage were obtained. The fill factor and efficiency are found from equations (3.5) and (3.6). This data can be plotted on the HP 7475A or stored on a floppy disk for later use.

The difference between SCA1 and SCACON is that SCACON calculates the concentration ratio. It accomplishes this by requiring the user to input the short circuit current of the unconcentrated cell. It then uses the equation

$$C = \frac{I_{scc}}{I_{sc}} \tag{5.1}$$

where I_{scc} and I_{sc} are the short circuit current for concentrated and unconcentrated light respectively. The efficiency was determined by substituting this value into the following equation.

$$\eta = \frac{P_{max}}{P_i \times A_c \times C} \tag{5.2}$$

where P_c and A_c are the input intensity and active area of the solar cell, respectively.

It should be noted that SCA1 and SCACON were modifications of two previously written programs called E1 and ECON. For further information on these programs, refer to Sengil [Ref. 14: pp. 8-10].

2. SCAV3 and SCAVC3

SCAV3 and SCAVC3 are very similar to SCA1 and SCACON in obtaining the I-V curves and electrical parameters. The major difference between these programs is SCAV3 and SCAVC3 will test a string of GaAs solar cells. The number of cells in the string ranged from two to six sells. In addition, because the open circuit voltage of the string was greater than 1.0098 volts, the power supply combination output range had to be changed from the low output range to the high output range. This was accomplished by changing the four digit code that was sent to the power supply combination. By

changing the first digit of the code to a two, the power supply combination voltage output range was put into the high output range[3] .

A copy of SCAVC3 is found in Appendix A. By eliminating lines 4080, 4100, 4105, 4110 and changing line 4145, the user has a copy of SCAV3. Line 4145 must be changed by eliminating 'CON' out of the denominator and verify the intensity level. The discussion on how to find the intensity level is found in Section F of this chapter.

a. Voltage Resolution Determination

It should be noted that by going from a low to a high output range, the voltage step resolution was changed from 1.47 mV per step to 14.7 mV per step. This meant that there was less data points taken for the I-V curves measurements.

The 14.7 mV per step was found by following the procedure outline by Gold [Ref. 13: pp. 63-66]. By changing the digital code from 1999 to 2999 and from 1000 to 2000, the maximum and minimum voltage was changed from 1.0098 volts to 7.63 volts and from -0.1429 to -7.097 volts respectively. Substituting these values into this equation

$$\frac{(V_{max} - V_{min})}{999} \tag{5.3}$$

yields 14.74 mV per step.

b. Calibration of the HP 6825A and 59501B Power Supply Combination

Periodically the HP 6825A and 59501B power supply combination had to be checked to see if they were still within calibration. This was accomplished by following steps 1 through 8 of the procedures outline in Gold [Ref. 13: pp. 65-66]. In addition, three steps were added to verify the maximum, minimum, and zero voltage output of the power supply when it was in the high voltage output range. The steps added are:

- Type IBWRT "2999" at the psupp: prompt. This drives the power supply to its maximum voltage in the high voltage output range. It should be +7.631 volts.
- Next, type IBWRT "2000". This drives the power supply to the minimum voltage output. This reading should be -7.098 volts.
- Next, type IBWRT "2482". The power supply should be at +0.008 volts.

---

3 By having the first digit of the code as a one the power supply would be placed into the low voltage output range.

Each of the above values should be within ± 0.001 volts. If this is not the case then *repeat the entire procedure.* It should be noted that after performing Gold's procedures the maximum, minimum, and zero voltage always came out to be the above values.

D. ILLUMINATION LEVEL AND PLANAR WAVE PROBLEM

As mentioned earlier, one of the main objectives of the test was to see the SCA's output under AM0 condition. This meant that the illumination of intensity level of the light source or sources used had to be approximately 1353 W/m^2, and the lightwaves had to be planar. Several different configurations were tried and in all cases, the illumination level reached only a small fraction needed. Furthermore, any attempt to increase the intensity by adding more light sources would result in creating additional spot areas produce by the same fresnel lens. For example, if three light sources were used, three spot areas would be produced by the same lens. Only one of the spots would fall on the intended solar cell. The other two would miss the cell entirely.

The light sources tried were the Kratos SS2500 Solar Simulator, 375 watt and 175 watt flood lights, and three slide projectors. The solar simulator produces an illumination level equal to AM0, but only if the solar cells are within 15 inches from the light. At that distance, only a small portion of the array was illuminated.

Since the intensity level could not be brought up to AM0 condition and because the numerous spots per lens, the number of light sources used was reduced to one. The light source used was the Kratos SS 2500 Solar Simulator because it had the largest intensity of all the sources available. The use of one source eliminated the multiple spots from each lens.

By using the solar simulator the SCA had to be placed on its side for conducting the string test. This prevented testing of the entire SCA. The frame was design to counteract the weight of the fresnel lenses when the SCA was lying parallel to the floor. The horizontal stiffness was very small. With the SCA on its side, the the majority weight from all nine lenses would be acting horizontally to the array. Consequently, after putting more than four lenses on the frame would deform significantly. Since the frame could support three lenses without any significant deformation, the test was reduced to testing the top, middle, bottom strings only. It should be noted that it took a considerable amount of time to adjust the three lenses in order for all three spots to fall on their respective cell.

E. TEST PROCEDURE

1. General

Because of the illumination problem mentioned in the previous section, a complete test of the SCA could not be achieved. However, this did not prevent an accurate and reliable test to be conducted. One procedure in testing an array is to test the cells under AM0 condition with concentrated and unconcentrated light. From this information, the array's output performance can be accurately obtained [Ref. 2: pp. 77-78]. In addition, the concentration ratio could still be tested as long as the light source had a sufficient intensity so that the solar cells could produce current.

The test consisted of:

- Testing one GaAs solar cell under AM0 condition with and without the fresnel lens.
- Testing the individual strings of the SCA, both under unconcentrated and concentrated light.

2. Single GaAs Solar Cell Test

Prior to testing the GaAs solar cell under AM0 conditions, the solar simulator had to be calibrated. This was accomplished by placing a standard solar cell on the test block. The cell's temperature was allowed to reach equilibrium and the intensity of the solar simulator was adjusted until the I-V curves matched. When this was achieved, the solar simulator was at AM0.

Next, the GaAs solar cell was placed on the test block and the unconcentrated and concentrated I-V curves were generated. For comparison the two curves were plotted on the same semi-log graph. These curves are shown in Figure 23 on page 62 through Figure 25 on page 64, respectively. The electrical parameters are listed in each of the figures.

3. Test and Calculation of the Light Source Intensity.

The intensity of the light source was determined by using the same solar cell and measuring its I-V curve at the SCA's location. A program called SCA11D was used to obtain the curve. This program is the same as SCA1, except the current axis scale on the graph was changed to micro amps. Figure 26 on page 66 shows one of the results of this test. The jaggedness of the curve is due to the intensity fluctuation, noise, and the small amount of current being generated. Several tests were run in an attempt to get a smoother curve, but the results were the same.

The parameters needed in doing the calculations were the cell efficiency at AM0 and the maximum power measurement at the unknown intensity. These values are ob-

tained from the figures. Refering to Figure 23 on page 62, the cell's efficiency is 19.56%. The maximum power is obtain from Figure 26 on page 66 and is 0.0325 mW. Substituting these values into equation (3.6), the illumination level, p_{in}, is found to be 1.321 mW. This value was substituted into line 4145 in programs SCAV3 and SCAVC3. Because of the light intensity fluctuation, this test and subsequent calculations were performed prior to every string test. If the illumination level was different form the previous values the new value was substituted into line 4145.

4. SCA String Test

This test was primarily conducted to find out if the SCA's thermal design was adequate and to verify that the fresnel lenses provided a 150X concentration ratio. The thermal design was checked by checking the steady state cell operating tempersature. If correctly design the SCA would have an operating temperature of 50.7°C. The test was conducted for each string after performing the light intensity check described by the previous section. Eight tests were conducted during a four hour period. The I-V curve results for the top, middle, and bottom strings are found in Appendix C through E.

F. DISCUSSION OF TEST RESULTS

1. GaAs Cell at AM0 Conditions

Table 1 lists the electrical parameters of the GaAs solar cell under AM0 conditons. It can be seen from the table that the cell's concentrated output has increased significantly from the unconcentrated. The biggest increases were obtained in I_{sc}, P_{max}, and I_{max}.

Table 1. GAAS SOLAR CELL TEST RESULTS AT AM0

	V_A (mV)	I_{SC} (mA)	P_{MAX}* (mW)	V_{MAX} (mV)	I_{MAX} (mA)	F.F.	EFF (%)
UNCON	930.85	4.51	3.32	780.7	4.2	.791	19.56
CON	1007.54	56.76	48.19	885.47	54.42	.842	22.54

Figure 25 on page 64 compares the two I-V curves on a semi-log scale. Notice that the concentration ration is only 12.57. This was due to the 9.125 inches lens to cell spacing. Because of this, the lens was only approximately 4 inches from the light source. At this distance, the illuminated area of the lens was 2.66 inches in diameter. Substituting these values into equations (3.1) and (3.2) yields a concentration ratio of 12.57.

2. SCA Output Computation and Analysis

As mentioned earlier, one procedure in finding the SCA's output is by obtaining the I-V curve and electrical parameters from a single cell. In this case, it is sufficient to use the electrical parameters of the GaAs solar cell tested at AM0 under concentrated and unconcentrated light. The electrical parameters needed are the open circuit voltage, short circuit current, maximum power, maximum voltage, and maximum current. These values are mutiplied by the number of cells in series, N_s, the number of cells (or strings) connected in parallel, N_p, or the total number of cells in the SCA, N_t, whichever is applicable. In equation form these become

$$V_a = N_s \times V_{oc} \tag{5.4}$$

$$I_{sc} = N_p \times I_{sc}' \tag{5.5}$$

$$P_{max} = N_t \times P_{max}' \tag{5.6}$$

$$I_{max} = N_p \times I_{max}' \tag{5.7}$$

where the prime marks denote the single GaAs cell values. The number of cells in series and number of cells in parallel are both equal to three. Total number of cells is nine. The value of the electrical parameters are obtained from Table 1 on page 45. Table 2 on page 47 shows the results of the SCA output analysis. From this table a substantial increase in the SCA's output is seen. However, it must be pointed out that this is for a concentration ratio of 12.57X not the 150X the lens is designed to produce. If the light source had illuminated the entire lens, then the SCA's concentrated output would have been much larger. Specificially, I_{sc} and I_{max} would have been approximately 2.03 A and 1.89 A respectively.[4] The value of the SCA's open circuit and maximum voltage, would have increased slightly.

---

4 These values were obtained by multiplying I_{sc} and I_{max} of the unconcentrated cell by 150 and then multiplying them by 3.

Table 2. SCA OUTPUT ANALYSIS RESULTS

	V_A (mV)	I_{SC} (mA)	P_{MAX}* (mW)	V_{MAX} (mV)	I_{MAX} (mA)
UNCON	2792.55	13.53	29.88	2342.1	12.6
CON	3022.61	170.29	433.71	2656.4	163.26

* MULTIPLIED BY 9. ALL OTHERS MULTIPLIED BY 3.

3. String Test Results

Table 3 on page 48 shows the top string test results. The first test, S3T1, is the string under unconcentrated light. The remaining tests, SC3T1 through SC3T8, are the test results of string under concentrated light. The average result is given at the bottom of the table. Notice the unconcentrated string's short circuit current is 0.055 mA. This was due to the low intensity level of the light source. From the average line, the concentration ratio was 152.3 and the fill factor (F.F) was 0.889. Comparing this with the unconcentrated test, the SCA's string output increased significantly. Similar results were obtained for the middle and bottom strings. These results are listed in Table 4 on page 101 and Table 5 on page 102 (Appendix F), respectively. All I-V curves for the top, middle, and bottom strings are found in Appendix C through E.

Due to the low intensity level of the light source, the steady state solar cell operating temperature of the individual strings never exceeded 27°C. This prevented the verification of the SCA's thermal design. The cell operating temperature is a critical factor in determining the SCA's ability to be used in space.

G. EXPERIMENTAL ACCURACY

The Kratos SS2500 Solar Simulator spectral quality is considered to be accurate to within $\pm$ 1% [Ref 13 p. 38]. The power fluctuation from other test equipment being turned on and off in the building did cause the light intensity to fluctuate. This fluctu-

ation was not significant when testing one solar cell on the test block. To make sure the data measurements were accurate, each data point was measured 20 times.

Table 3. TEST RESULTS OF TOP STRING

NAME	CR	I_{SC} (mA)	V_{OC} (mV)	P_{MAX} (mW)	V_{MAX} (mV)	I_{MAX} (mA)	F.F.
S3T1	1	.055	2169.5	.095	1823.1	.052	.794
SC3T1	151.8	8.35	2675.8	21.7	2651.5	8.2	.905
SC3T2	154.5	8.5	2869.7	21.8	2622.2	8.32	.890
SC3T3	149.1	8.2	2874.8	21.2	2622.2	8.1	.896
SC3T4	148.2	8.15	2874.8	21.0	2607.0	8.1	.896
SC3T5*	150.9	8.3	2874.8	21.3	2622.6	8.1	.893
SC3T6	157.4	8.5	2890.3	21.8	2608.8	8.3	.884
SC3T7	157.0	8.5	2875.9	21.1	2638.1	7.99	.854
SC3T8	150.0	8.1	2876.2	20.9	2607.4	8.0	.896
AVG	152.3	8.3	2851.5	21.4	2622.5	8.1	.889

The intensity fluctuation was very apparent in testing the SCA's strings for unconcentrated light. The major cause of this was the low intensity level of the light source at the SCA's location. This combined with the power fluctuation caused each unconcentrated string I-V curve to be very jagged. Figure 26 on page 66 provides a good example of this problem.

The planar wave problem caused the efficiency readings of the SCA's string to be inaccurate. By adjusting the fresnel lenses individually to ensure that the concentrated spot covers each cell, the incident light angle to the normal was changed. With the lenses, this angle was approximately zero degrees. Without the lenses, the angle was slightly greater than two degrees. Even though this angle was small, it was large enough to yield unreliable efficiency results. For example, the efficiency of the top string was 18.4% unconcentrated and 26.1% concentrated. The maximum theoretical efficiency of the GaAs solar cell is 28% and at the present time, the highest efficiency ever achieved in a laboratory is 27.0% [Ref. 4]. The strings efficiency were left on each I-V curve just for information purposes.

VI. CONCLUSIONS AND RECOMMENDATIONS

A. CONCLUSIONS

The first conclusion is a Gallium Arsenide Solar Concentrator Array using fresnel lenses can be constructed. The materials needed to build the SCA are readily available with costs being the only limiting consideration.

Next, it can be concluded from Table 1 on page 45, that the fresnel lens did significantly increase the SCA's output. Since the entire lens was not illuminated by the light source, the actual increase is not known. However, tables 3 through 5 showed that the lenses did provide a 150X concentration ratio. If the light source was large enough to illuminate the entire lens, then it is reasonable to believe that the concentrated short circuit current would have been approximately 676.5 mA. The open circuit voltage of the concentrated cell would have increased too, but not as much as the short circuit current. This was seen from Figure 5 on page 15. From this information, it is reasonable to state that the SCA would have had a substantial increase in its maximum power output.

As stated in the introduction, a critical factor that determines the SCA effectiveness is its ability to reject thermal heat. The SCA did maintain a constant 27°C during four hours of illumination, but this was not at AM0 conditition. Due to the low intensity level of the light source, the effectiveness of its thermal design could not adequately be determine.

B. RECOMMENDATIONS

It is recommended that further research be continued in this area. There are three improvements that could be done to the SCA. The first would be to use fresnel lenses with smaller focal lengths. At the time of this writting, a fresnel lens with a 1.0 inch focal length was being developed by the 3M Company [Ref. 4]. This will reduce the size of the SCA considerably. Secondly, smaller arrays could be built by using only one of the fresnel lenses and putting four or five GaAs solar cells within the spot area. By using only one lens, the array could be tested using the Kratos SS2500 Solar Simulator already set up in the lab. The shortcoming is getting the simulator to illuminate the entire lens. The third recommendation would be to develop a light source capable of illuminating the entire SCA under AM0 conditions. This will make it possible to evaluate the thermal design of the array. The last recommendation is to test the SCA in a radiation en-

vironment. From this test, the improvement of the array's survivability can be evaluated.

APPENDIX A. GAAS SOLAR CONCENTRATOR ARRAY TEST PROGRAM

```
10 '*****************************************************************
15 '*                                                               *
20 '*                    SCAVC3.BAS                                 *
25 '* ------------------------------------------------------------- *
30 '*                                                               *
35 '* IT PROVIDES AN AUTOMATIC  METHOD FOR DETERMINING THE I-V      *
40 '* CURVE OF A N BY M GALLIUM ARSENIDE SOLAR CONCENTRAROR         *
45 '* ARRAY. N IS THE NUMBER OF SOLAR CELLS IN SERIES AND M IS THE  *
50 '* NUMBER OF STRINGS IN THE ARRAY.  THE GaAs CELLS USED HAVE AN  *
55 '* ACTIVE AREA DIAMETER OF 4mm.  THE MAXIMUM NUMBER OF CELLS IN  *
60 '* IN A STRING IS SIX.  THIS PROGRAM IS MENU DRIVEN AND REQUIRES*
65 '* THE USER TO HAVE  AN IBM DATA ACQUISITION CARD, A GPIB INTER- *
70 '* FACE CARD, AN IEEE-488 CAPABLE MULTIMETER, AND AN IEEE-488   *
75 '* CAPABLE  POWER SUPPLY.  THE GRAPHICS IS FOR AN HP 7475A PLOT-*
80 '* TER. THE PROGRAM IS MODIFIED FROM PROGRAMS WRITTEN IN REF-   *
85 '* ERENCES 12 AND 13.                                           *
90 '*                                                               *
95 '*****************************************************************
340 '
350 '
360 '   **********START OF GPIB DRIVER**********
370 '
380       CLEAR   ,59309!          ' IBM BASICA Declarations
390       IBINIT1 = 59309!
400       IBINIT2 = IBINIT1 + 3    ' Lines 1 through 6 MUST be included.
410       BLOAD "bib.m",IBINIT1
420       CALL IBINIT1(IBFIND,IBTRG,IBCLR,IBPCT,IBSIC,IBLOC,IBPPC,IBBNA,IBONL,IBRSC,IBSRE,IBRSV,
          IBPAD,IBSAD,IBIST,IBDMA,IBEOS,IBTMO,IBEOT,IBRDF,IBWRTF)
430       CALL IBINIT2(IBGTS,IBCAC,IBWAIT,IBPOKE,IBWRT,IBWRTA,IBCMD,IBCMDA,IBRD,IBRDA,IBSTOP,
          IBRPP,IBRSP,IBDIAG,IBXTRC,IBRDI,IBWRTI,IBRDIA,IBWRTIA,IBSTA%,IBERR%,IBCNT%)
440       REM Optionally include the following declarations in your program.
450       REM They provide appropriate mnemonics by which
460       REM to reference commonly used values.  Some mnemonics (GET%, ERR%,
470       REM END%, ATN%) are preceded by "B" in order to distinguish them from
480       REM BASICA keywords.
490       REM
500       REM GPIB Commands
510       UNL% = &H3F      ' GPIB unlisten command
520       UNT% = &H5F      ' GPIB untalk command
530       GTL% = &H1       ' GPIB go to local
540       SDC% = &H4       ' GPIB selected device clear
550       PPC% = &H5       ' GPIB parallel poll configure
560       BGET% = &H8      ' GPIB group execute trigger
570       TCT% = &H9       ' GPIB take control
580       LLO% = &H11      ' GPIB local lock out
590       DCL% = &H14      ' GPIB device clear
```

```
600     PPU% = &H15     ' GPIB ppoll unconfigure
610     SPE% = &H18     ' GPIB serial poll enable
620     SPD% = &H19     ' GPIB serial poll disable
630     PPE% = &H60     ' GPIB parallel poll enable
640     PPD% = &H70     ' GPIB parallel poll disable
650     REM
660     REM GPIB status bit vector
670     REM global variable IBSTA% and wait mask
680     EERR% = &H8000  ' Error detected
690     TIMO% = &H4000  ' Timeout
700     END% = &H2000   ' EOI or EOS detected
710     SRQI% = &H1000  ' SRQ detected by CIC
720     RQS% = &H800    ' Device needs service
730     CMPL% = &H100   ' I/O completed
740     LOK% = &H80     ' Local lockout state
750     REM% = &H40     ' Remote state
760     CIC% = &H20     ' Controller-In-Charge
770     ATN% = &H10     ' Attention asserted
780     TACS% = &H8     ' Talker active
790     LACS% = &H4     ' Listener active
800     DTAS% = &H2     ' Device trigger state
810     DCAS% = &H1     ' Device clear state
820     REM
830     REM Error messages returned in global variable IBERR%
840     EDVR% =  0      ' DOS error
850     ECIC% =  1      ' Function requires GPIB-PC to be CIC
860     ENOL% =  2      ' Write function detected no Listeners
870     EADR% =  3      ' Interface board not addressed correctly
880     EARG% =  4      ' Invalid argument to function call
890     ESAC% =  5      ' Function requires GPIB-PC to be SAC
900     EABO% =  6      ' I/O operation aborted
910     ENEB% =  7      ' Non-existent interface board
920     EOIP% = 10      ' I/O operation started before previous op completed
930     ECAP% = 11      ' No capability for operation
940     EFSO% = 12      ' File system operation error
950     EBUS% = 14      ' Command error during device call
960     ESTB% = 15      ' Serial poll status byte lost
970     ESRQ% = 16      ' SRQ remains asserted
980     REM
990     REM EOS mode bits
1000    BIN% = &H1000   ' Eight bit compare
1010    XEOS% = &H800   ' Send EOI with EOS byte
1020    REOS% = &H400   ' Terminate read on EOS
1030    REM
1040    REM Timeout values and meanings
1050    T10S% =  13     ' Timeout of 10 s (ideal)
```

```
1060      REM
1070      REM Miscellaneous
1080      S% = &H8          ' Parallel Poll sense bit
1090      LF% = &HA         ' Line feed character
1100      REM
1110      REM Application program variables passed to
1120      REM GPIB functions
1130      REM
1140      CMD$ = SPACE$(10)       ' command buffer
1150      RD$ = SPACE$(255)       ' read data buffer
1160      WRT$ = SPACE$(255)      ' write data buffer
1170      BNAME$ = SPACE$(7)      ' board name buffer
1180      BDNAME$ = SPACE$(7)     ' board or device name buffer
1190      FLNAME$ = SPACE$(50)    ' file name buffer
1200 '   ************END OF GPIB DRIVER******************
1210 '
1220      DEF SEG = 0
1230      DATA.SEGMENT = PEEK(&H511) * 256 + PEEK(&H510)
1240 BDNAME$ = "PSUPP"
1250 DEF SEG = DATA.SEGMENT
1260 CALL IBFIND (BDNAME$,PSUPP%)
1270 BDNAME$ = "DMM"
1280 CALL IBFIND (BDNAME$,DMM%)
1290 B$ = "F5N5ZOT1"
1300 CALL IBWRT(DMM%,B$)
1310 '
1320 '
1330 '   ********DAAC BASICA HEADER**********************
1340  '
1350 'NAME:  Data Acquisition And Control (DAAC)
1360 '       HEADER for BASICA
1370 '
1380 'FILE NAME:  DACHDR.BAS
1390 '
1400 'DOS DEVICE NAME:  DAAC
1410 '
1420 'RESERVED FUNCTION NAMES:
1430 '          AINM, AINS, AINSC, AOUM, AOUS,
1440 '          BINM, BINS, BITINS, BITOUS, BOUM, BOUS,
1450 '          CINM, CINS, CSET, DELAY
1460 'RESERVED DEF SEG VALUE NAME:  DSEG
1470 '
1480 'NAMES DEFINED AND USED BY HEADER:
1490 '          ADAPT%, AI, COUNT, FOUND%,
1500 '         .HNAME$, SG%, STAT%
1510 '
```

```
1520 FOUND% = 0
1530 SG% = &H2E
1540 'Start searching the interrupt vectors until you find
1550 'one that points to the DAAC device driver.
1560 'Do a DEF SEG to that segment.
1570 WHILE ((SG% <= &H3E) AND (FOUND% = 0))
1580       DEF SEG = 0
1590       DSEG = PEEK(SG%) + PEEK(SG% + 1) * 256
1600       DEF SEG = DSEG
1610       HNAME$=""
1620       FOR AI=10 TO 17
1630              HNAME$ = HNAME$ + CHR$(PEEK(AI))
1640       NEXT AI
1650       IF HNAME$ = "DAAC    " AND PEEK(18) + PEEK(19) <> 0 THEN FOUND% = 1
1660       SG% = SG% + 4
1670 WEND
1680 IF FOUND% = 0 THEN PRINT "ERROR: DEVICE DRIVER DAC.COM NOT FOUND" : END
1690 'Now initialize all function name variables for calls
1700 'to access the device driver.
1710 AINM        = PEEK(&H13) * 256 + PEEK(&H12)
1720 AINS        = PEEK(&H15) * 256 + PEEK(&H14)
1730 AINSC       = PEEK(&H17) * 256 + PEEK(&H16)
1740 AOUM        = PEEK(&H19) * 256 + PEEK(&H18)
1750 AOUS        = PEEK(&H1B) * 256 + PEEK(&H1A)
1760 BINM        = PEEK(&H1D) * 256 + PEEK(&H1C)
1770 BINS        = PEEK(&H1F) * 256 + PEEK(&H1E)
1780 BITINS      = PEEK(&H21) * 256 + PEEK(&H20)
1790 BITOUS      = PEEK(&H23) * 256 + PEEK(&H22)
1800 BOUM        = PEEK(&H25) * 256 + PEEK(&H24)
1810 BOUS        = PEEK(&H27) * 256 + PEEK(&H26)
1820 CINM        = PEEK(&H29) * 256 + PEEK(&H28)
1830 CINS        = PEEK(&H2B) * 256 + PEEK(&H2A)
1840 CSET        = PEEK(&H2D) * 256 + PEEK(&H2C)
1850 DELAY       = PEEK(&H2F) * 256 + PEEK(&H2E)
1860 DIM V%(50)
1880 DIM VOLT(1000)
1890 DIM CURR(1000)
1900 DIM POW(1000)
1910 DIM VIN%(20)
1920 Z$=SPACE$(14)
1930 ' initialize global variables
1940 DEV%=9
1950 ADAPT% = 0
1960 COUNT = 1
1970 STAT% = 0
1980 DEF SEG = DSEG
```

```
1990 CALL DELAY (ADAPT%, COUNT, STAT%)
2000 '
2010 '   *******END OF DAAC BASICA HEADER*****************
2020 '
2030  CLS
2040  SCREEN 0
2050  CLS
2060  BEEP
2070  PRINT "THE FOLLOWING OPTIONS ARE AVAILABLE FOR USE WITH THIS"
2080  PRINT "PROGRAM. SELECT A NUMBER AND THEN ENTER RETURN. NUMBER"
2090  PRINT "1 MUST BE SELECTED FIRST."
2100  PRINT
2110  PRINT "1.  RUN CALIBRATION ROUTINE."
2120  PRINT
2130  PRINT "2.  RUN SOLAR CELL PARAMETER TEST."
2140  PRINT
2150  PRINT "3.  PLOT I-V CURVE ON HP PLOTTER."
2160  PRINT
2170  PRINT "4.  WRITE DATA ON FLOPPY."
2180  PRINT
2190  PRINT "5.  READ DATA FROM FLOPPY."
2200  PRINT
2210  PRINT "6.  EXIT TO SYSTEM."
2280  PRINT
2290 INPUT ">",X
2300 IF X <> 1 THEN 2320
2310 GOTO 2640
2320 IF X <> 2 THEN 2340
2330 GOTO 2980
2340 IF X <> 3 THEN 2360
2350 GOTO 4480
2360 IF X <> 4 THEN 2380
2370 GOTO 5620
2380 IF X <> 5 THEN 2400
2390 GOTO 6010
2400 IF X <> 6 THEN 2420
2410 SYSTEM
2420 PRINT " INPUT MUST BE 1-6,TRY AGAIN "
2430 INPUT " TYPE ENTER TO RETURN MENU >",C$
2440 GOTO 2040
2620 '   ******* CALIBRATION SUBROUTINE *****************
2630 '
2640 CLS
2650 PRINT "COMMENCING CALIBRATION ROUTINE"
2660 BEEP
2670 PRINT
```

```
2680 PRINT "CONNECT STANDARD CELL TO TEST MODULE AND PLACE"
2690 PRINT "CAL/RUN SWITCH TO CAL POSITION.  ENTER THE VALUE"
2700 INPUT "OF THE STANDARD CELL VOLTAGE WHEN PROMPTED >",A
2710 PRINT
2720 CHAN% = 0: CTRL% = 0: MODE% = 0
2730 STOR% = 0: COUNT = 20: RATE =1000
2740 STAT% = 0
2750 DEF SEG = DSEG
2760 CALL AINM(ADAPT%,DEV%,CHAN%,CTRL%,MODE%,STOR%,COUNT,RATE,VIN%(0),STAT%)
2770 VIN = 0
2780 FOR G = 0 TO  19
2790 VIN = VIN%(G) + VIN
2800 NEXT G
2810 C1 = VIN/8192 - A
2820 PRINT "C1=";C1
2830 CHAN% = 2: CTRL% = 0: MODE% = 0
2840 STOR% = 0: COUNT = 20: RATE =1000
2850 STAT% = 0
2860 DEF SEG = DSEG
2870 CALL AINM(ADAPT%,DEV%,CHAN%,CTRL%,MODE%,STOR%,COUNT,RATE,VIN%(0),STAT%)
2880 VIN = 0
2890 FOR G = 0 TO  19
2900 VIN = VIN%(G) + VIN
2910 NEXT G
2920 C2 = VIN/8192 - A
2930 PRINT "C2=";C2
2940 BEEP
2950 PRINT "CALIBRATION COMPLETED. PLACE THE CAL/RUN INTO THE RUN POSITION"
2955 INPUT "CHECK C1,C2 (SHOULD EQUAL TO APPROX. 5.0 ).IF OK ENTER RETURN >",X$
2960 GOTO 2040
2970 '
2980 ' COMMENCING TEST
2990 '
3000 DEF SEG=DATA.SEGMENT
3010 BDNAME$="PSUPP"
3020 A$="2482"  'THIS CODE SETS THE POWER SUPPLY TO APPROX ZERO VOLTS.
3030 CALL IBWRT(PSUPP%,A$)
3050 INPUT "CONNECT SOLAR CELL ,LIGHT ON IT,ADJUST C,TYPE ANY LETTER > ",X$
3060 N=2482
3070 DEF SEG=DSEG
3210 COUNT= 5 : CHAN%=0
3220 CALL AINM(ADAPT%,DEV%,CHAN%,CTRL%,MODE%,STOR%,COUNT,RATE,VIN%(0),STAT%)
3230 VIN = 0
3240 FOR G = 0 TO  4
3250 VIN = VIN%(G) + VIN
3260 NEXT G
```

```
3280 V=VIN/2048-C1
3290 'CHECK FOR V=0
3300 IF V > 0 THEN 3500          'IF VOLTAGE STILL POSITIVE GO TO DECREASE
3301 '                            VOLTAGE SUBROUTINE
3310 VOLT(0)=0
3320 DEF SEG=DATA.SEGMENT
3330 BDNAME$="DMM"
3340 CALL IBRD(DMM%,Z$)
3350 CURR(0)=VAL(Z$)
3360 INPUT "CHECK FOR ISC,ADJUT CONCENTRATION > ",X$
3370 INPUT "YOU WANT AMC CAL.PRINT 0,YOU WANT GO ON PRINT 1 > ",ZT
3380 IF ZT=0 THEN 2980
3390 GOTO 3600
3400 '*************************************************
3500 'SUBROUTINE FOR TO DECREASE THE VOLTAGE UNTIL IT GETS TO ZERO VOLTS.
3510 N=N-1
3520 DEF SEG=DATA.SEGMENT
3530 BDNAME$="PSUPP"
3540 B$=STR$(N)
3550 B$=RIGHT$(B$,4)
3560 CALL IBWRT(PSUPP%,B$)
3570 GOTO 3070
3580 '*************************************************
3590 '*************************************************
3600 I=1 'SUBROUTINE FOR CURR=0
3610 N=N+1
3620 B$=STR$(N)
3630 B$=RIGHT$(B$,4)
3640 DEF SEG=DATA.SEGMENT
3650 BDNAME$="PSUPP"
3660 CALL IBWRT(PSUPP%,B$)
3670 'READ VOLT AND CURRENT
3680 DEF SEG=DSEG
3690 COUNT= 5 : CHAN%=0
3695 CALL DELAY (ADAPT%,COUNT,STAT%)
3700 CALL AINM(ADAPT%,DEV%,CHAN%,CTRL%,MODE%,STOR%,COUNT,RATE,VIN%(0),STAT%)
3710 VIN = 0
3720 FOR G = 0 TO  4
3730 VIN = VIN%(G) + VIN
3740 NEXT G
3750 V=VIN/2048-C1
3760 VOLT(I)=V
3780 'READ CURRENT
3790 DEF SEG=DATA.SEGMENT
3810 BDNAME$="DMM"
3820 CALL IBRD(DMM%,Z$)
```

```
3823 CURR(I)=VAL(Z$)
3825 IF CURR(I) < 0 THEN 3870
3830 I=I+1
3840 GOTO 3610
3850 '*****************************************************
3860 'ENTERPOLATIONS FOR EDGE VALUES OF THE VOLTAGE.  THIS IS USED TO GET AN
3861 'REASONABLE APPROXIMATION OF ZERO VOLTS.
3870 CURR(I)=0
3880 VOLT(I)=(VOLT(I)+VOLT(I-1))/2
3890 PMAX=0
3900 '*****************************************************
4000 '*****************************************************
4010 FOR T=0 TO I
4020 POW(T)=VOLT(T)*CURR(T)
4030 IF POW(T) < PMAX THEN 4070
4040 PMAX=POW(T)
4050 VMAX=VOLT(T)
4060 IMAX=CURR(T)
4070 NEXT T
4071 VOC=VOLT(I)
4072 ISC=CURR(0)
4073 FF=PMAX/(VOC*ISC)
4074 INPUT "DISCONNECT CELL,INPUT TEMPERATURE > ",TEMP
4075 INPUT "INPUT CELL NAME > ",CELL$
4076 INPUT "INPUT TODAY'S DATE > ",TAR$
4077 PRINT "THE NEXT SET OF PROMPTS WILL GIVE YOU YOUR ELECTRICAL PARAMETERS"
4078 PRINT "OF THE SOLAR CONCENTRATOR ARRAY UNDER TEST.  YOU MUST INPUT THE "
4079 PRINT "VALUE GIVEN OR ROUNDOFF TO THE TO THE DESIRED ACCURACY"
4080 INPUT "HIT RETURN WHEN YOU ARE READY TO CONTINUE. > ",ERT
4081 CLS
4085 INPUT "AMO Isc OF THIS CELL (mA) = ",ISC1  'THIS IS THE UNCONCENTRATED
4086                                            'SHORT CIRCUIT CURRENT.
4090 PRINT "GIVE VALUE OF Isc IF Isc = ",ISC*1000
4095 INPUT "Isc = ",ISC
4100 CON=(ISC)/(ISC1)
4105 PRINT "GIVE VALUE OF CONCENTRATION IF CON = ",CON
4110 INPUT "CON = ",CON
4136 INPUT "GIVE THE NUMBER OF SOLAR CELLS PER STRING > ", NCELL
4137 INPUT "GIVE THE NUMBER OF STRING(S) IN THE ARRAY > ", NSTR
4145 EFF=(PMAX /(.001457 * .1257 * NCELL * NSTR * CON ))*100
4146 PRINT "GIVE THE VALUE OF EFF IF EFF = ",EFF
4147 INPUT "EFF = ",EFF
4160 PRINT "GIVE VALUE OF Voc IF Voc = ",VOC*1000
4165 INPUT "Voc = ",VOC
4170 PRINT "GIVE VALUE OF Pmax IF Pmax = " ,PMAX*1000
4175 INPUT "Pmax = " ,PMAX
```

```
4180 PRINT "GIVE VALUE OF Vmax IF Vmax = ",VMAX*1000
4185 INPUT "Vmax = ",VMAX
4190 PRINT "GIVE VALUE OF Imax IF Imax = ",IMAX*1000
4195 INPUT "Imax = ",IMAX
4200 PRINT "GIVE VALUE OF F.F. IF  F.F. = ",FF
4205 INPUT "F.F. = ",FF
4210 EFF=INT(EFF*100)/100
4240 GOTO 2040
4250 '*************************************************
4480 '**********PLOTTING SUBROUTINE**********************
4490 '
4500 CLS
4510 INPUT "READY PLOTTER ENTER RETURN >",C$
4520 OPEN "COM2:9600,S,7,1,RS,CS65535,DS,CD" AS #1
4530 PRINT #1,"IN;SP1;IP2000,2400,8400,7000;"
4540 PRINT #1,"SC0,3000,0,15;"
4550 '
4560 '
4570 '
4580 PRINT #1,"PU0,0PD3000,0,3000,15,0,15,0,0PU"
4590 PRINT #1,"SI.2,.3;TL1.5,0"
4600 FOR X=0 TO 3000 STEP 300
4610 PRINT #1,"PA";X,",0;XT;"
4620 IF X<100 THEN PRINT #1,"CP-1.3,-1;LB";X;CHR$(3)
4630 IF X<1000 AND X>99 THEN PRINT #1,"CP-2.3,-1;LB";X;CHR$(3)
4640 IF X>999 THEN PRINT #1,"CP-2.8,-1;LB";X;CHR$(3)
4650 NEXT X
4660 FOR Y=0 TO 15 STEP 3
4670 PRINT #1,"PA 0,",Y,"YT;"
4680 IF Y<100 THEN PRINT #1,"CP-3,-.25;LB";Y;CHR$(3)
4690 IF Y>99 THEN PRINT #1,"CP-4,-.25;LB";Y;CHR$(3)
4700 NEXT Y
4710 PRINT #1,"SI.35,.5"
4720 PRINT #1,"PA1000,0;CP-1,-1.8;LBVOLTAGE  (mV)"+CHR$(3)
4730 PRINT #1,"PA0,3;DI0,1;CP-1,1.4;LBCURRENT  (mA)"+CHR$(3)
4735 PRINT #1,"VS 20"
4737 PRINT #1,"SC0,3000,0,1500;"
4740 PRINT #1,"DI;PU"
4750 FOR N=0 TO I
4760 PRINT #1,"PA";INT(VOLT(N)*1000);INT(CURR(N)* 100000!);"PD"
4770 NEXT N
4780 PRINT #1,"PU"
4790 '
4800 '
4810 '
4820 PRINT #1,"SP2;SI.15,.25"
```

```
4830 PRINT #1,"PU;PA500,650;CP0,0;LBIsc  = ";ISC     ;CHR$(3)
4840 PRINT #1,"CP;LBVoc  = ";VOC     ;CHR$(3)
4850 PRINT #1,"CP;LBPmax = ";PMAX     ;CHR$(3)
4860 PRINT #1,"CP;LBVmax = ";VMAX     ;CHR$(3)
4870 PRINT #1,"CP;LBImax = ";IMAX     ;CHR$(3)
4880 PRINT #1,"CP;LBFF   = ";FF;CHR$(3)
4890 PRINT #1,"CP;LBEff  = ";EFF;CHR$(3)
4900 PRINT #1,"PU;PA1200,650;CP0,0;LBmA";CHR$(3)
4910 PRINT #1,"CP;LBmV"+CHR$(3)
4920 PRINT #1,"CP;LBmV"+CHR$(3)
4930 PRINT #1,"CP;LBmV"+CHR$(3)
4940 PRINT #1,"CP;LBmA"+CHR$(3)
4950 PRINT #1,"CP;CP;LB%"+CHR$(3)
4960 PRINT #1,"SP2;SI.15,.25"
4970 '
4980 '
4990 '
5000 PRINT #1,"PU;PA 2125,1400;CP0,0;LBCELL NO: ";CELL$;CHR$(3)
5010 PRINT #1,"CP;LBDATE : ";TAR$ ;CHR$(3)
5020 PRINT #1,"CP;LBTEMP (C) : "TEMP;CHR$(3)
5030 PRINT #1,"CP;LBC        : "CON;CHR$(3)
5600 GOTO 2040
5610 '*************END OF PLOTTING************************
5620 '*************DISK WRITE SUBROUTINE*******************
5630 CLS
5720 INPUT "FLOPPY DISK TO DRIVE A,TYPE ENTER WHEN YOU READY,AND GIVE CELL NAME > ",CELL$
5730 FILE$="A:"+CELL$+".DAT"
5740 OPEN FILE$ FOR OUTPUT AS #2
5750 WRITE #2,PMAX,VMAX,IMAX,EFF,FF,TEMP,I,ISC,VOC,TAR$,CON
5760 FOR T=0 TO I
5770 WRITE #2,VOLT(T),CURR(T)
5780 NEXT T
5790 CLOSE
5800 GOTO 2040
5810 '***************END OF DISK WRITE*********************
6000 '***************DISK READ SUBROUTINE******************
6010 CLS
6020 INPUT "PLACE DISK DRIVE A, AND TYPE CELL NAME >",CELL$
6030 FILE$="A:"+CELL$+".DAT"
6040 OPEN FILE$ FOR INPUT AS #2
6050 INPUT #2,PMAX,VMAX,IMAX,EFF,FF,TEMP,I,ISC,VOC,TAR$,CON
6060 FOR T=0 TO I
6070 INPUT #2,VOLT(T),CURR(T)
6080 NEXT T
6090 CLOSE
6100 GOTO 2040
```

APPENDIX B. I-V CURVE TEST RESULTS FOR SINGLE GAAS SOLAR CELL

This appendix contains the I-V curve for the single GaAs solar cell test. Figures 23 and 24 are the unconcentrated and concentrated curves. Figure 25 is the comparison of the two curves on semi-log scale.

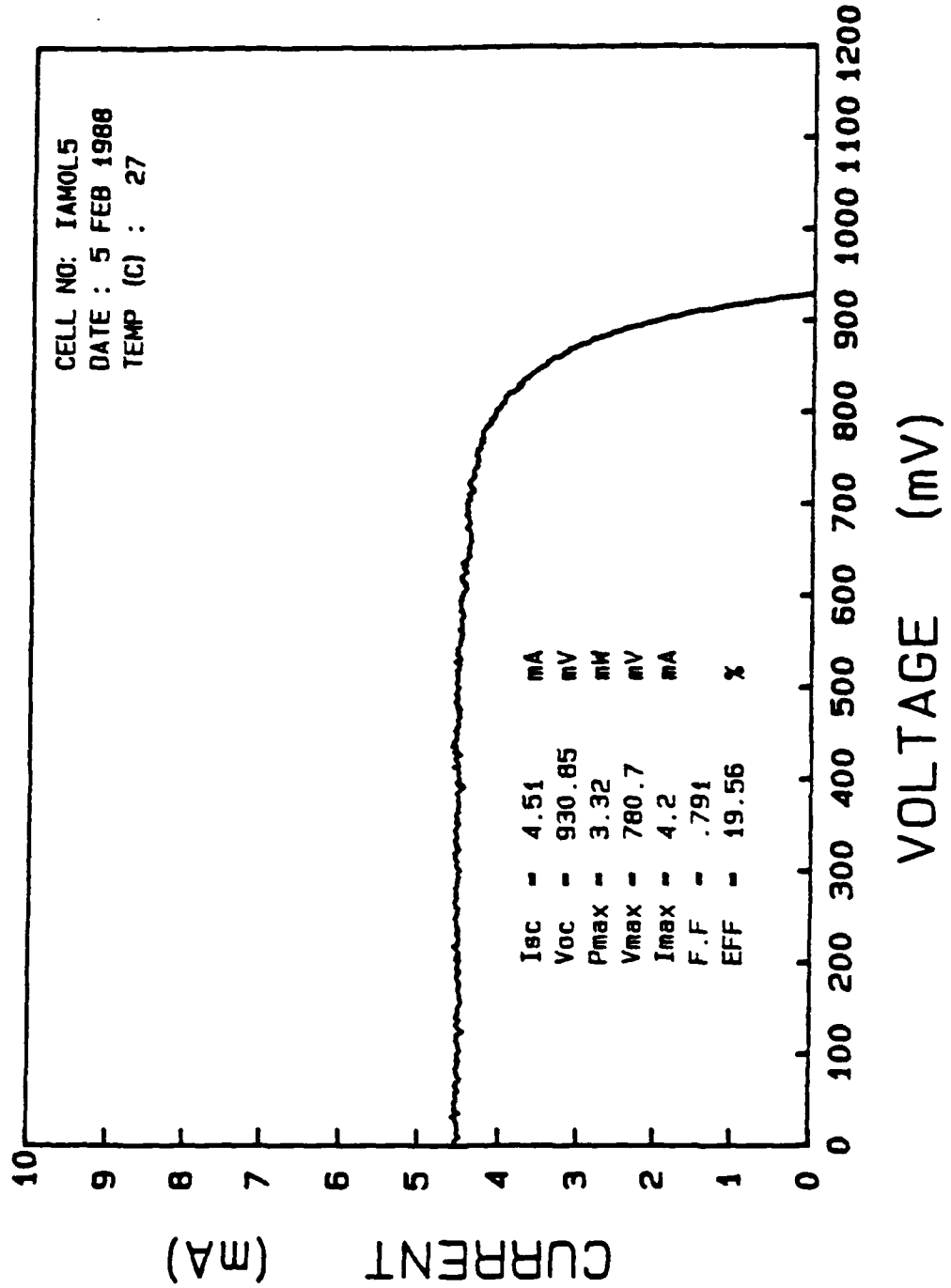

Figure 23. GaAs Solar Cell I-V Curve (Unconcentrated)

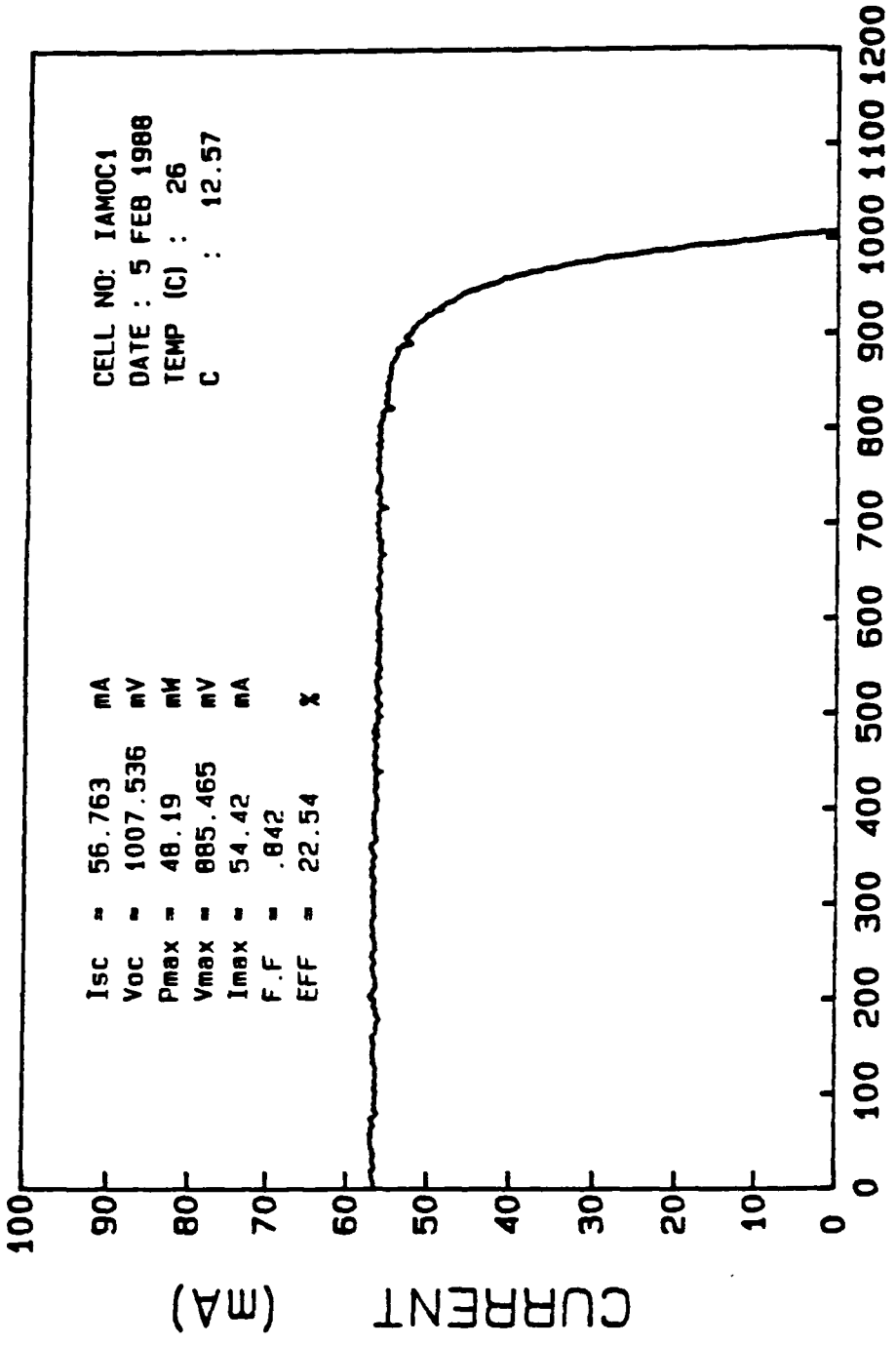

Figure 24. GaAs Solar Cell I-V Curve (Concentrated)

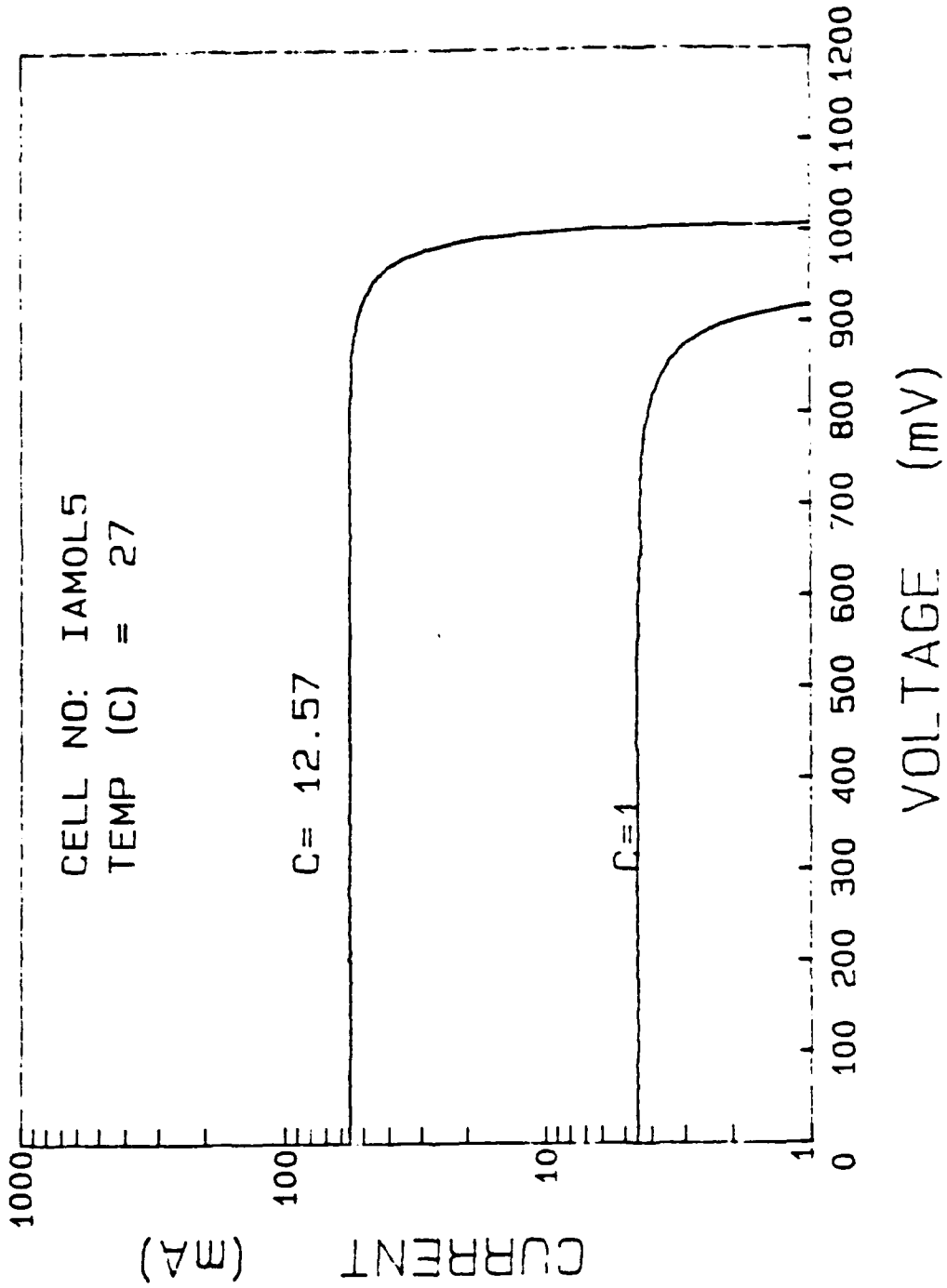

Figure 25. Comparison of the GaAs Solar Cell at 1X and 12.57X

APPENDIX C. SCA I-V CURVE TEST RESULT FOR TOP STRING

Figure 26 on page 66 gives the I-V curve of the intensity test for the top string. Figure 27 on page 67 is the I-V curve of the top string at a concentration ratio (CR) equal to one. Figure 28 on page 68 is the comparison of the unconcentrated curve to the average concentrated curve. Figure 29 on page 69 through Figure 36 on page 76 are the I-V curves of the eight concentrated string test.

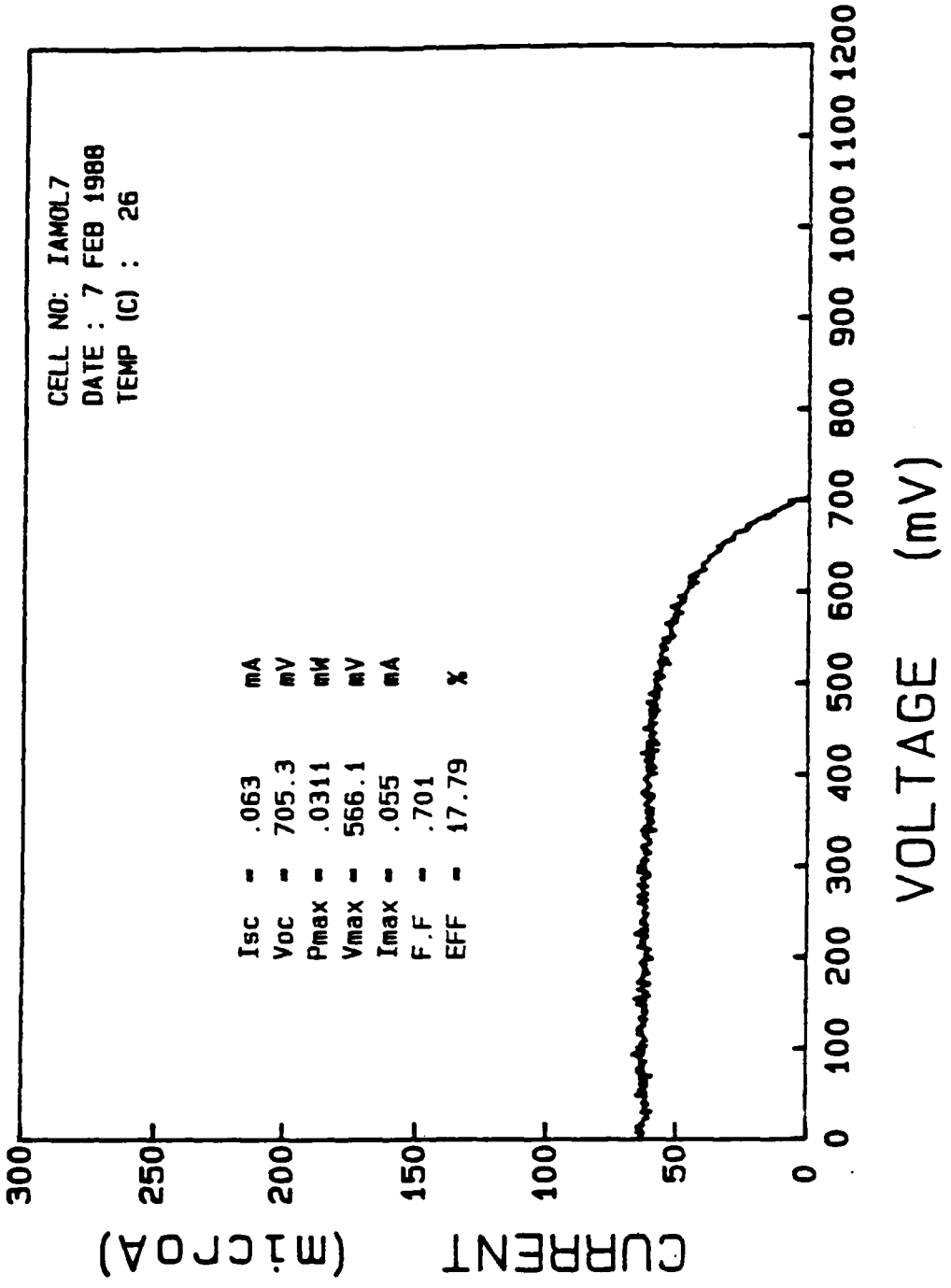

Figure 26. I-V Curve of the Top String Intensity Test

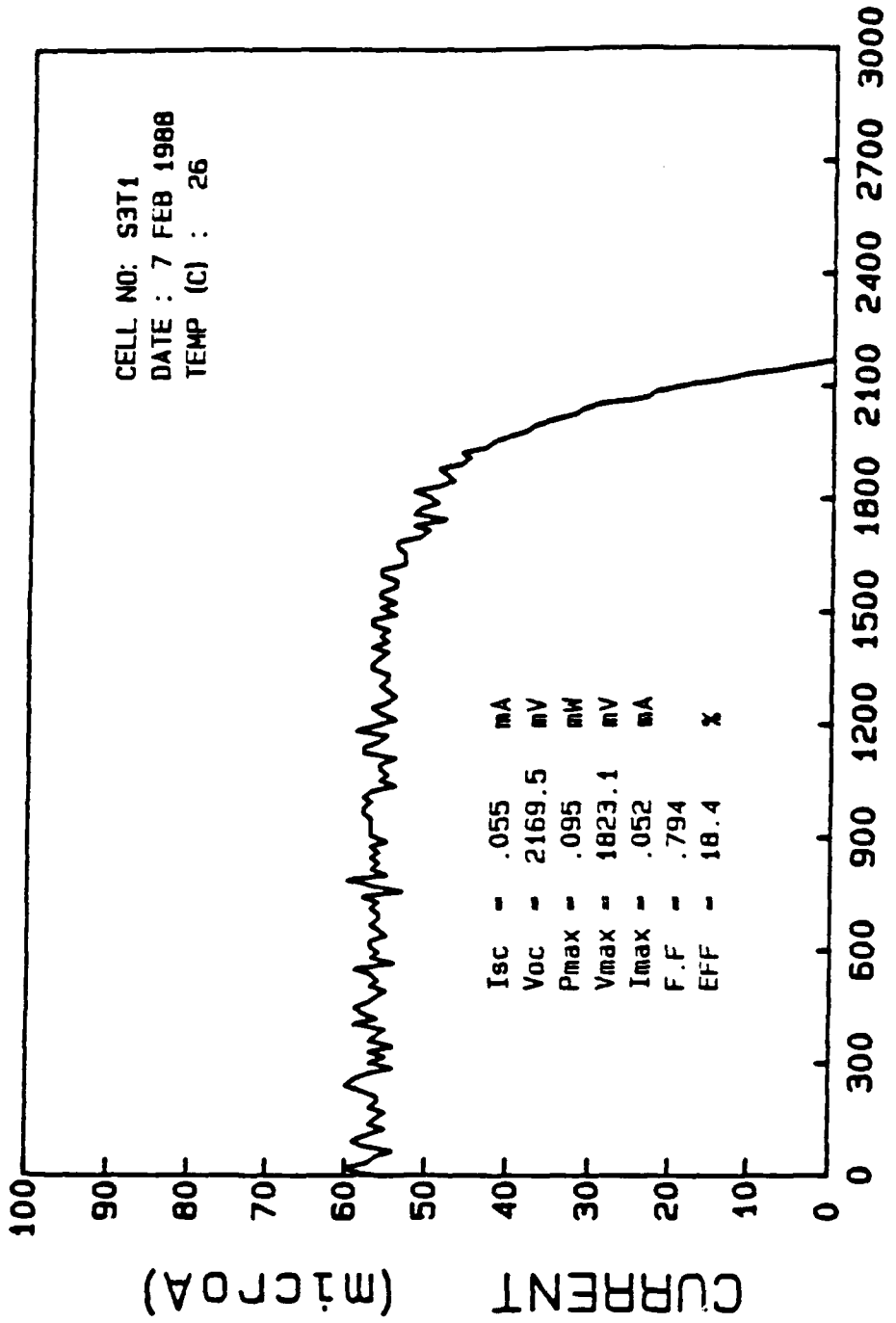

Figure 27. I-V Curve of Top String (Unconcentrated)

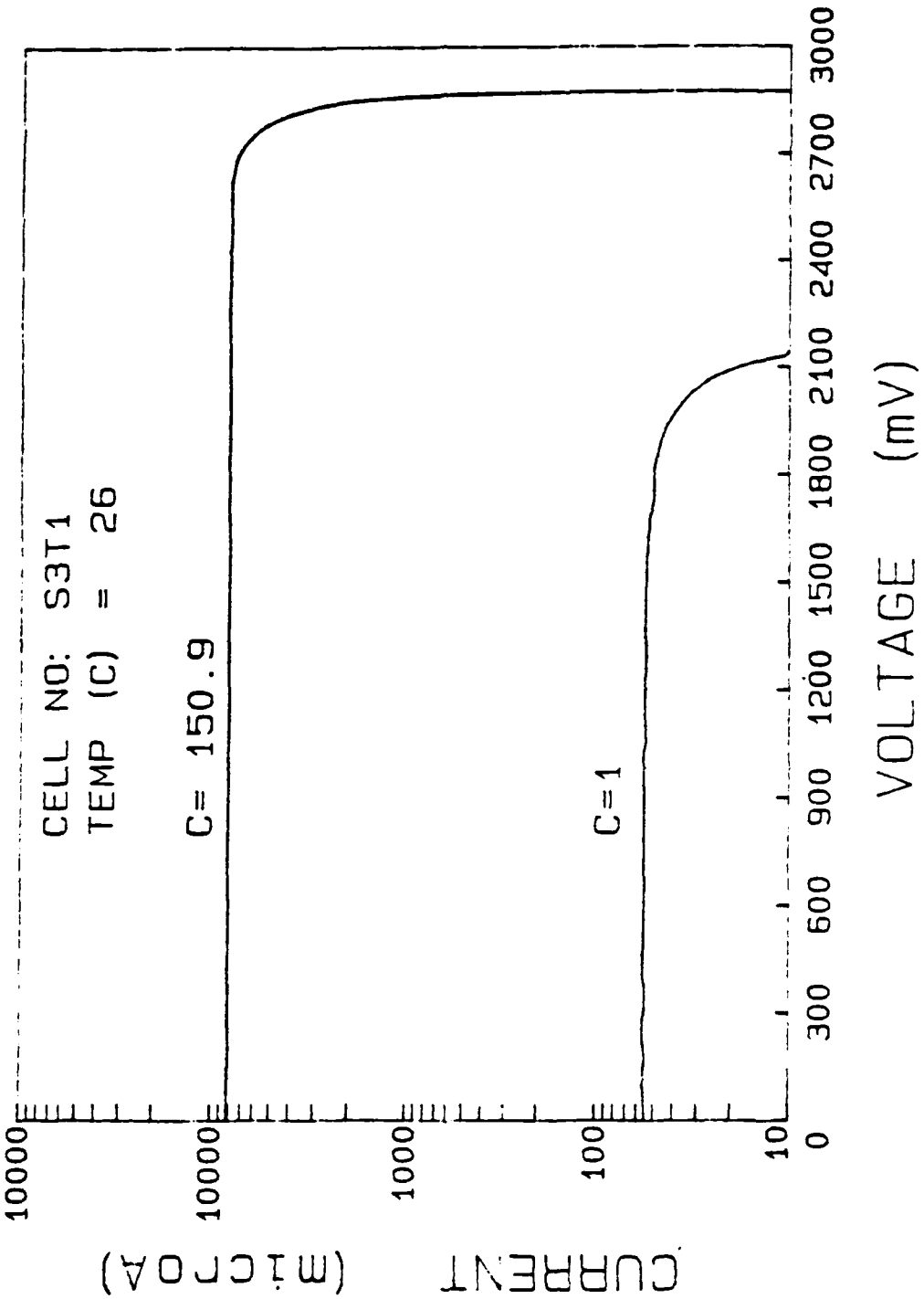

Figure 28. Comparison of the Top String I-V Curves at 1X and 150.9X

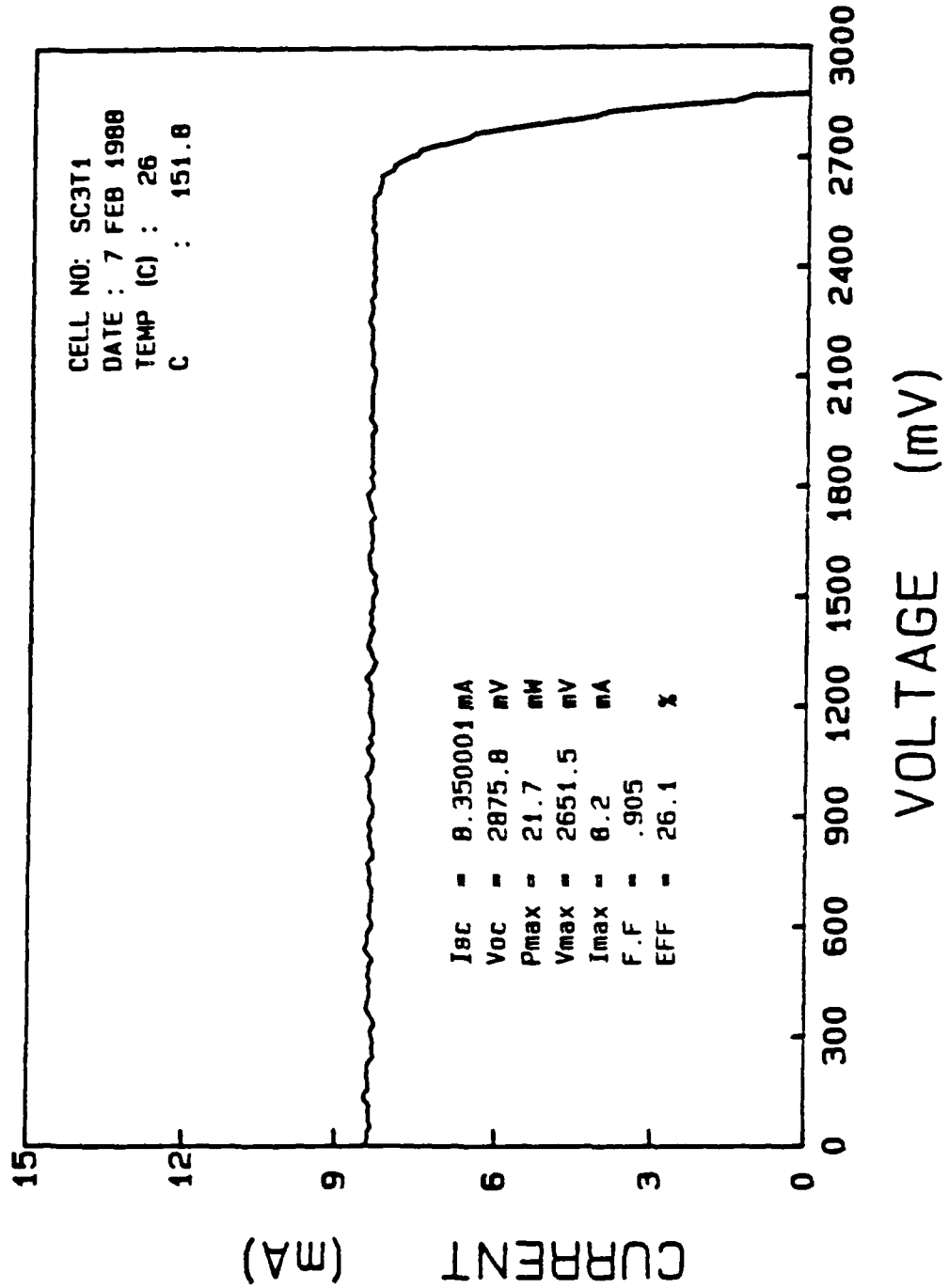

Figure 29. I-V Curve of Top String at 151.8X

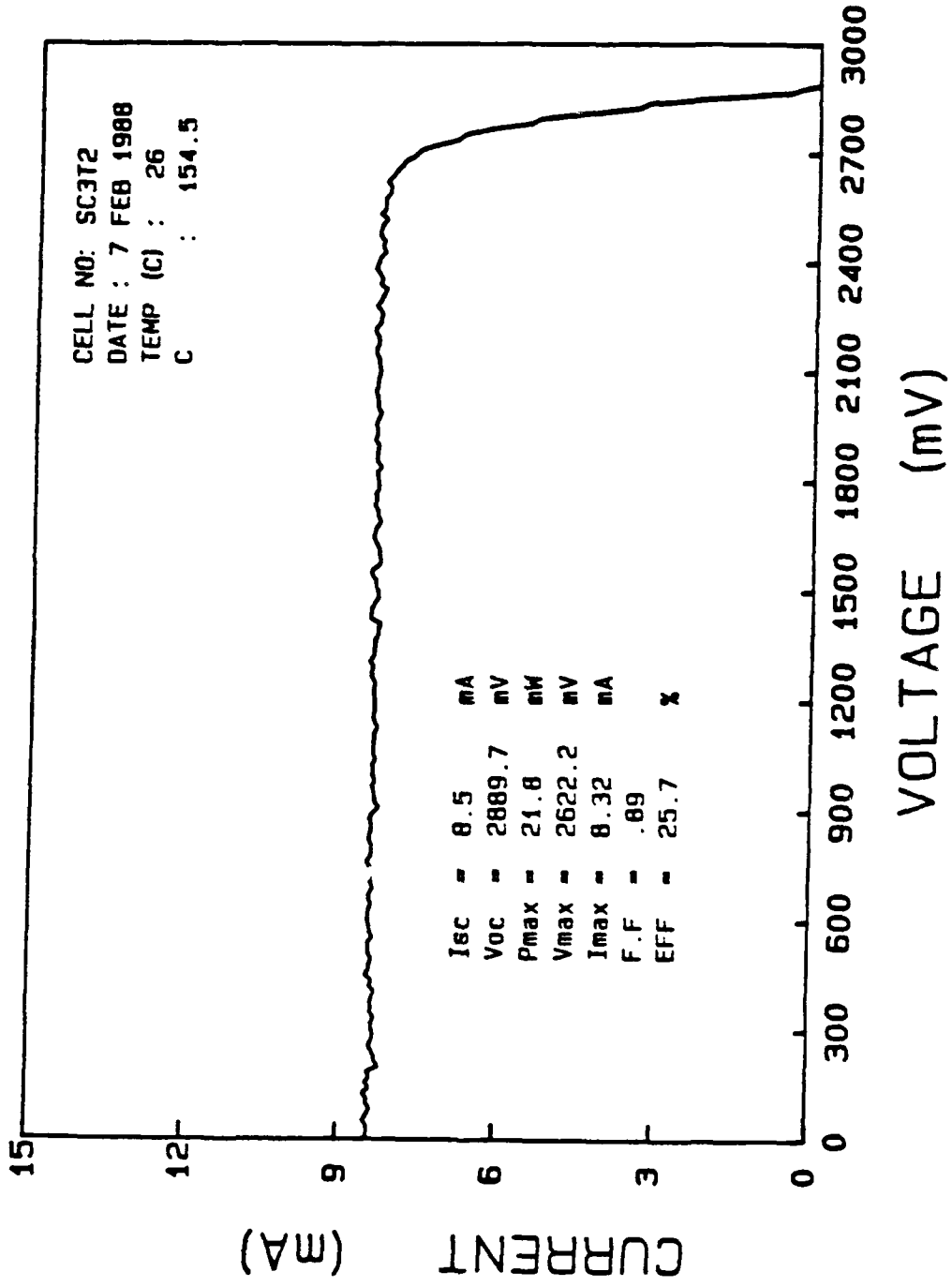

Figure 30. I-V Curve of Top String at 154.5X

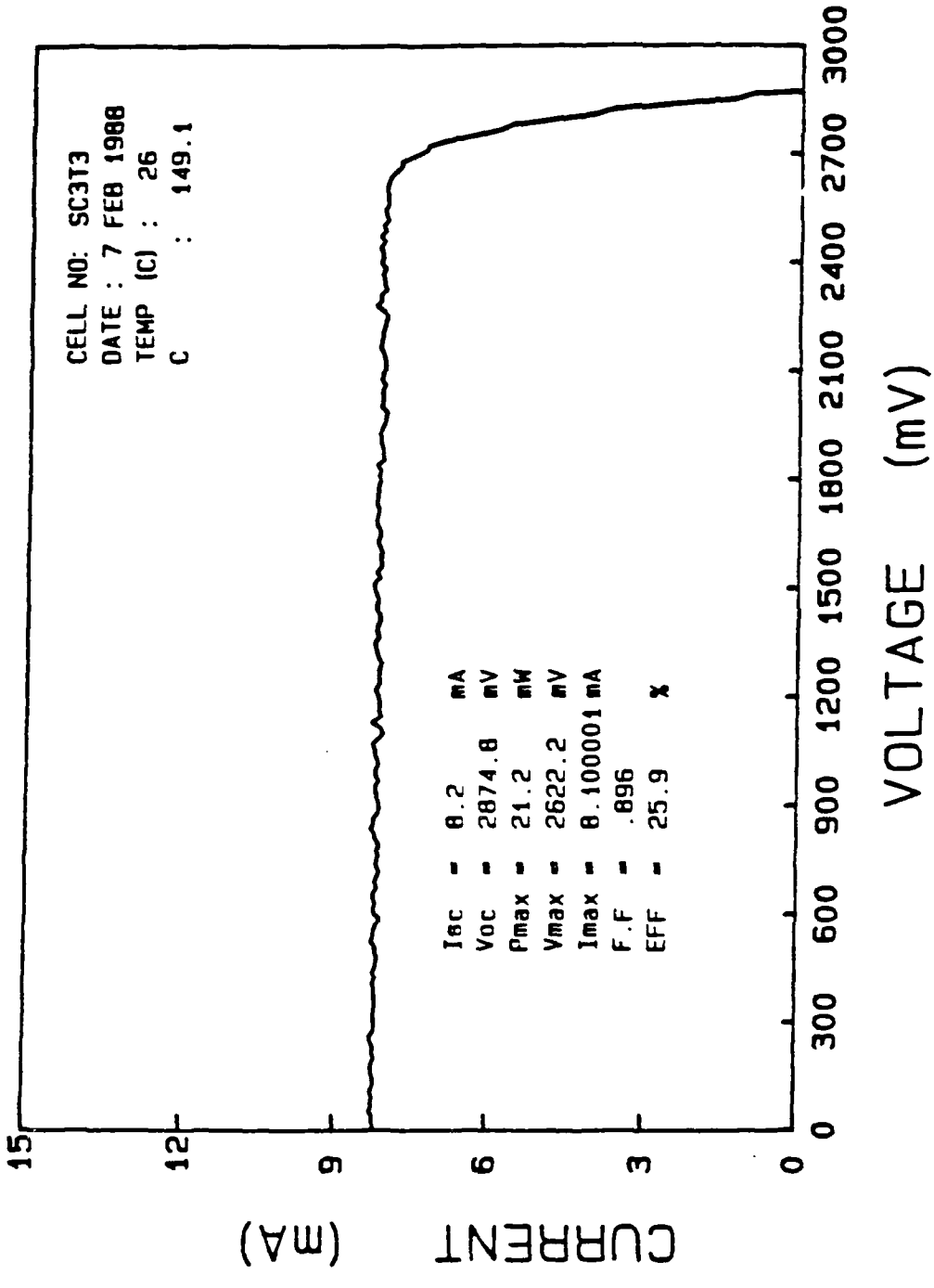

Figure 31. I-V Curve of Top String at 149.1X

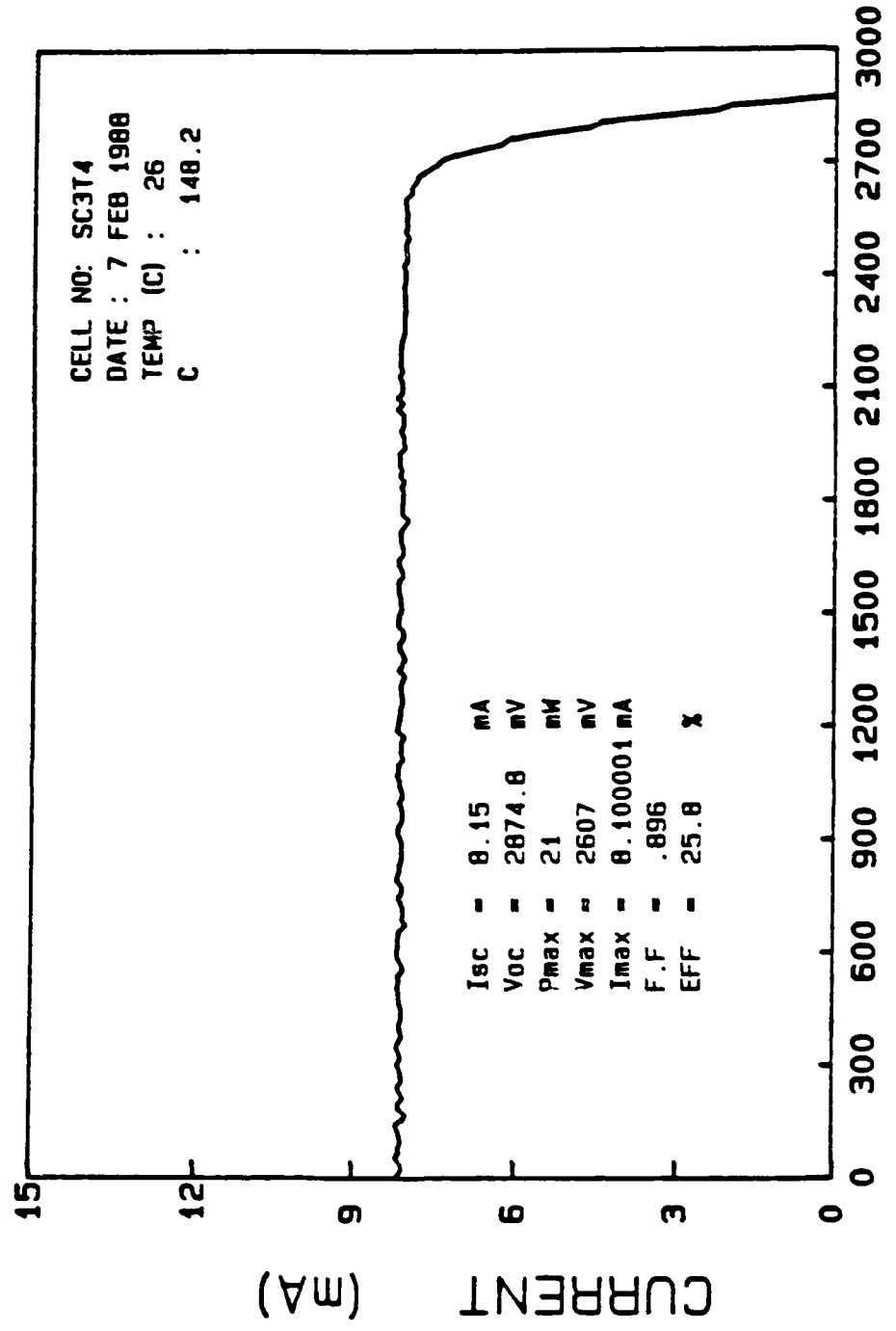

Figure 32. I-V Curve of Top String at 148.2X

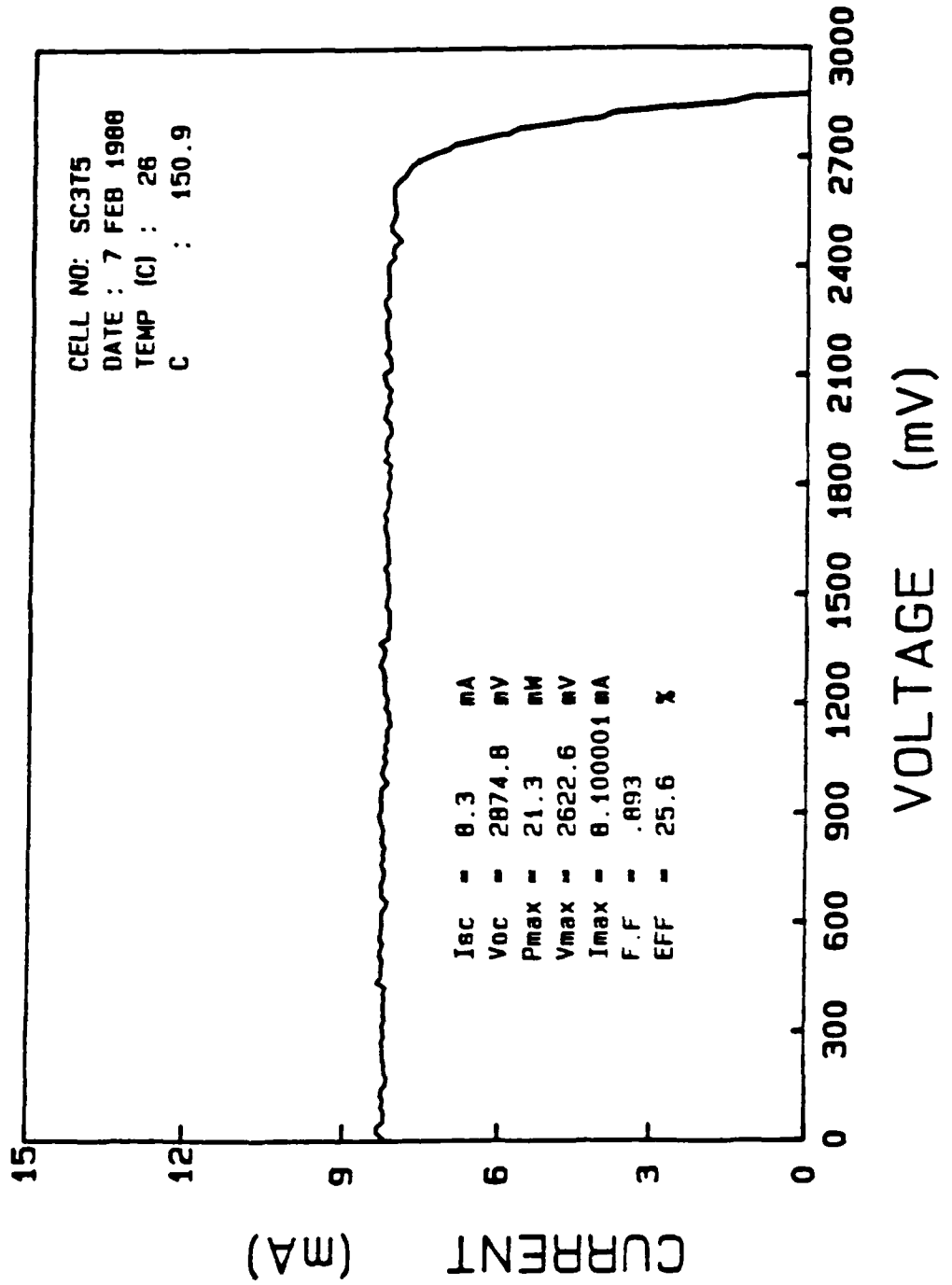

Figure 33. I-V Curve of Top String at 150.9X

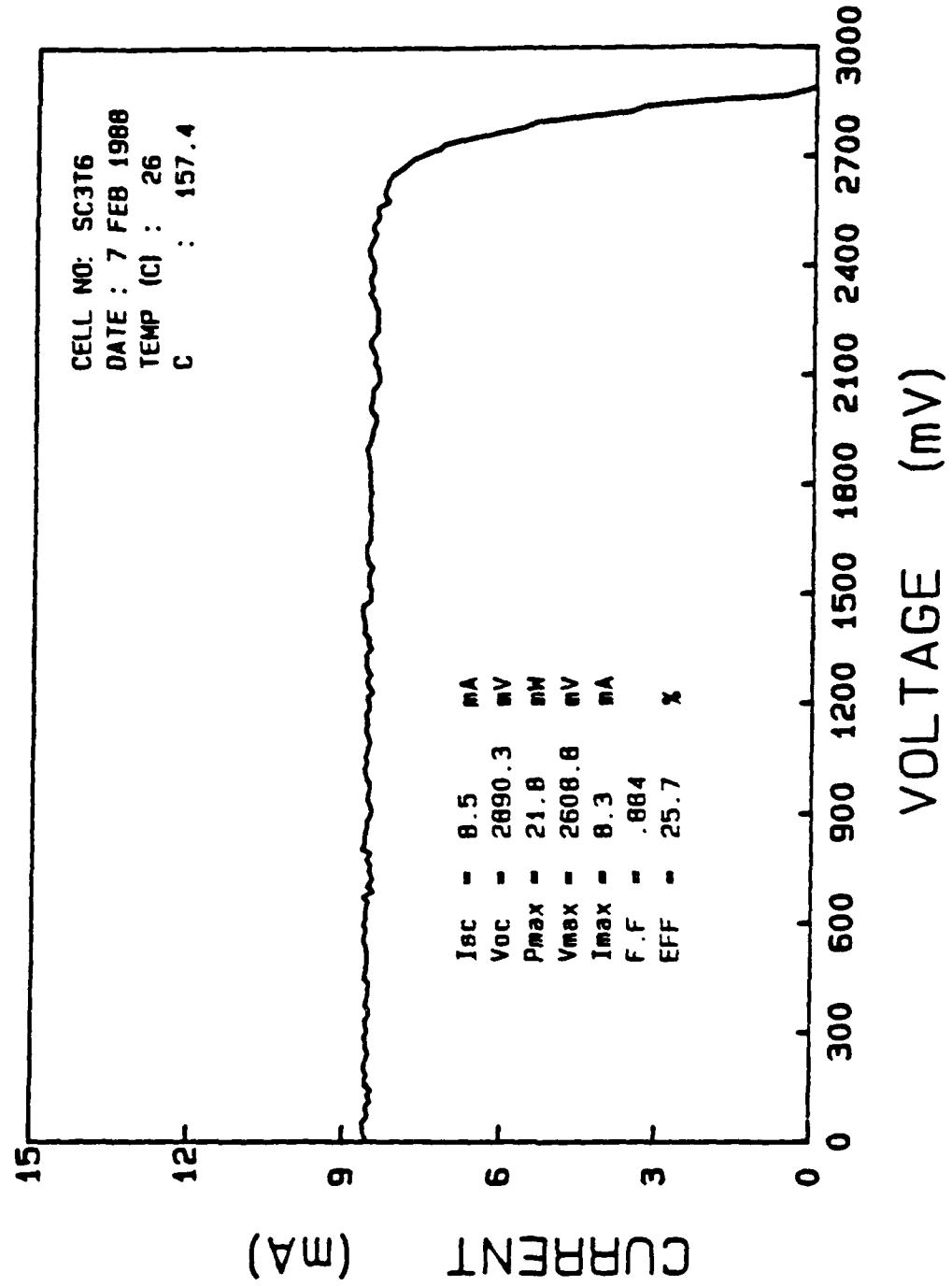

Figure 34. I-V Curve of Top String at 157.4X

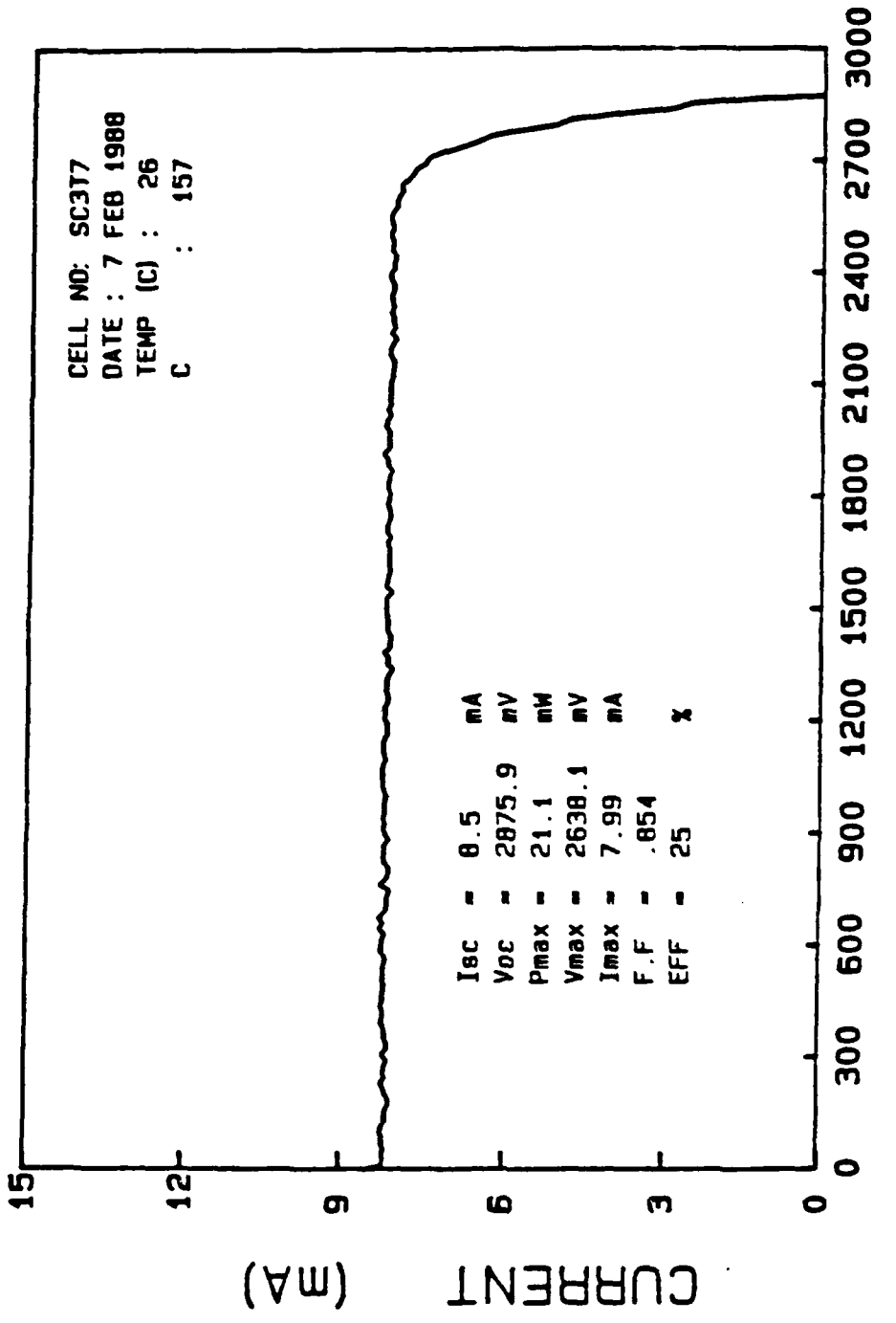

Figure 35. I-V Curve of Top String at 157.0X

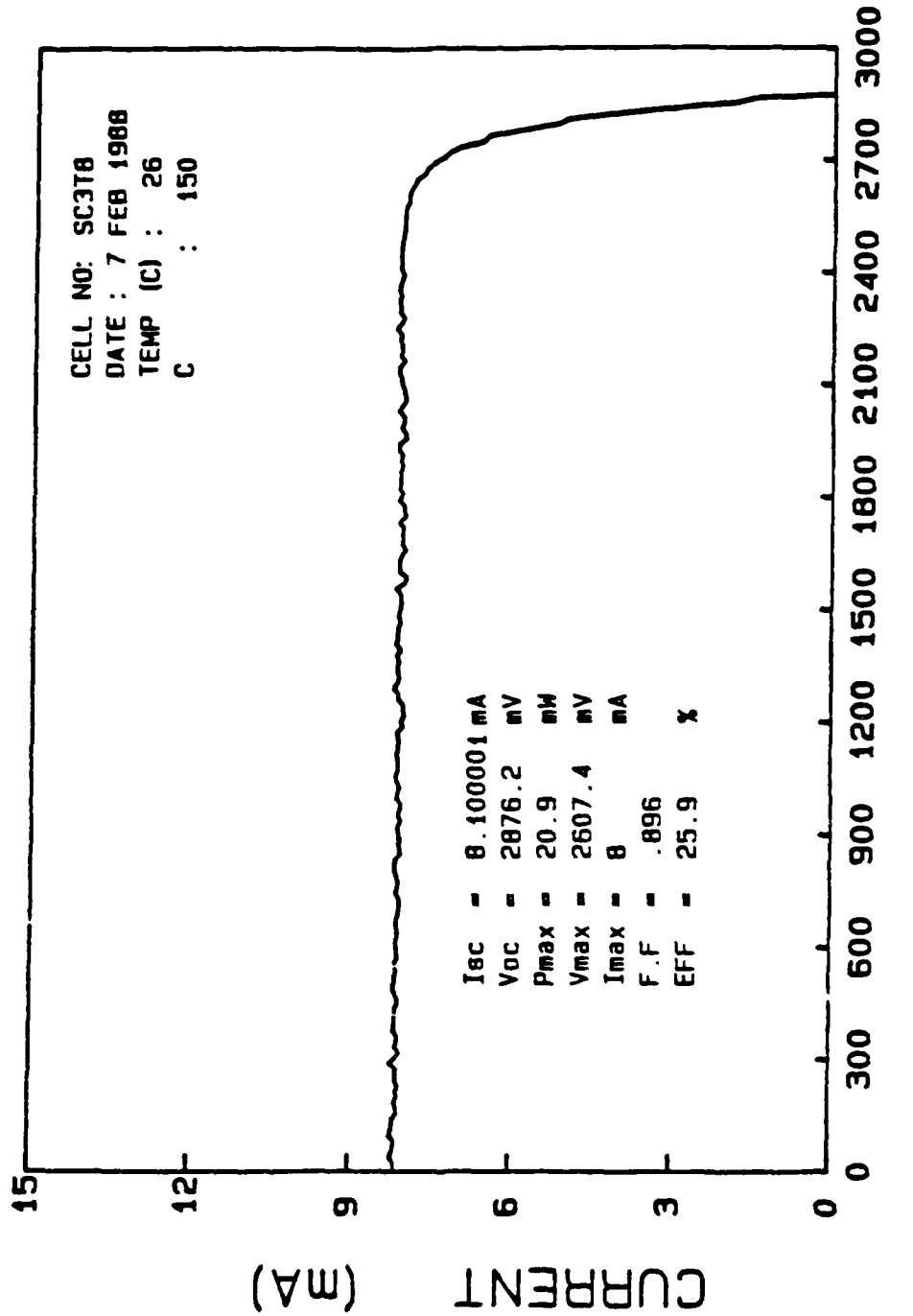

Figure 36. I-V Curve of Top String at 150.0X

APPENDIX D. SCA I-V CURVE TEST RESULTS FOR MIDDLE STRING

Figure 37 on page 78 gives the I-V curve of the intensity test for the middle string. Figure 38 on page 79 is the I-V curve of the middle string at a concentration ratio (CR) equal to one. Figure 39 on page 80 is the comparison of the unconcentrated curve to the average concentrated curve. Figure 40 on page 81 through Figure 47 on page 88 are the I-V curves of the eight concentrated middle string test.

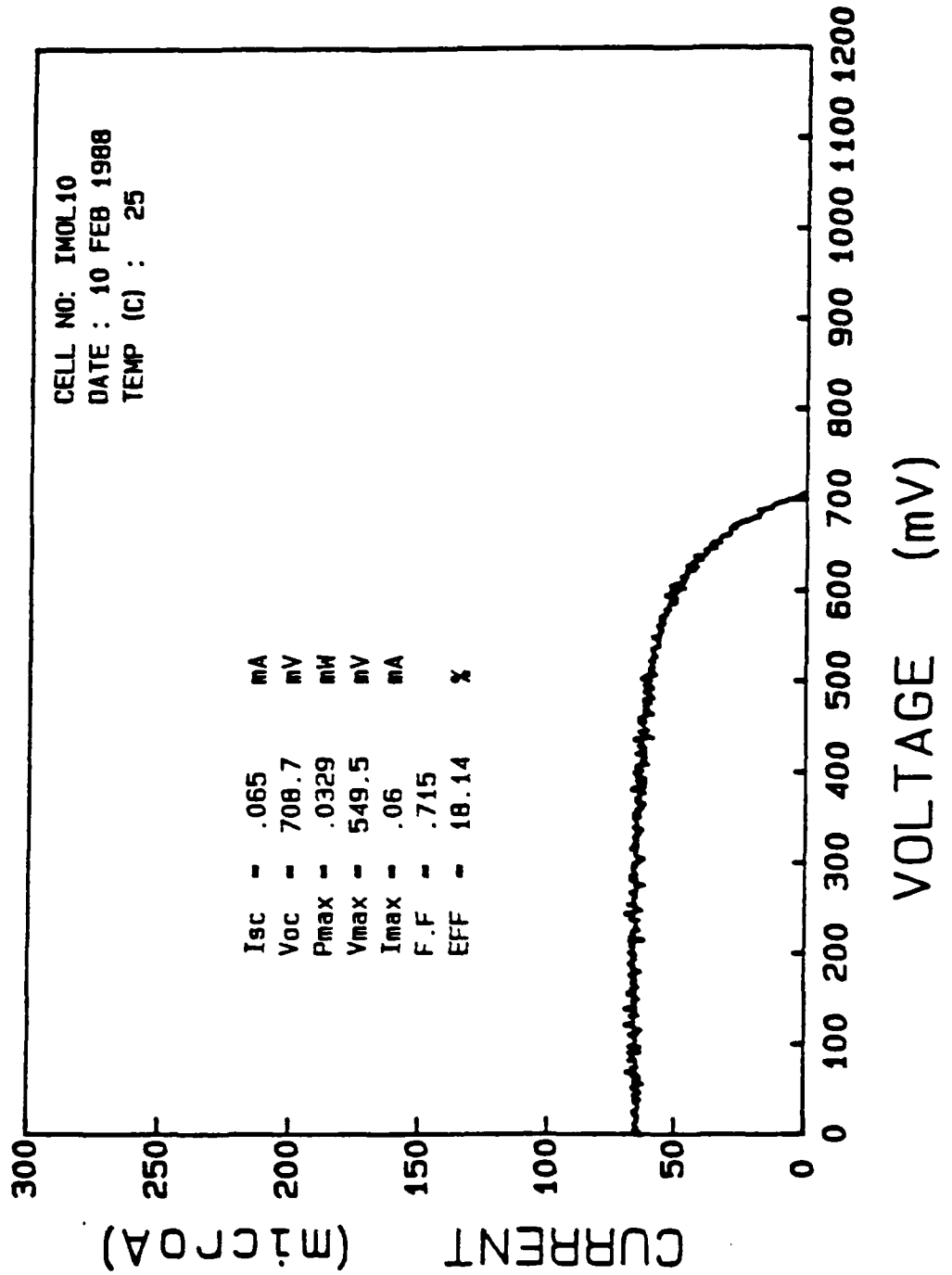

Figure 37. I-V Curve of the Middle String Intensity Test

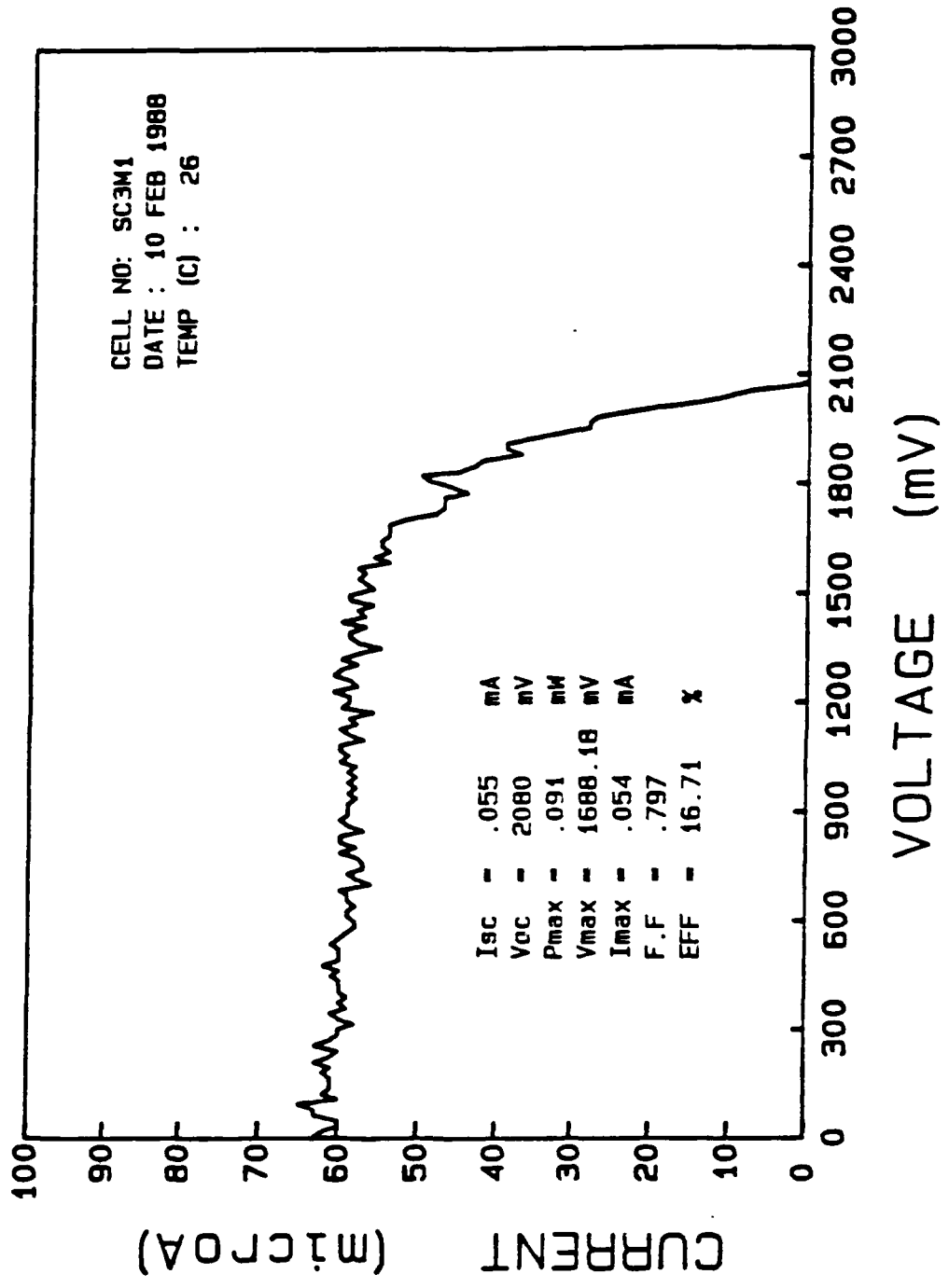

Figure 38. I-V Curve of Middle String (Unconcentrated)

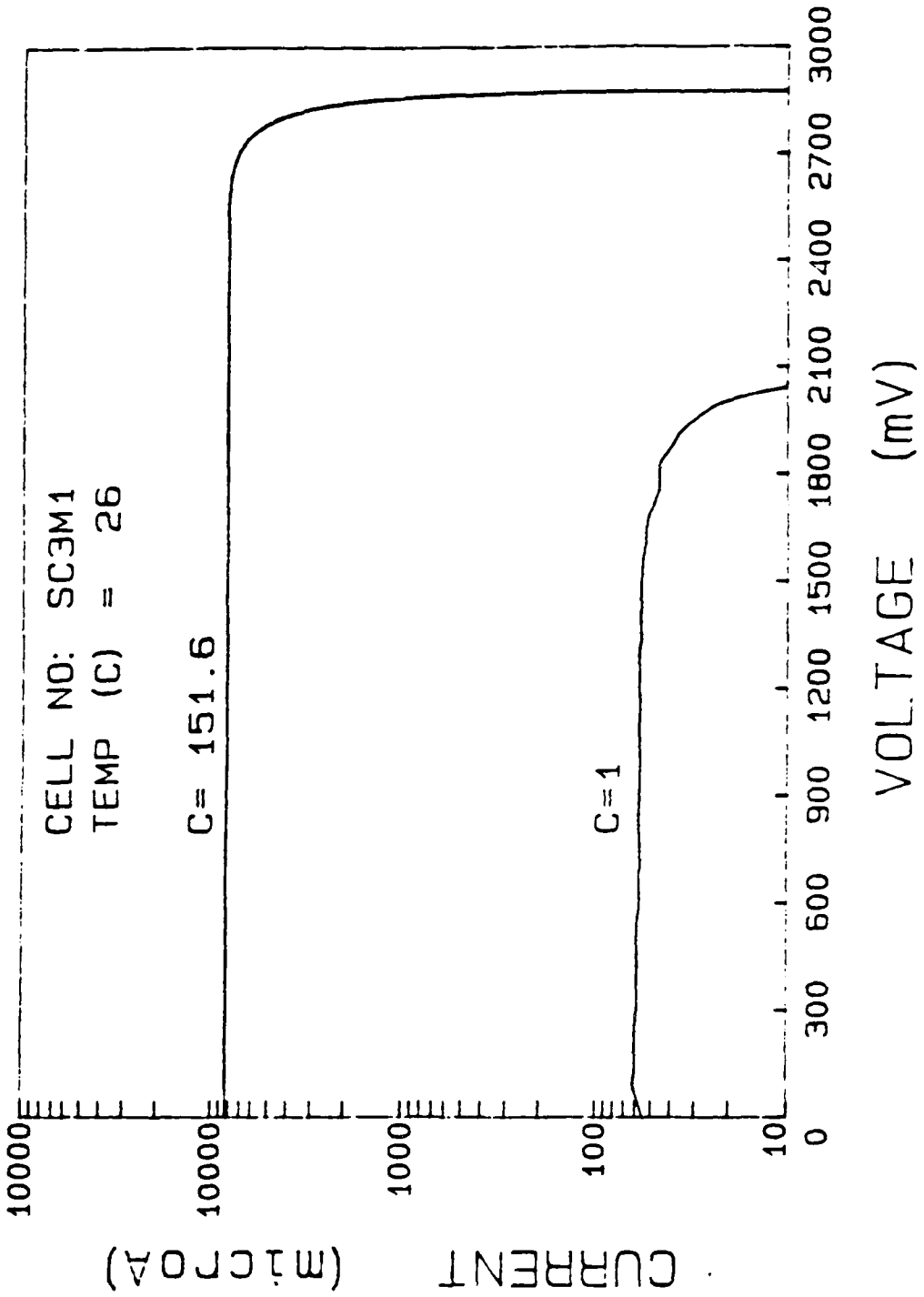

Figure 39. Comparison of the Middle String I-V Curves at 1X and 151.6X

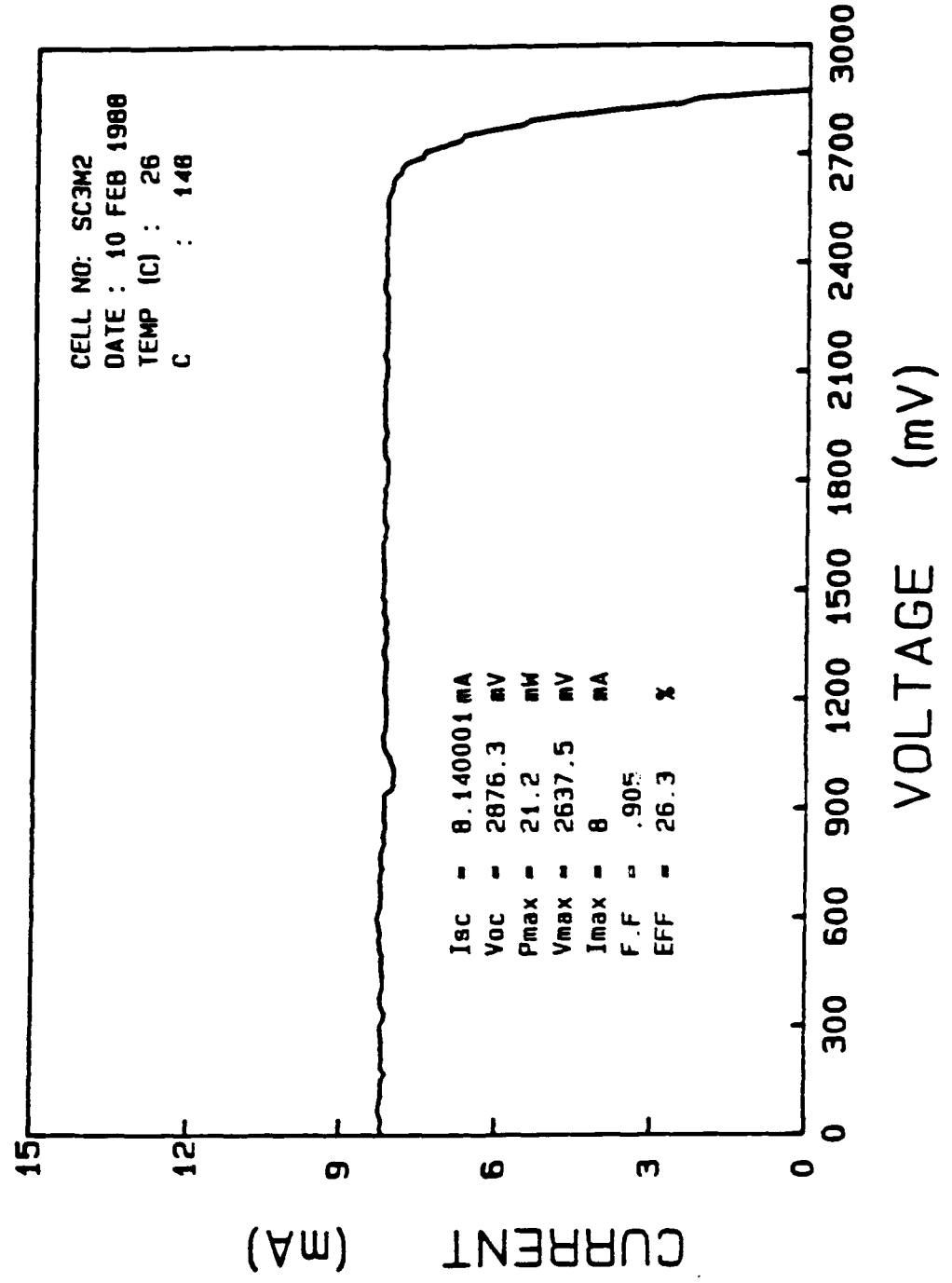

Figure 40. I-V Curve of Middle String at 148.0X

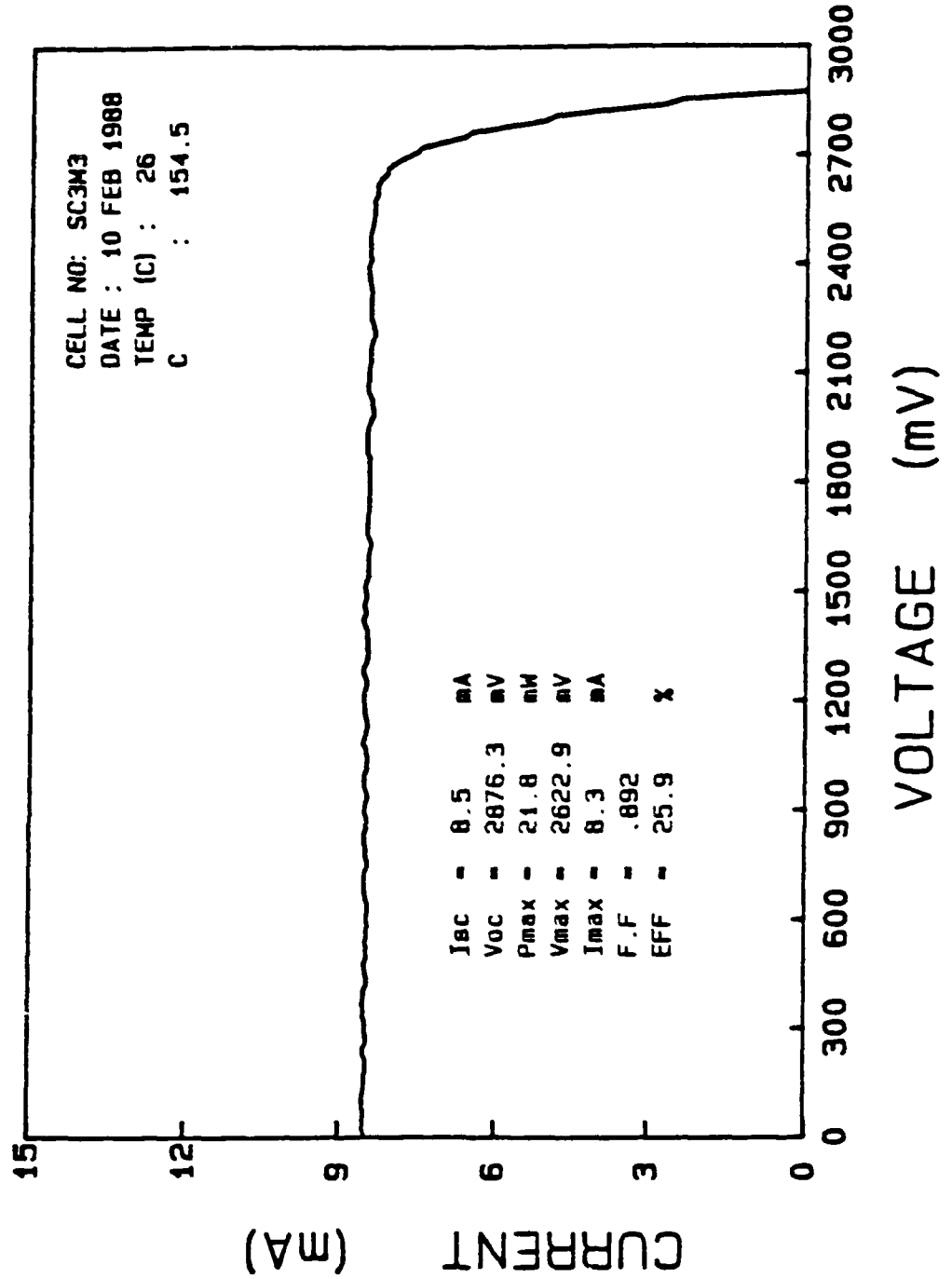

Figure 41. I-V Curve of Middle String at 154.5X

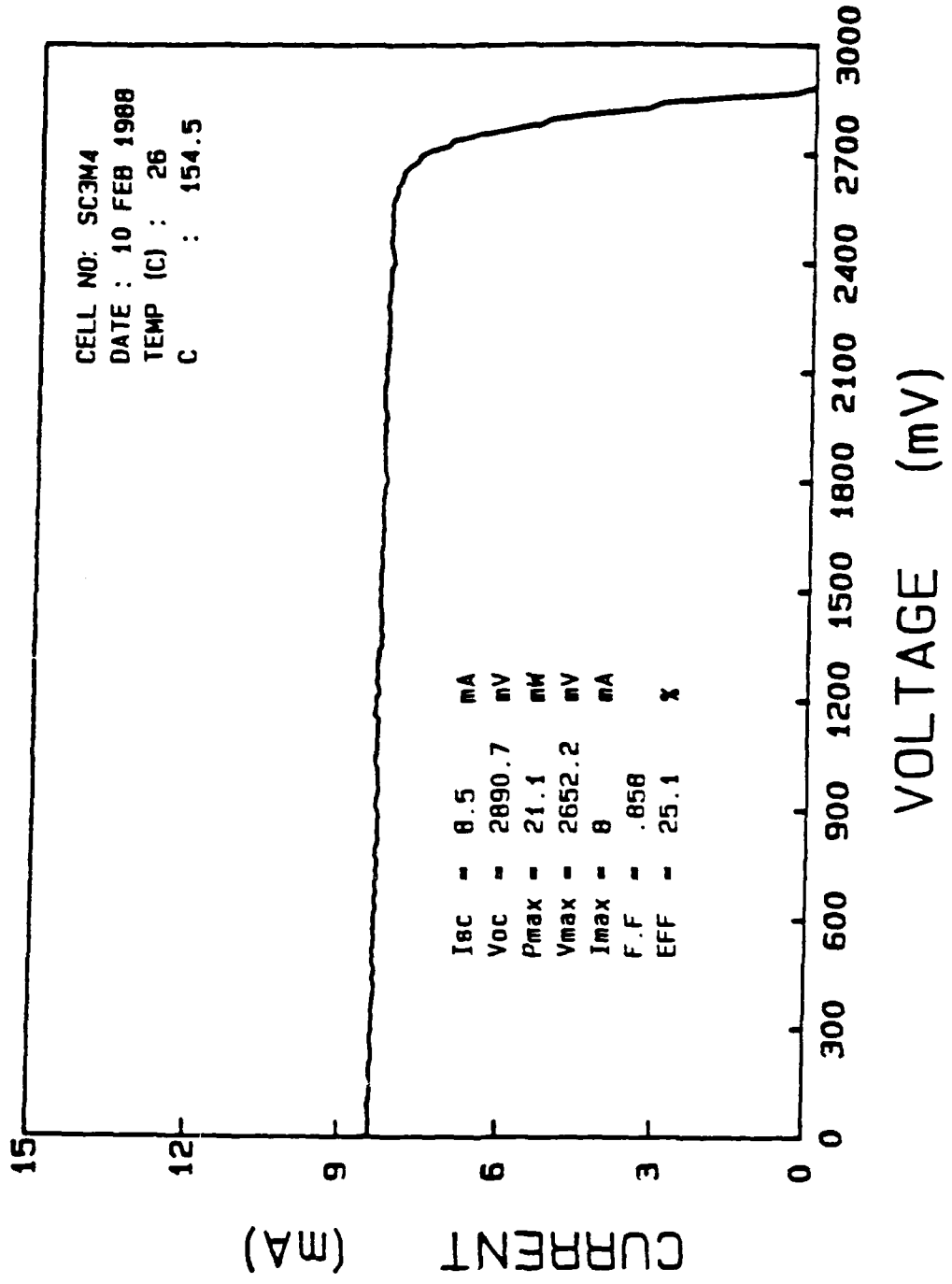

Figure 42. I-V Curve of Middle String at 154.5X

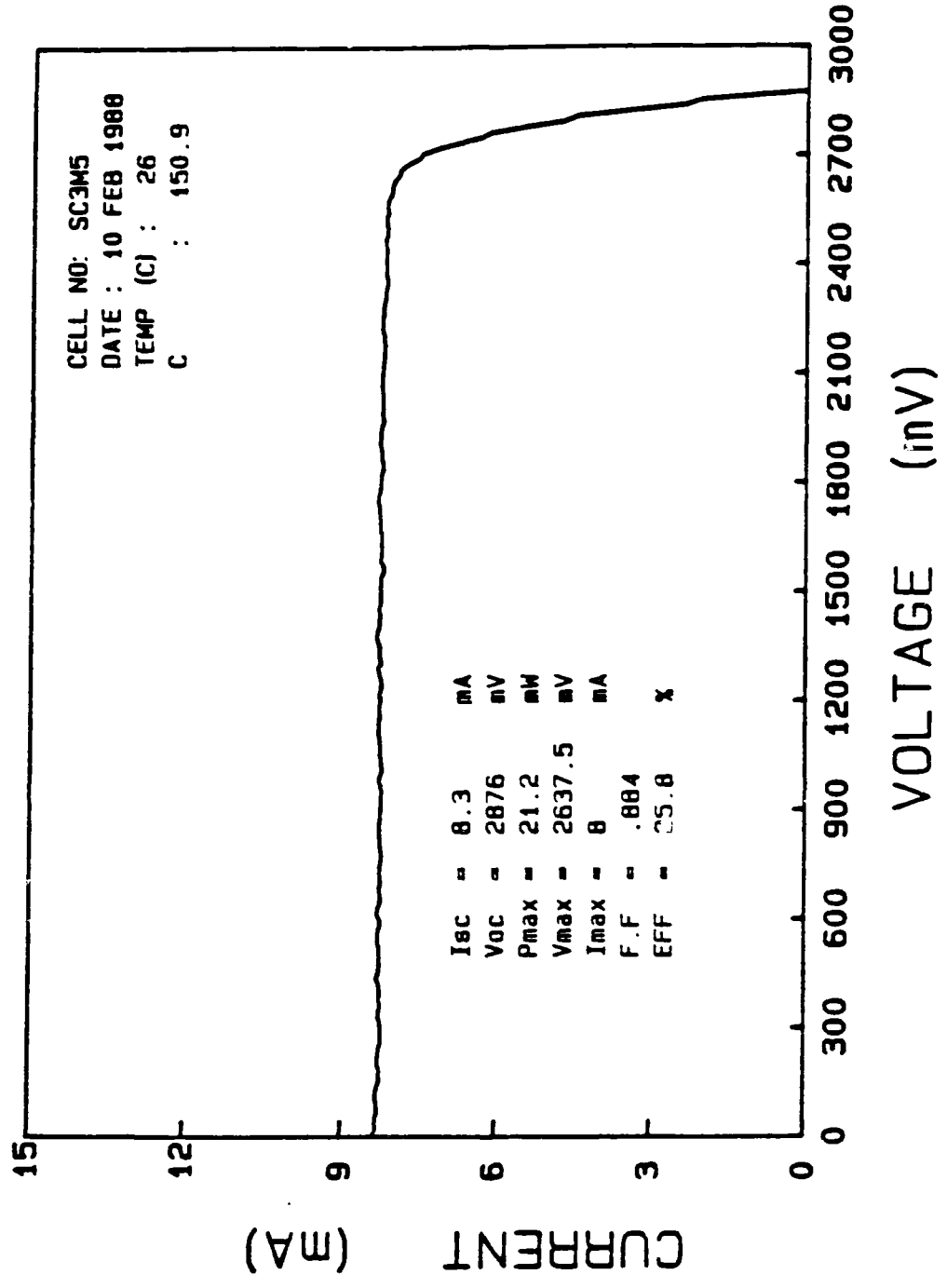

Figure 43. I-V Curve of Middle String at 150.9X

AD-A194 658 CONSTRUCTION OF GALLIUM ARSENIDE SOLAR CONCENTRATOR FOR SPACE USE(U) NAVAL POSTGRADUATE SCHOOL MONTEREY CA C L HUDEC MAR 88 2/2

UNCLASSIFIED F/G 9/1 NL

END
DATE FILMED
8 8

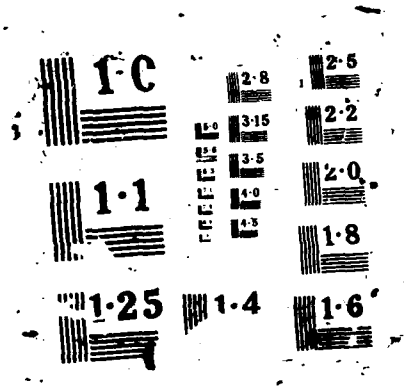
1·C
1·1
1·25
2·8
3·15
3·5
4·0
4·5
1·4
2·5
2·2
2·0
1·8
1·6

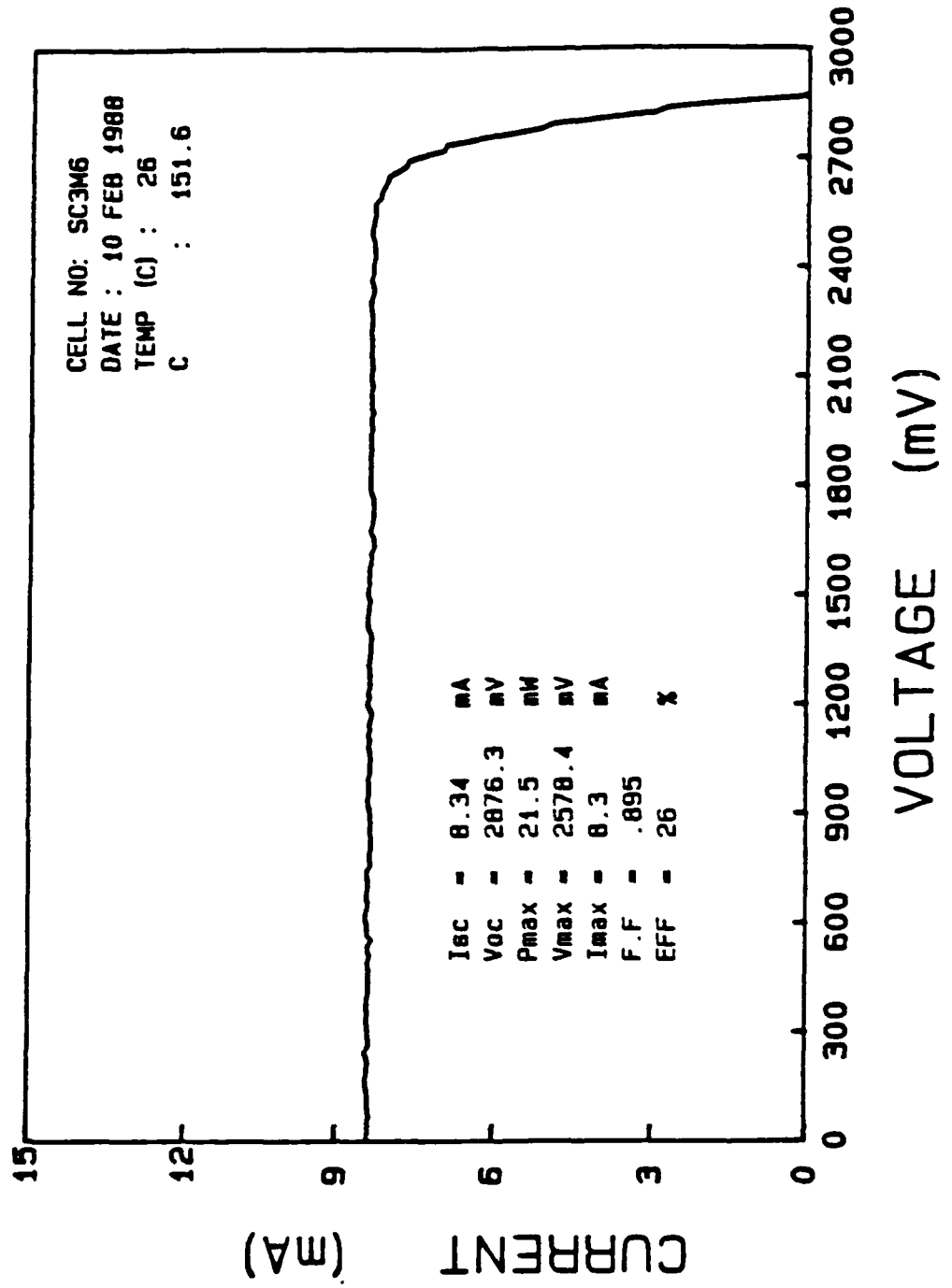

Figure 44. I-V Curve of Middle String at 151.6X

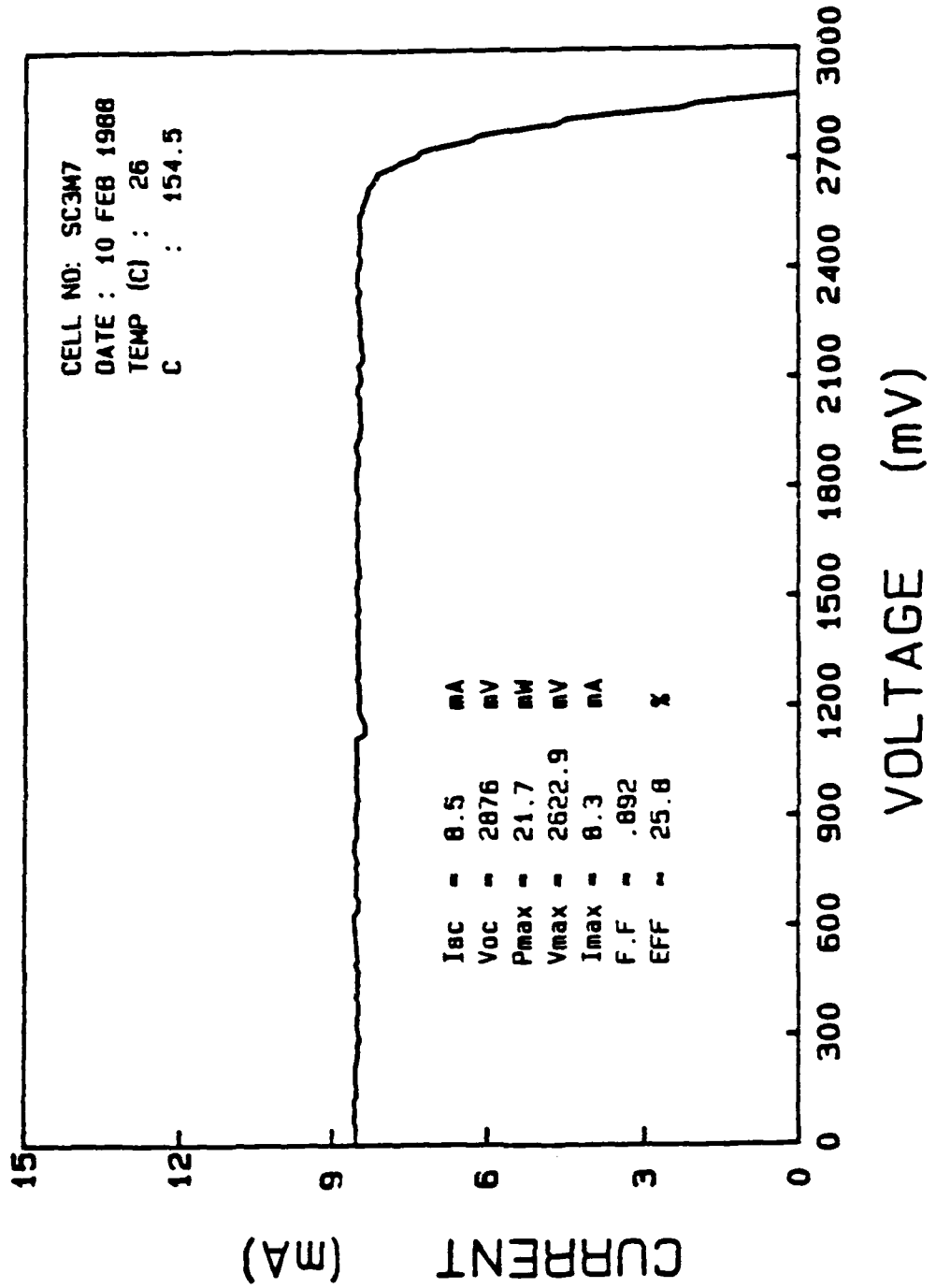

Figure 45. I-V Curve of Middle String at 154.5X

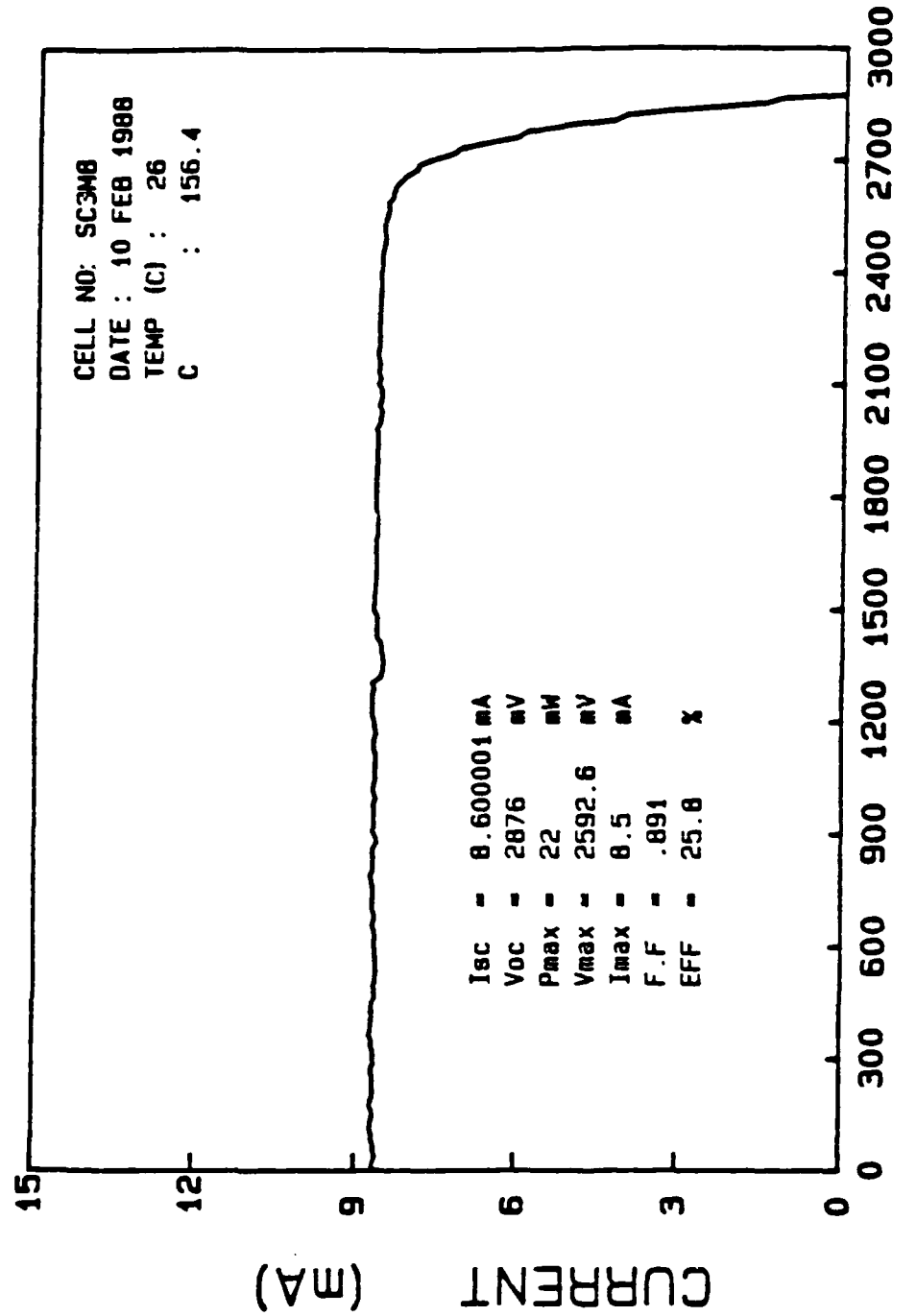

Figure 46. I-V Curve of Middle String at 156.4X

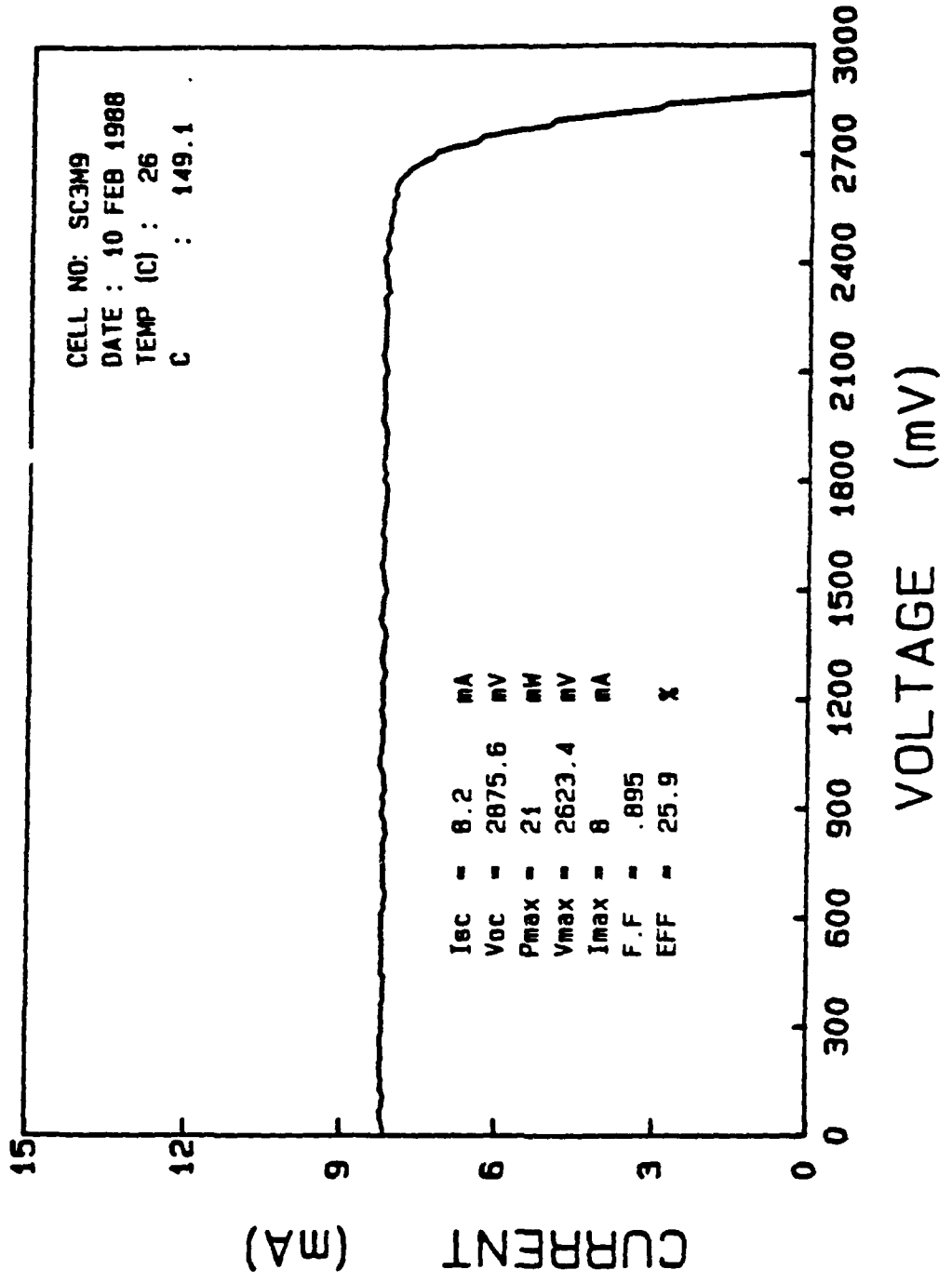

Figure 47. I-V Curve of Middle String at 149.1X

APPENDIX E. SCA I-V CURVE TEST RESULTS FOR BOTTOM STRING

Figure 48 on page 90 gives the I-V curve of the intensity test for the bottom string. Figure 49 on page 91 is the I-V curve of the bottom string at a concentration ratio (CR) equal to one. Figure 50 on page 92 is the comparison of the unconcentrated curve to the average concentrated curve. Figure 51 on page 93 through Figure 58 on page 100 are the I-V curves of the eight concentrated bottom string test.

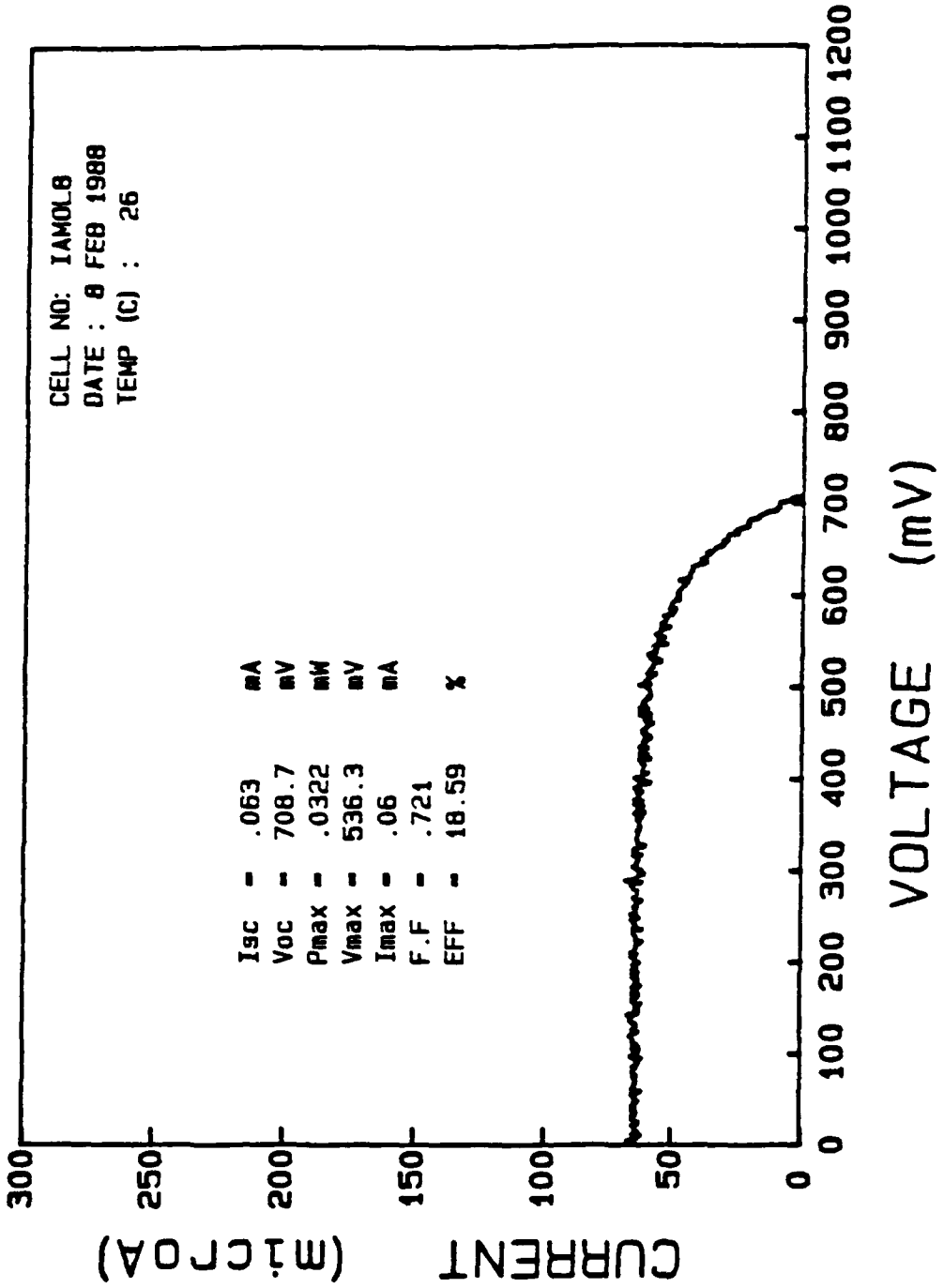

Figure 48. I-V Curve of the Bottom String Intensity Test

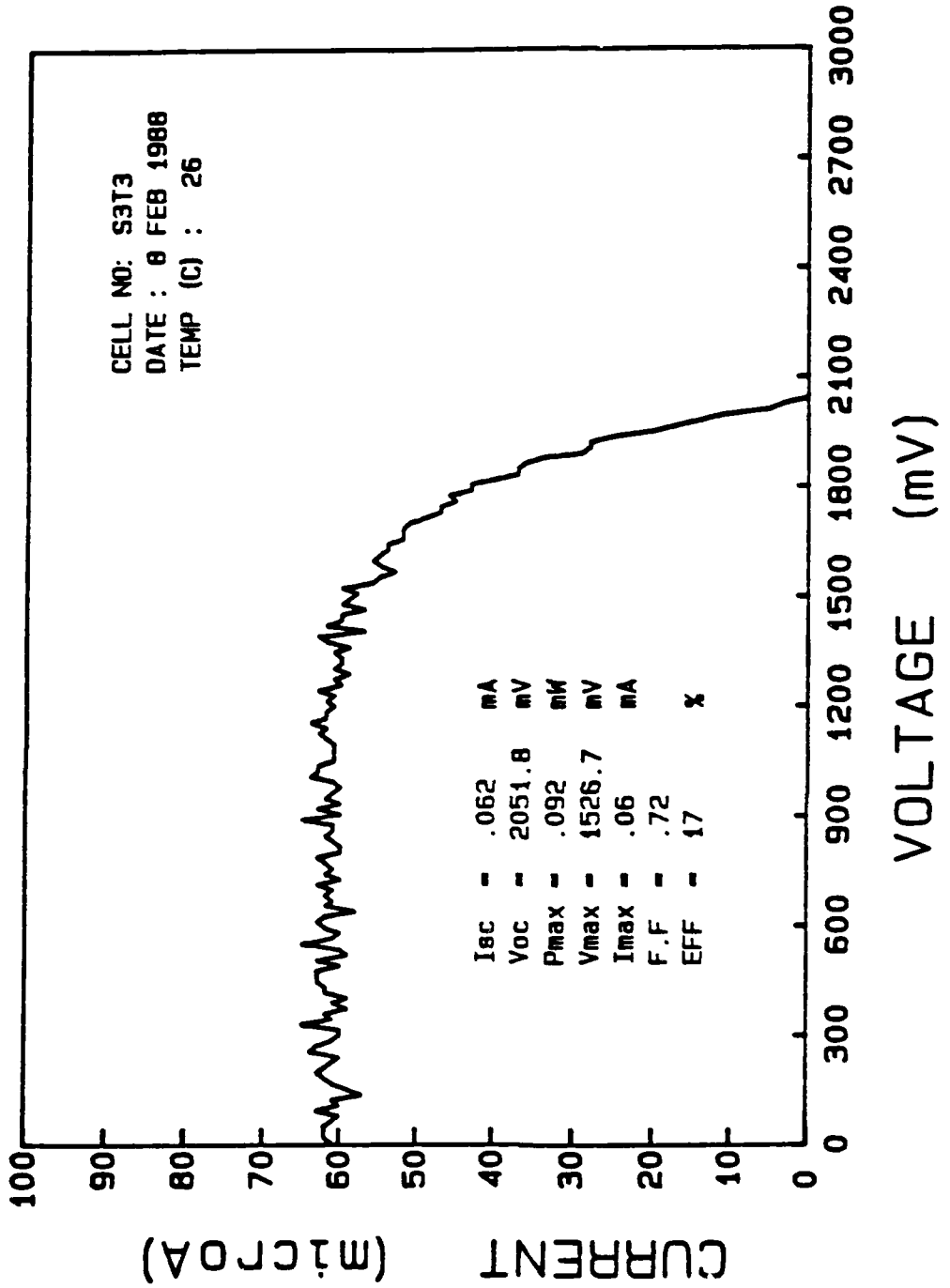

Figure 49. I-V Curve of Bottom String (Unconcentrated)

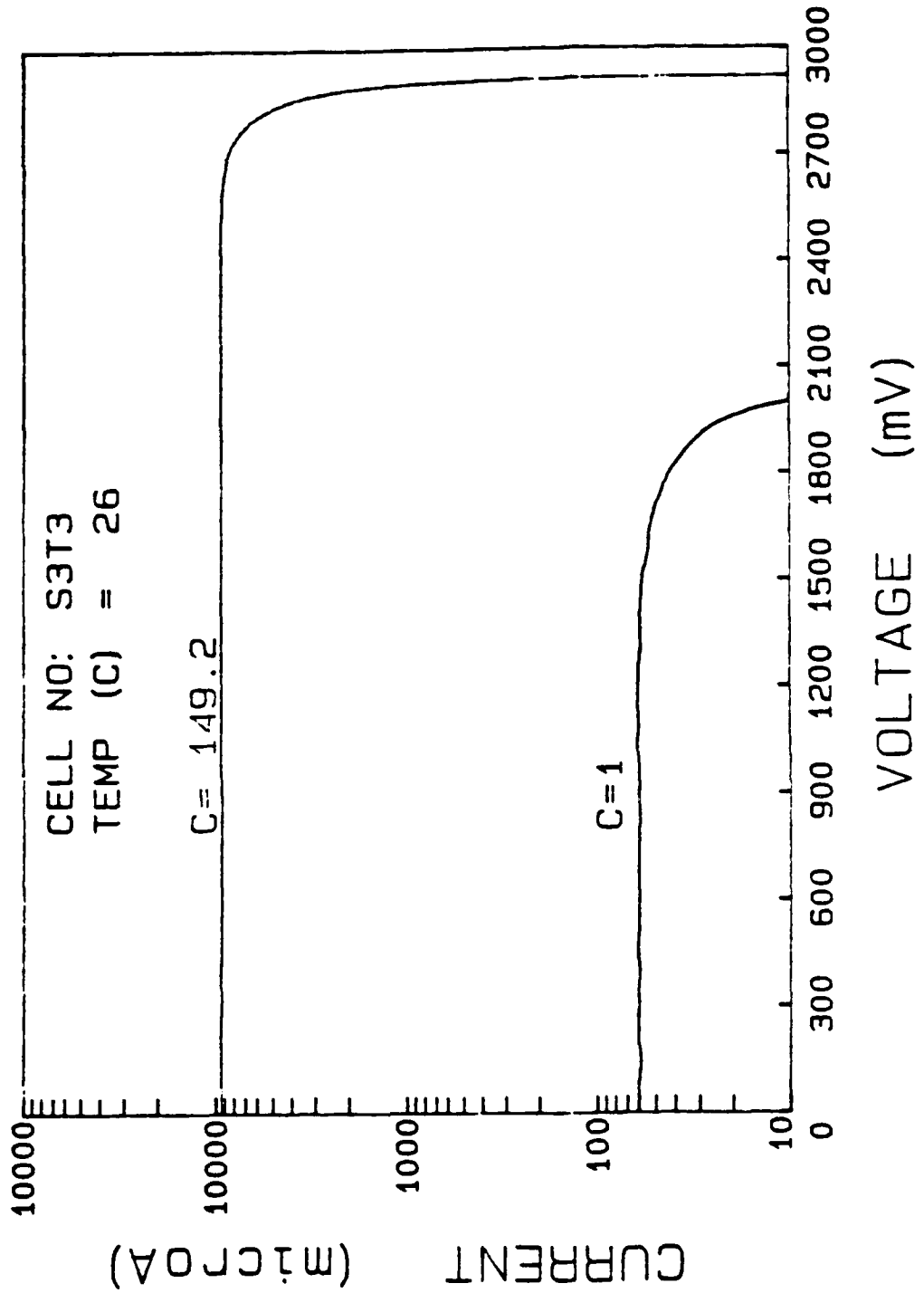

Figure 50. Comparison of the Bottom String I-V Curves at 1X and 149.2X

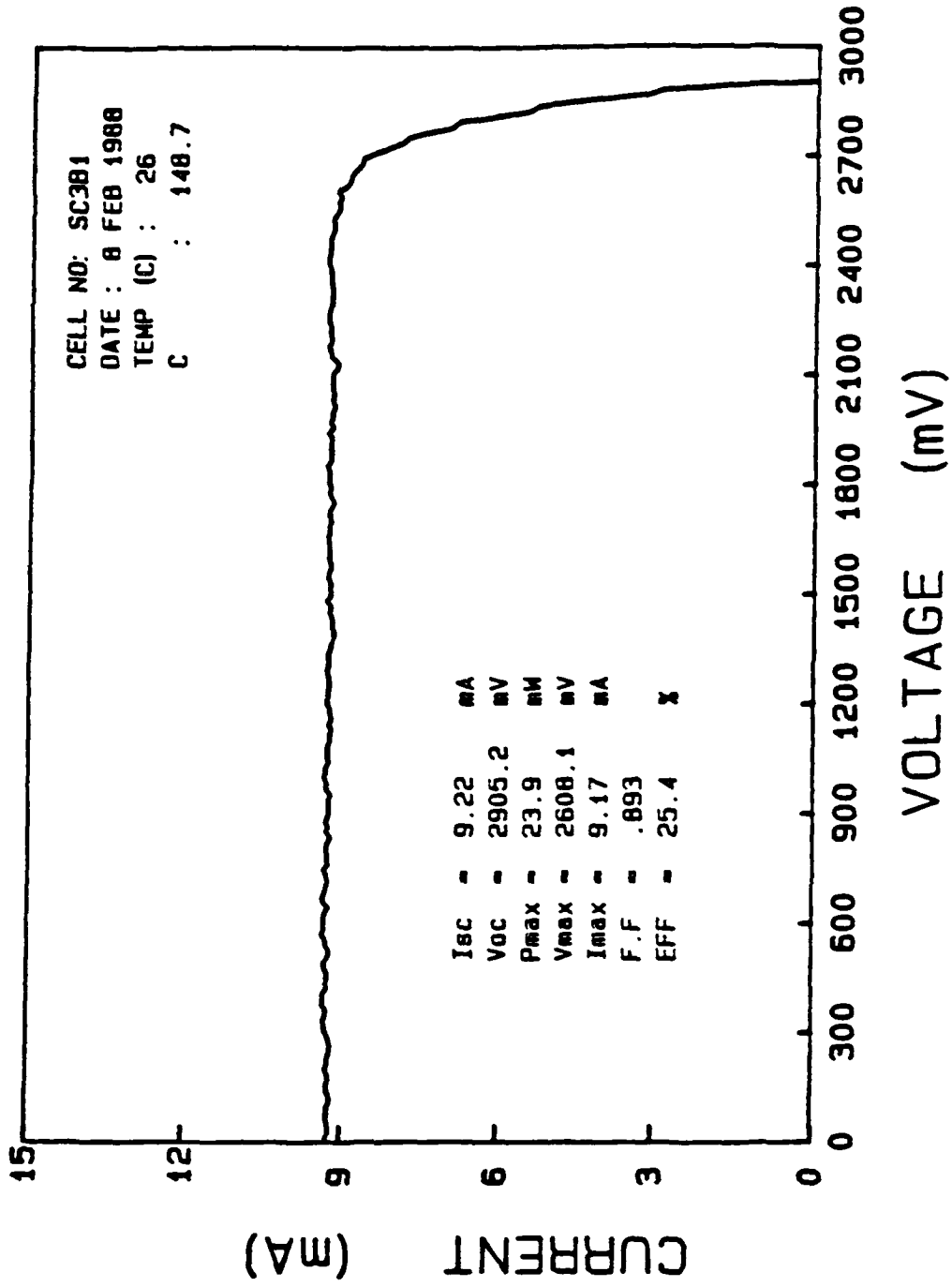

Figure 51. I-V Curve of Bottom String at 148.7X

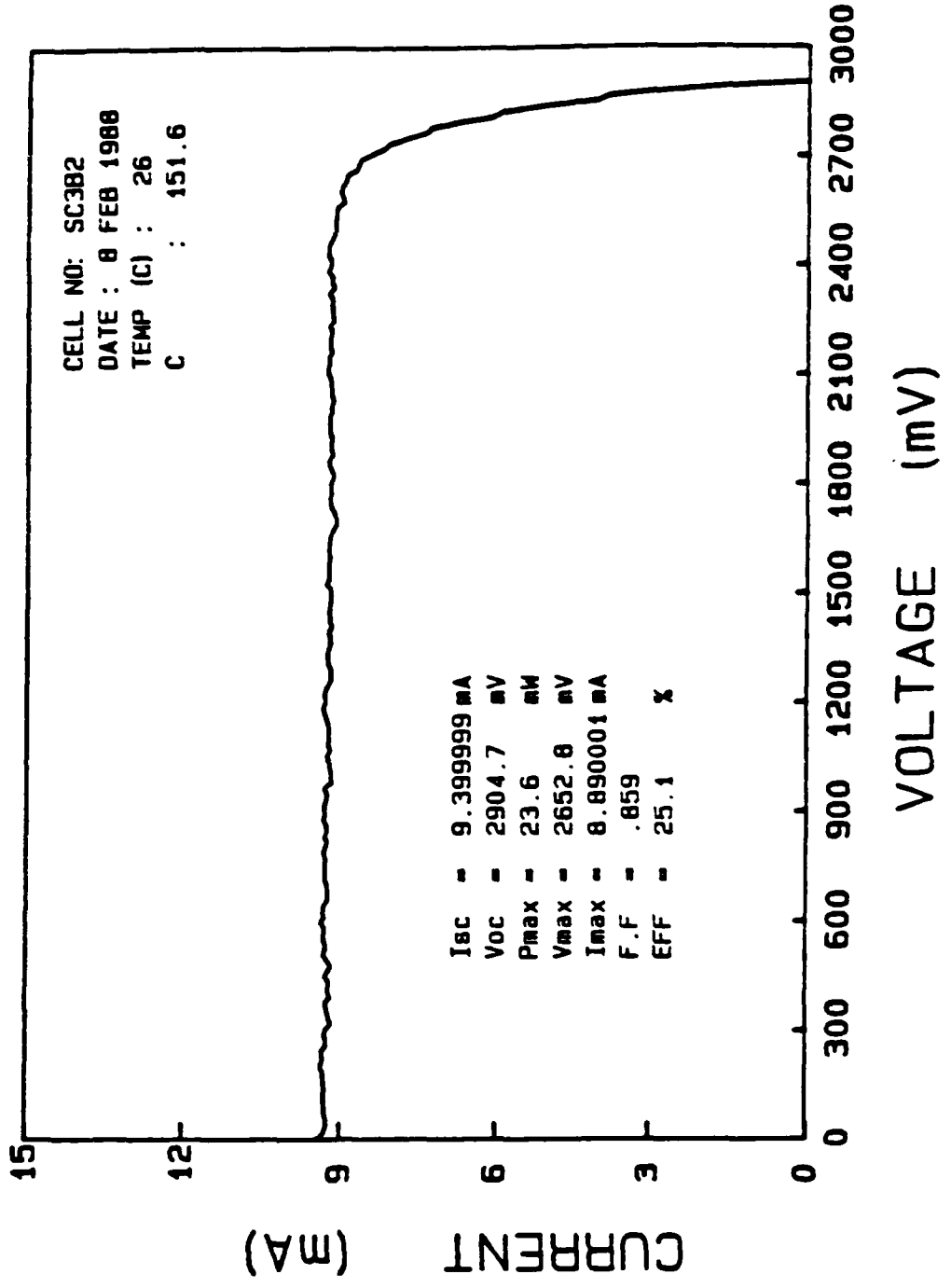

Figure 52. I-V Curve of Bottom String at 151.6X

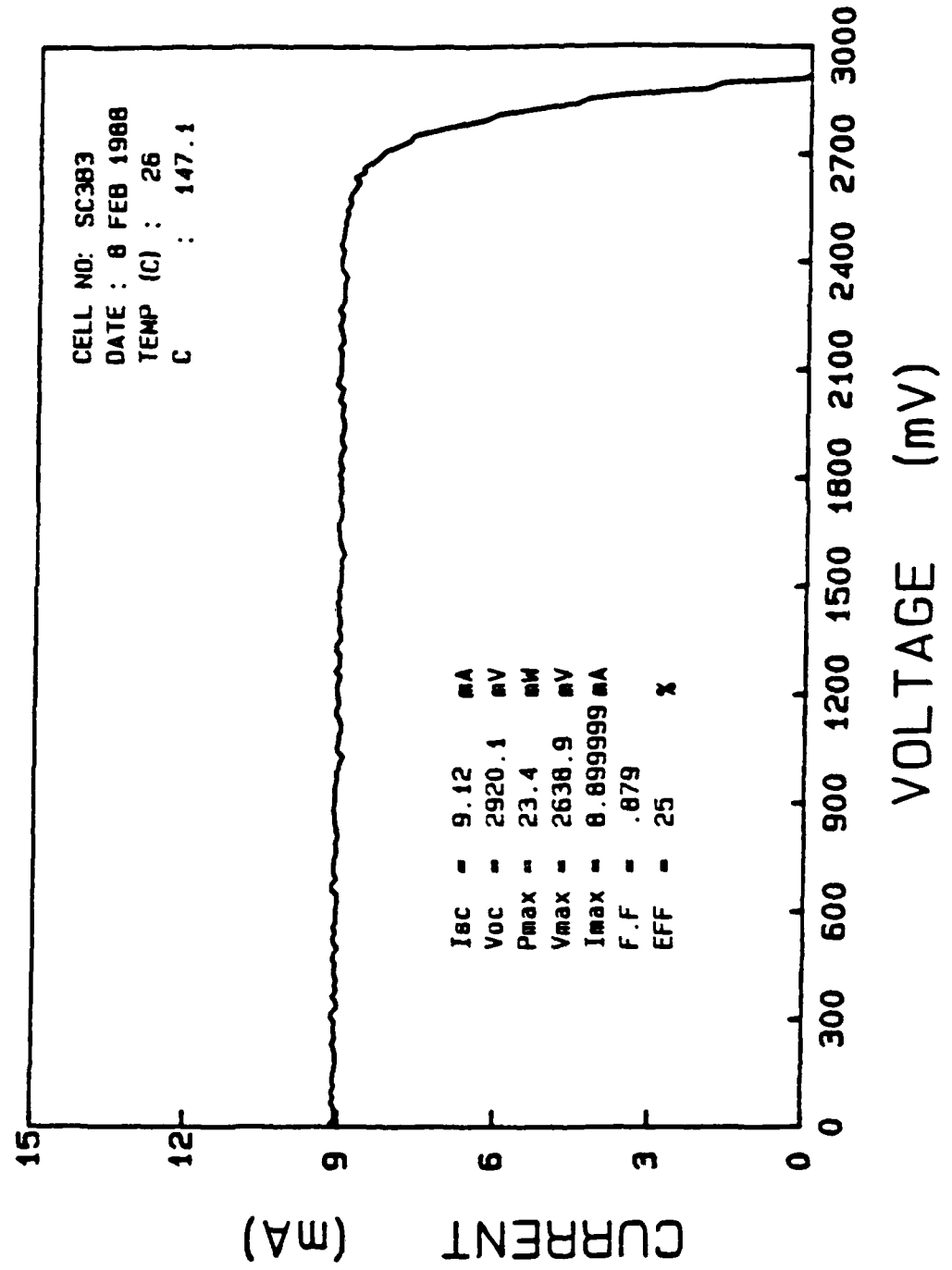

Figure 53. I-V Curve of Bottom String at 147.1X

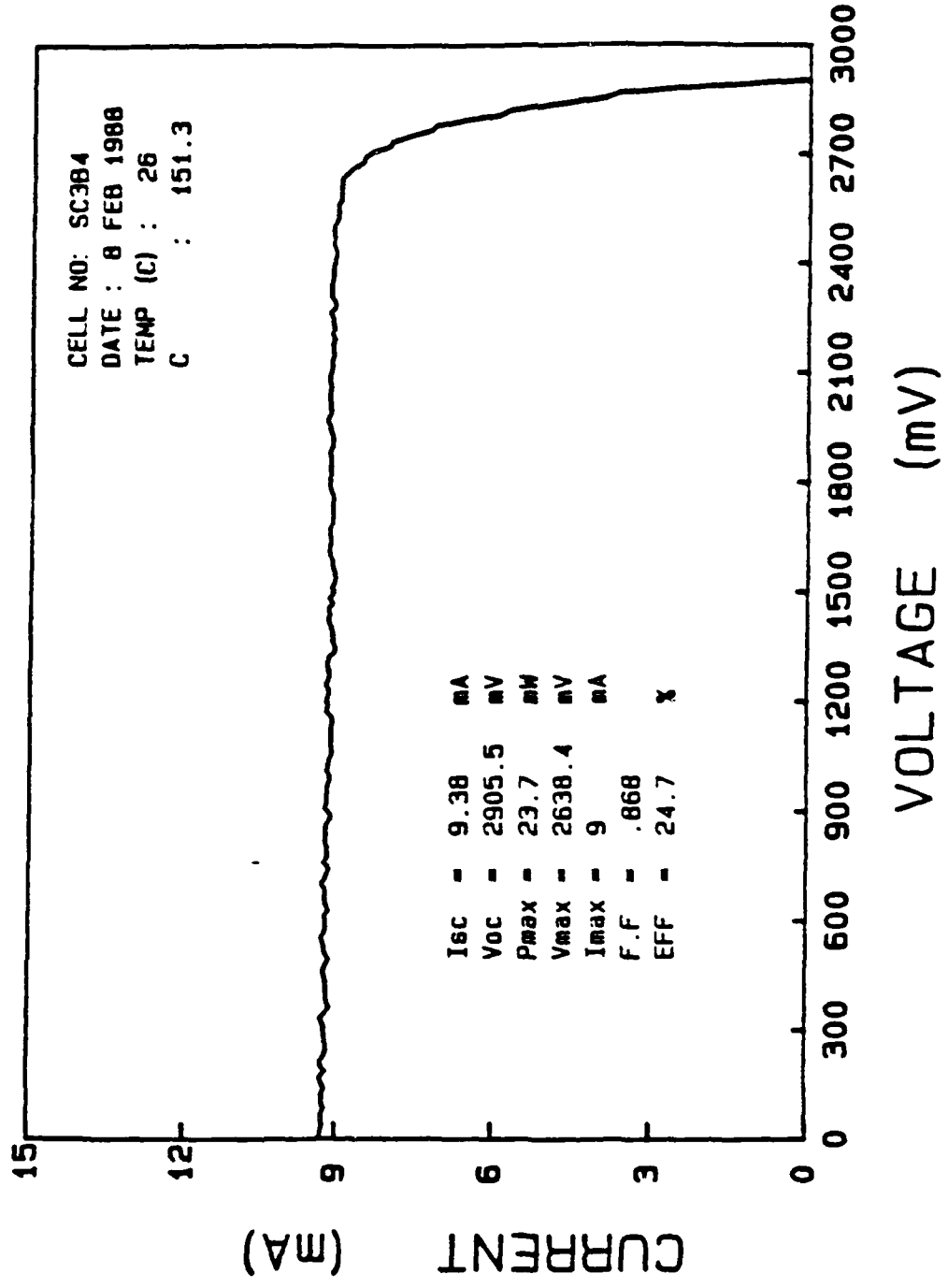

Figure 54. I-V Curve of Bottom String at 151.3X

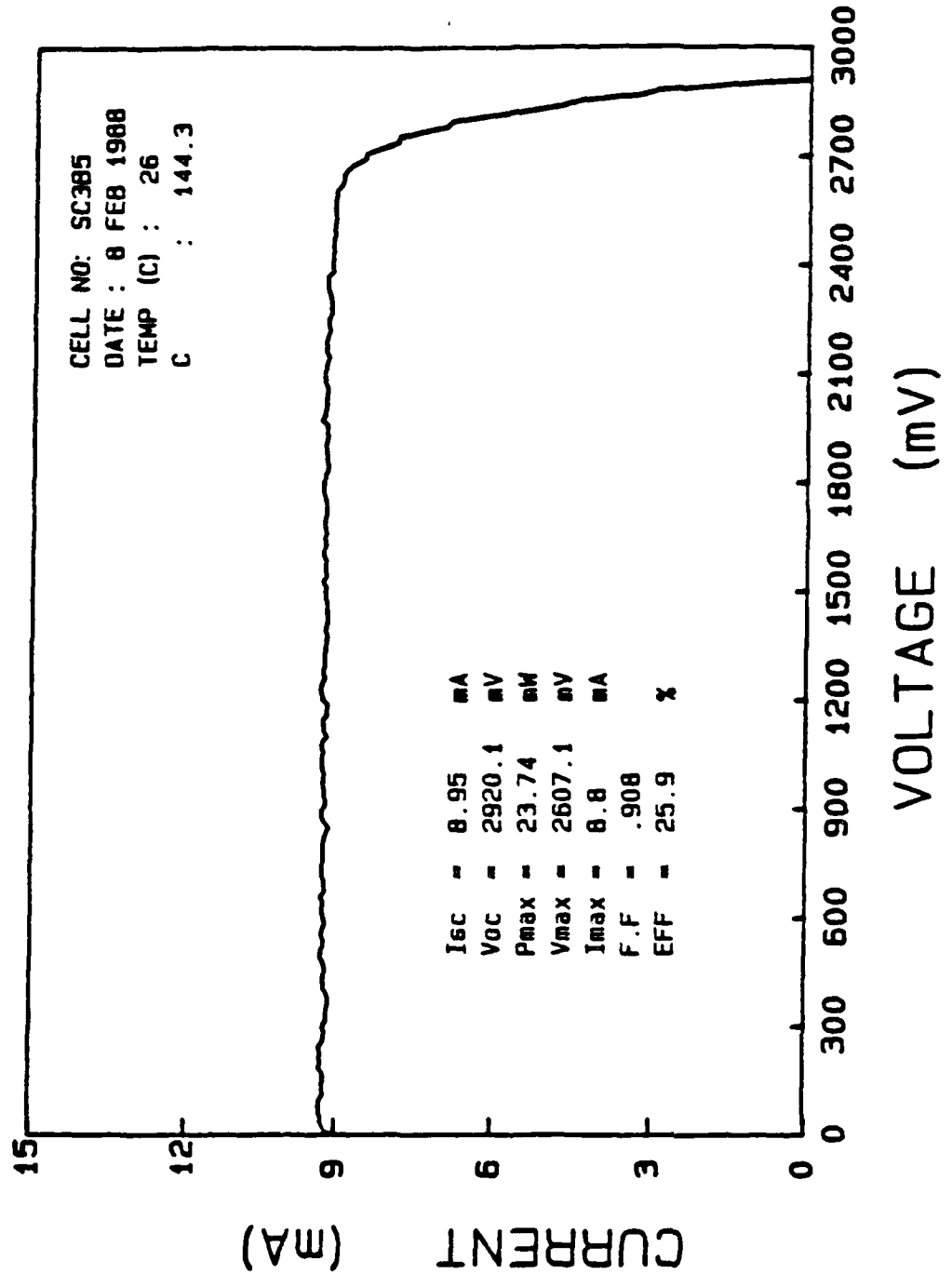

Figure 55. I-V Curve of Bottom String at 144.3X

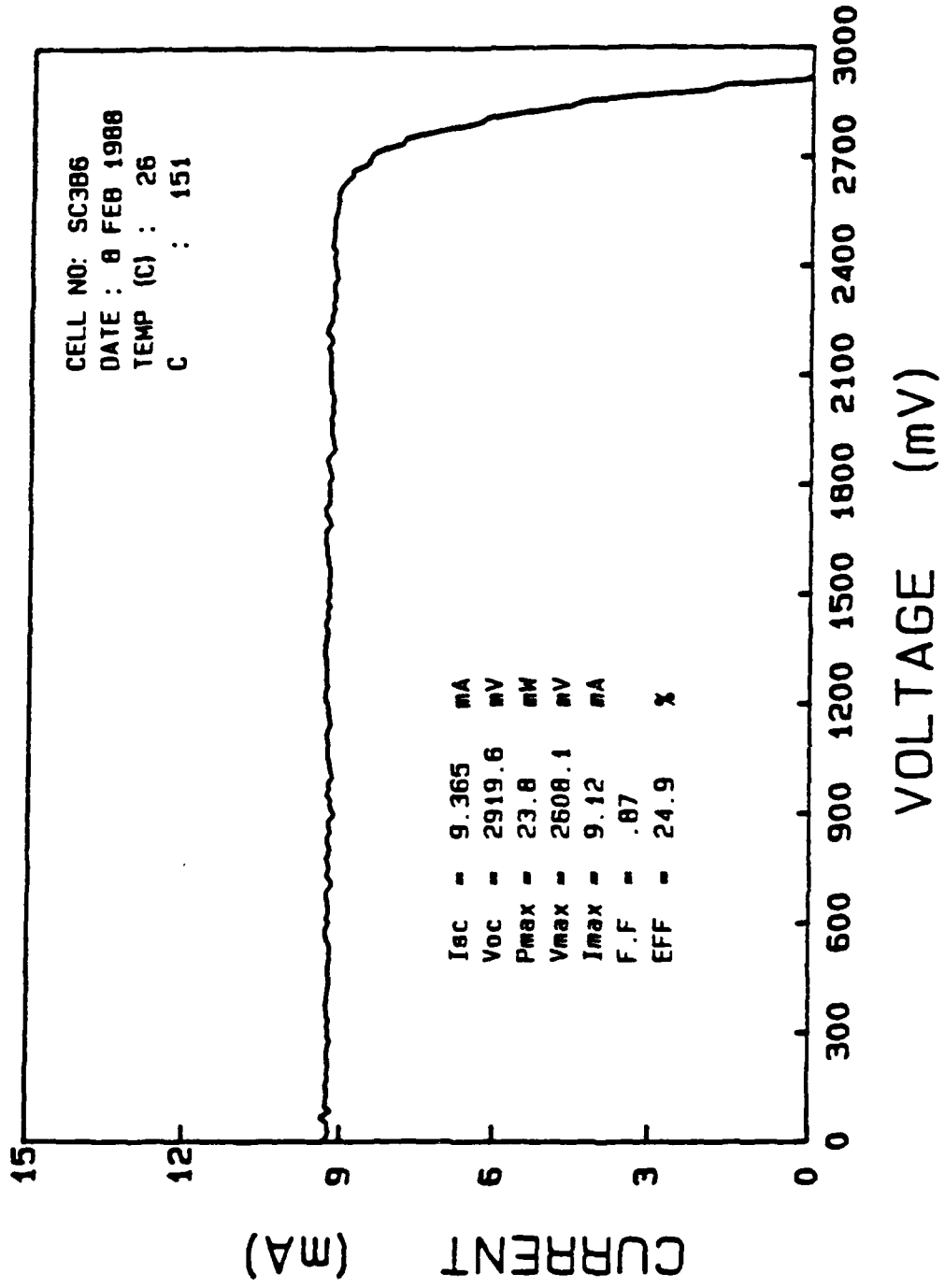

Figure 56. I-V Curve of Bottom String at 151.0X

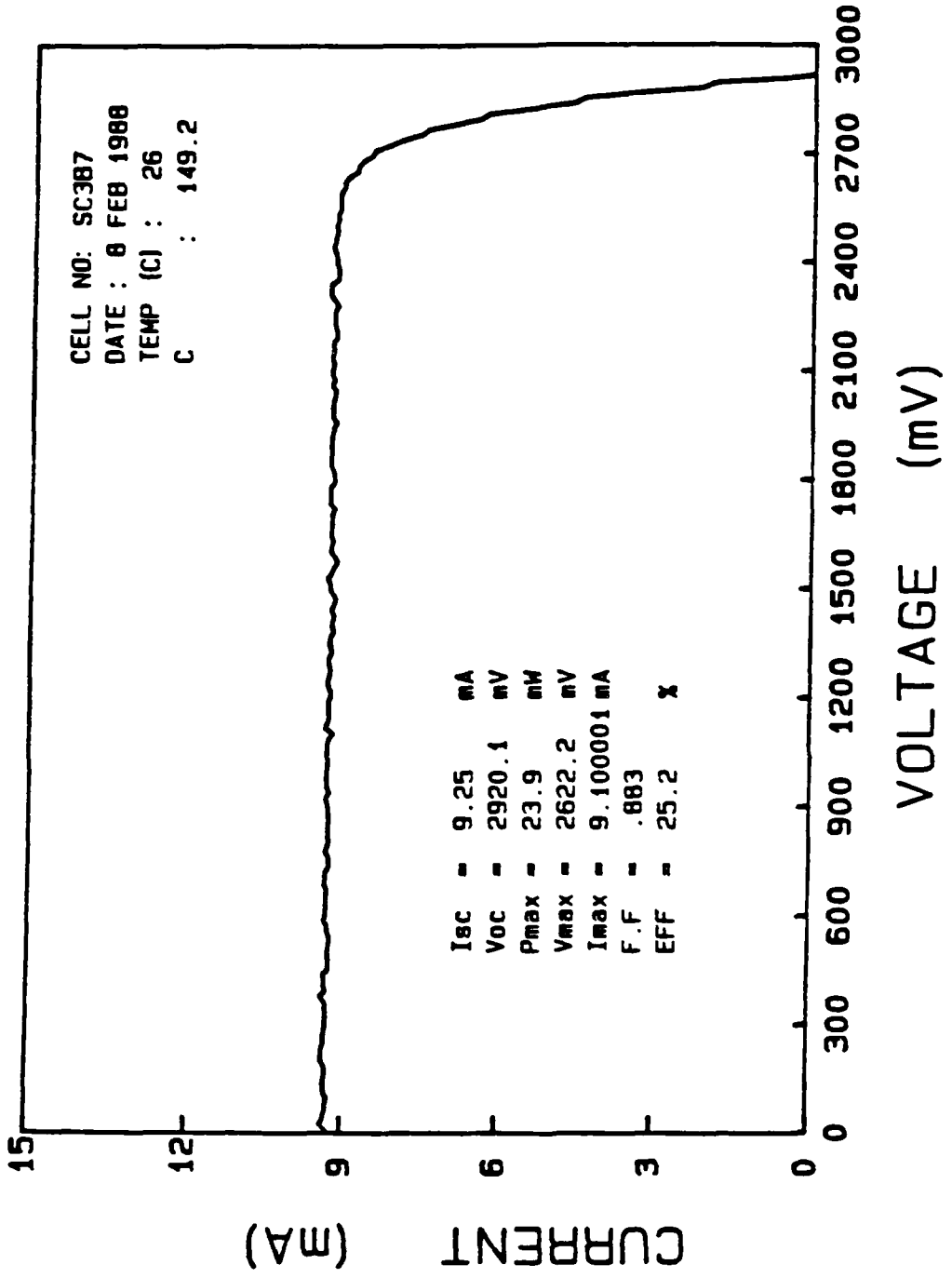

Figure 57. I-V Curve of Bottom String at 149.2X

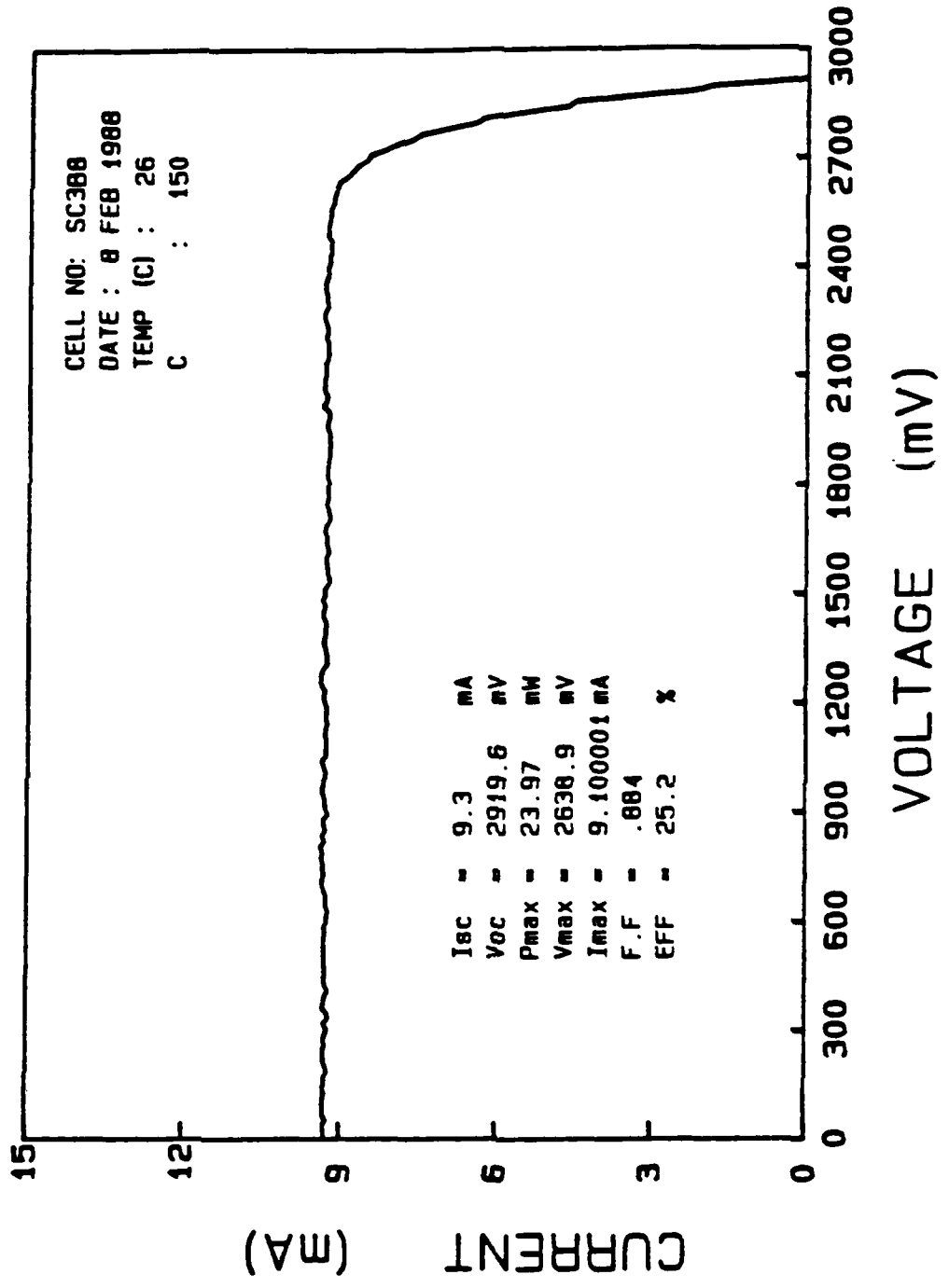

Figure 58. I-V Curve of Bottom String at 150.0X

APPENDIX F. RESULTS OF MIDDLE AND BOTTOM STRING TEST

The test results of the middle and bottom string are listed in Tables 4 and 5, respectively. A discussion of these test results may be found Chapter V.

Table 4. TEST RESULTS OF MIDDLE STRING

NAME	CR	I_{SC} (mA)	V_{OC} (mV)	P_{MAX} (mW)	V_{MAX} (mV)	I_{MAX} (mA)	F.F.
SC3M1	1	.055	2080.0	.091	1688.2	.054	.797
SC3M2	148.0	8.14	2876.3	21.2	2637.5	8.0	.905
SC3M3	154.5	8.5	2876.3	21.8	2622.9	8.3	.892
SC3M4	154.5	8.5	2890.7	21.1	2652.2	8.0	.858
SC3M5	150.9	8.3	2876.0	21.2	2637.5	8.0	.884
SC3M6	151.6	8.3	2876.3	21.5	2578.4	8.3	.895
SC3M7	154.5	8.5	2876.0	21.7	2622.9	8.3	.892
SC3M8	156.4	8.6	2876.0	22.0	2592.6	8.5	.891
SC3M9	149.1	8.2	2875.6	21.0	2623.4	8.0	.895
AVG	152.4	8.4	2877.9	21.4	2621.4	8.2	.889

Table 5. TEST RESULTS OF BOTTOM STRING

NAME	CR	I_{SC} (mA)	V_{OC} (mV)	P_{MAX} (mW)	V_{MAX} (mV)	I_{MAX} (mA)	F.F.
S3T3	1	.062	2051.8	.092	1526.7	.06	.720
SC3B1	148.7	9.22	2905.2	23.9	2608.1	9.17	.893
SC3B2	151.6	9.4	2904.7	23.6	2652.8	8.89	.859
SC3B3	147.1	9.12	2920.1	23.4	2638.9	8.89	.879
SC3B4	151.3	9.38	2905.5	23.7	2638.4	9.0	.868
SC3B5	144.3	8.95	2920.1	23.7	2607.1	8.8	.908
SC3B6	151.0	9.37	2919.6	23.8	2608.1	9.12	.876
SC3B7	149.2	9.25	2920.1	23.9	2622.2	9.10	.883
SC3B8	150.0	9.3	2919.6	24.0	2638.9	9.10	.884
AVG	149.2	9.25	2914.4	23.8	2626.8	9.01	.881

LIST OF REFERENCES

1. Geis, J.W., *Concentrating Photovoltaics: A Candidate for the Next Generation of Satellite Power System*, Journal of Energy, Vol. 6, No. 2, March-April 1982.

2. Rauschenbach, H. S., *Solar Cell Array Design Handbook*, Van Nostrand Reinhold Co., 1980.

3. Rauschenbach, H. S., *Solar Cell Array Design handbook*, Jet Propulsion Laboratory Publication 43-38, Vol I, October 1978.

4. Personal communication with Dr. Mark O'Neill, ENTECH, INC., 31 July 1987.

5. Patterson, R.E. and others, "Low Cost, High Concentration Ratio Solar Cell Array For Space Application." an unpublished paper.

6. Cobb, S. Jr., *Development and Evaluation of an Improved Efficiency Polymeric Web Point-Focus Fresnel Lens*, Sandia National Laboratory Report SAND 86-7046, April 1987.

7. Tada, H. Y. and others, *Solar Cell Radiation Handbook*, Jet Propulsion Laboratory Publication 82-69, 1 November 1982.

8. Agrawal, B. N., *Design of Geosynchronous Spacecraft*, Prentice-Hall, Inc, 1986.

9. Personal communication with Dr. P. Iles, Applied Solar Energy Corporation, 10 October 1987.

10. Telephone conversation with Dr. Dennis Flood, NASA Lewis Research Center, 02 October 1987.

11. Telephone conversation with Dr. Frank Hoe, Applied Solar Energy Corporation, 01 October 1987.

12. Kraus, A. D., *Steady State Thermal Analysis User's Manual*, InterCept Software, June 1985.

13. Gold, D. W., *High Energy Electron Radiation Degradation of GaAs Solar Cell*, M.S. Thesis, Naval Postgraduate School, Monterey, California, March 1986

14. Sengil, N., *Solar Cell Concentrator System*, M.S. Thesis, Naval Postgraduate School, Monterey, California, March 1986.

BIBLIOGRAPHY

Hawkins, D. and others, *Photovoltaics, Technical Information Guide*, U.S. Government Printing Office, Februrary, 1985.

Hewlett Packard Company, *Model 6825A Bipolar Power Supply/Amplifier, Operating and Service Manual*, 1974.

Hewlett Packard Company, *Model 59501B HP-IB Isolated DAC/Power Supply Programmer, Operating and Service Manual*, 1983.

Holman, J. P., *Heat Transfer*, McGraw Hill Book Co., 1981.

International Business Machine Corporation, *IBM Personal Computer Data Acquisition and Control Adapter Programming Support*, November 1984.

International Business Machine Corporation, *PC Options and Adapters Tecnical Reference Manual-Data Acquisition Adapter*, 1984.

Levy, S. L. and L. Stoddard, *New Developments in a High(500x) Concentration PV Module Design*, Eighteenth IEEE Photovoltaic Specialists Conference, 1985.

Lienhard, J., *A Heat Transfer Textbook*, Prentice-Hall, Inc., 1987.

McDanal, A. J., *A Crossed Lens Photovoltaic Concentrator For Use With a 160x Silicon Cells and 500x Gallium Arsenide Cells*, Eighteenth IEEE Photovoltaic Specialists Conference, 1985.

National Instruments Corporation, *GPIB-PC Users Manual For the IBM Personal Computer and Compatibles*, October 1984.

O'Neill, M. J., and M. Piszczor, *Development of a Dome Fresnel Lens/Gallium Arsenide Photovoltaic Concentrator For Space Application,* Ninteenth IEEE Photovoltaic Specialists Conference, 1987.

Shepard, N. F., Jr., *A Point-Focus Concentrating Photovoltaic Array For Space Application,* Eighteenth IEEE Photovoltaic Specialists Conference, 1985.

Siegel, R. and J. R. Howell, *Thermal Radiation Heat Transfer,* McGraw Hill Book Co., 1981.

INITIAL DISTRIBUTION LIST

		No. Copies
1.	Defense Technical Information Center Cameron Station Alexandria, VA 22304-6145	2
2.	Library, Code 0142 Naval Postgraduate School Monterey, CA 93943-5002	2
3.	Professor S. Michael Code 62Mi Naval Postgraduate School Monterey, CA 93943	2
4.	Professor A. Kraus Code 62Ks Naval Postgraduate School Monterey, CA 93943	2
5.	Professor J. Powers Chairman,Code 62 Department of Electrical and Computer Engineering Naval Postgraduate School Monterey, CA 93943	1
6.	Professor R. Panholzer Code 62Pz Naval Postgraduate School Monterey, CA 93943	2
7.	Department of the Navy Commender Space and Naval Warfare Systems Command, PDW 106-483 Attn: Ledr. R. Harding Washington, D.C. 20363-5100	2
8.	Major Chris L. Hudec United States Army Element Office Secratary of Defense (W1B3AA) Pentagon, VA 20310	4
9.	United States Army Space Command ATTN: Technical Library Peterson AFB, CO 80914	2

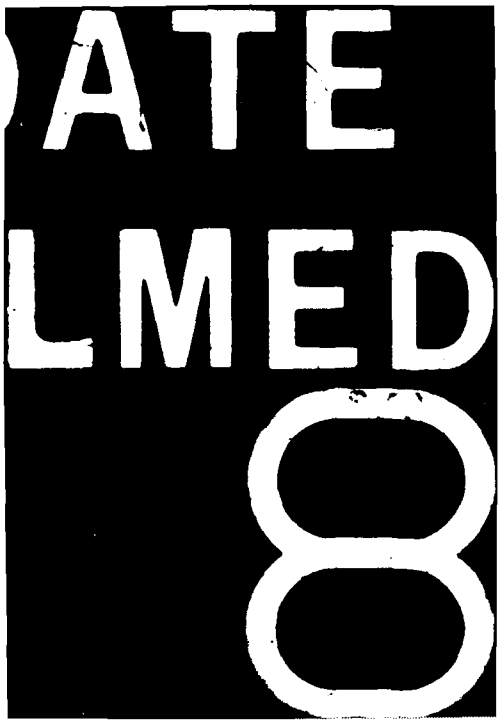
ATE
LMED
8